

**Immune perturbations in HIV-1-infected individuals who make broadly reactive
neutralizing antibodies**

by

M. Anthony Moody^{1,2,3,#}, Isabela Pedroza-Pacheco^{4,#}, Nathan A. Vandergrift^{1,5},
Cecilia Chui⁴, Krissey E. Lloyd¹, Robert Parks¹, Kelly A. Soderberg¹, Ane T. Ogbe⁴,
Myron S. Cohen⁶, Hua-Xin Liao^{1,5}, Feng Gao^{1,5}, Andrew J. McMichael⁴,
David C. Montefiori⁷, Laurent Verkoczy^{1,5,8}, Garnett Kelsoe^{1,2}, Jinghe Huang⁹,
Patrick R. Shea¹⁰, Mark Connors⁹, Persephone Borrow^{4*} and Barton F. Haynes^{1,2,5*}

¹Duke University Human Vaccine Institute, Duke University School of Medicine, Durham, NC 27710.

²Department of Immunology, Duke University School of Medicine, Durham, NC 27710.

³Department of Pediatrics, Duke University School of Medicine, Durham, NC 27710.

⁴Nuffield Dept. of Clinical Medicine, University of Oxford, Oxford OX3 7FZ, United Kingdom.

⁵Department of Medicine, Duke University School of Medicine, Durham, NC 27710.

⁶University of North Carolina at Chapel Hill, 27599.

⁷Department of Surgery, Duke University School of Medicine, Durham, NC 27710.

⁸Department of Pathology, Duke University School of Medicine, Durham, NC 27710.

⁹Laboratory of Immunoregulation, NIAID, NIH, Bethesda, MD 20814.

¹⁰Institute for Genomic Medicine, Columbia University, New York, NY 10032.

#co-first authors

*Correspondence to: Barton F. Haynes, MD

Director, Duke Human Vaccine Institute

Duke University Medical Center

Durham, North Carolina 27710

Phone: (919) 684-5279

Fax: 919-684-5230

E-mail: hayne002@mc.duke.edu

M. Anthony Moody, MD

Duke Human Vaccine Institute

Durham, North Carolina 27710

Phone: (919) 684-5384

Fax: 919-684-5230

E-mail: moody007@mc.duke.edu

40 Persephone Borrow, PhD
41 Nuffield Dept of Clinical Medicine,
42 University of Oxford,
43 NDM Research Building,
44 Old Road Campus, Headington,
45 Oxford OX3 7FZ, UK.
46 Phone: 44-1260-612909
47 E-mail: persephone.borrow@ndm.ox.ac.uk
48
49

Abstract (122 words)

Induction of broadly neutralizing antibodies (bnAbs) is a goal of HIV-1 vaccine development. BnAbs occur in some HIV-1-infected individuals and frequently have characteristics of autoantibodies. Here we have studied cohorts of HIV-1-infected individuals that made bnAbs and compared them to those who did not do so, and determined immune traits associated with the ability to produce bnAbs. HIV-1-infected individuals with bnAbs had a higher frequency of blood autoantibodies, a lower frequency of regulatory CD4⁺ T cells, a higher frequency of circulating memory T follicular helper CD4⁺ cells and a higher T regulatory cell level of programmed cell death-1 expression compared to HIV-1-infected individuals without bnAbs. Thus, induction of HIV-1 bnAbs may require vaccination regimens that transiently mimic immunologic perturbations in HIV-1-infected individuals.

One Sentence Summary (146 characters with spaces)

Blood autoantibodies and a reduced frequency of regulatory CD4⁺ T cells are associated with broadly neutralizing antibodies in HIV-1⁺ individuals.

Introduction

Development of a HIV-1 vaccine is the cornerstone of a comprehensive global HIV-1 preventive strategy (1). A critical component of a successful strategy is design of immunogens to induce broadly-reactive neutralizing antibodies (bnAbs) (2, 3). However, to date, no candidate HIV-1 vaccines have induced plasma bnAb activity (4-6). Only rarely do HIV-1-infected individuals make high levels of bnAbs, but over 2-4 years of infection, ~50% of infected individuals develop cross-reactive antibodies that neutralize ~50% of difficult-to-neutralize (tier 2) HIV-1 isolates (7-11).

Clues to the dearth of vaccine-induced bnAbs come from analysis of the physical characteristics of bnAbs (2, 12-14). All bnAbs isolated to date either have very high frequencies of somatic mutations, long third heavy chain complementarity determining regions, and/or autoreactivity—traits of B-cell antigen receptors that are negatively regulated by immune tolerance mechanisms (13, 15-26). One hypothesis is that some, or all bnAb development may be controlled by one or more immune tolerance mechanisms (2, 12, 13, 16).

Approximately 50% of HIV-1-infected individuals will produce autoantibodies during untreated HIV-1 infection (27-33). Here we have profiled the immune perturbations associated with HIV-1 infection and bnAb induction. We studied a cohort of 239 chronically HIV-1-infected individuals for serum ability to broadly neutralize HIV-1 strains, and selected 51 individuals with the highest blood bnAb activity versus 51 matched individuals with low neutralizing activity. We tested for the coincident presence of plasma autoantibodies, and for peripheral blood CD4⁺ T cell subset frequencies in the HIV-1-infected individuals that had made bnAbs, in those that had not made bnAbs, and in HIV-1-seronegative controls (including those with and without autoantibodies). We quantified total CD4⁺ T cells and

assessed the circulating frequency of resting memory T follicular helper cells (mTfh cells), a population defined as the PD-1⁺ CXCR3⁻ subset of CXCR5⁺ CD4⁺ T cells (34). We also determined the frequency of CD25⁺ Foxp3⁺ regulatory CD4⁺ T (Treg) cells — a population of cells that have been shown to suppress the development of autoantibody responses [reviewed in (35)] — as well as the proportion of circulating CD4⁺ T follicular-phenotype cells (ie, CD4⁺ CXCR5⁺ T cells) composed of CD25⁺ Foxp3⁺ CD4⁺ T follicular regulatory (Tfr) cells, the subset of CD4⁺ Treg cells that mediates control of B cell responses within germinal centers (36-42), and measured PD-1 expression on both Treg and Tfr cells.

Autoantibodies in HIV-1-infected individuals with high versus low HIV-1 neutralizing activity in plasma.

Cohort A consisted of 239 HIV-1-infected individuals of whom 214 (90%) were African (**Table S1 online**). Based on serum neutralization data, we selected 51 individuals who had the highest level of bnAbs and matched them with 51 individuals who did not have bnAbs (**Figure 1A; Figures S1-2 and Tables S1-9 online**). Thirty-three of 51 (65% of) HIV-1-infected individuals with bnAb activity had positive plasma reactivity in one or more autoantibody assays (**Figure 1C**). In contrast, only 16 of 51 (31%) in the non-bnAb HIV-1-infected control group had plasma autoantibodies ($\chi^2 = 11.4$, $p = 0.0008$; **Figure 1C**). Poisson regression results also showed the bnAb individuals to have a higher number of positive autoantibody tests than the non-bnAb HIV-1-infected control group ($\chi^2 = 14.7$, $p = 0.0001$; **Figure 1E**). Cohort A was infected primarily with clade C viruses (A.bnAb 33/51, 65%; A.Control 37/51, 73%; $p = 0.52$, Fisher's exact test; **Table S9 online**), but we

found that clade of infecting virus had no effect on either the presence of neutralization breadth or the presence of autoantibodies (**Tables S10-12 online**).

To determine the effect of geographic region of HIV-1 individual origin on autoantibody frequency in bnAb individuals, we studied a second confirmatory group (Cohort B; **Tables S13-16 online**) of HIV-1 infected individuals from the US comprised of subjects who produced bnAbs and those who had lower levels of plasma neutralizing antibodies (**Figure 1B**). Confirming the data in Cohort A, we found that 22 of 24 (92%) HIV-1-infected individuals in Cohort B with bnAb activity had at least one positive test, while only 12 of 21 (57%) Cohort B low level neutralizing antibody individuals had plasma autoantibodies ($\chi^2 = 7.2$, $p = 0.007$; **Figure 1D**). However, due to the lower number of subjects in Cohort B, Poisson regression analysis was unable to show a difference in the total number of positive autoantibody tests in Cohort B bnAb individuals than the non-bnAb controls ($\chi^2 = 1.8$, $p = 0.2$; **Figure 1F**). Moreover, the Cohort B HIV-1-infected non-bnAb control group was different from the non-bnAb control group of Cohort A. The US Cohort B control group had a greater level of neutralizing antibodies than the primarily African Cohort A control group (B Control total isolate tested geometric mean titer [GMT] = 32.7, A Control GMT = 12.2, $p < 0.0001$, t -test; **Tables S4, S14 online**).

Since HIV-1 infection is associated with polyclonal B cell activation (43), we next asked if overall levels of antibody production to HIV-1 and non-HIV-1 antigens were similar between the bnAb and control groups of both cohorts. Thus, we assayed for plasma antibody binding to HIV-1 Env gp120 and gp41, as well as to trivalent inactivated influenza vaccine (TIV2008). Binding to HIV-1 Env gp120 ($p < 0.0001$, t -test) and gp41 ($p < 0.0001$, t -test) proteins were elevated in the Cohort A bnAb group compared to the Cohort A control

group (**Figure 2A, 2B; Table S17 online**), while plasma antibodies to influenza were similar between the Cohort A control group and the bnAb group ($p = 0.19$, t -test; **Figure 2C**). In both Cohort B bnAb and control groups, antibodies to gp120, gp41 and TIV2008 were not statistically different ($p = 0.35, 0.46, 0.27$, respectively, t -test; **Figure 2D-F; Table S17 online**). Thus, the lack of increased antibodies to influenza in these cohorts suggests that the higher frequency of autoantibodies in HIV-1-infected individuals with bnAbs was not due to a general increase in antibody induction.

CD4⁺ T cell subsets in Cohort A bnAb group versus Cohort A control groups.

CD25⁺ Foxp3⁺ CD4⁺ Treg cells play an important role in prevention of autoimmunity, and loss or impairment of Treg function leads to autoantibody induction (35, 44, 45). Conversely, increased frequencies of CD4⁺ T follicular helper (Tfh) cells, which play a crucial role in the germinal center B-cell response, are often associated with autoantibody production (46-48). Thus, we determined the frequency of CD4⁺ Tfh and Treg cells in the Cohort A bnAb and non-bnAb groups from whom PBMC samples were available, and matched HIV-1-seronegative controls. The A.bnAb group had a higher mean viral load than the non-bnAb group (**Table S7 online**), although we found that the presence of autoantibodies was independent of viral load (**Tables S19-20 online**). Total CD4⁺ T cells in both groups of HIV-1-infected individuals were reduced compared to HIV-1-seronegative controls, and they were significantly lower in the A.bnAb group than in the A.Control group ($p = 0.0001$, t -test; **Figure 3A; Table S18 online**). Analysis of the circulating frequency of resting memory T follicular helper (mTfh) CD4⁺ T cells, defined as the PD-1⁺ CXCR3⁻ subset of CXCR5⁺ CD4⁺ T cells (34), revealed that mTfh were present at significantly

higher frequencies in the A.bnAb group than in the A.Control group or HIV-1-seronegative controls ($p < 0.0001$ and $p < 0.0001$, respectively, t -test; **Figure 3B; Table S18 online**). The frequency of CD25⁺ Foxp3⁺ CD4⁺ Treg cells within lymphocytes was also significantly lower in the A.bnAb group compared to the A.Control group ($p = 0.004$, t -test; **Figure 3C; Table S18 online**), although the frequency of Treg cells within CD4⁺ T cells did not differ significantly between groups (not shown).

The inhibitory receptor programmed cell death-1 (PD-1) has been associated with CD4⁺ and CD8⁺ T cell activation and/or dysfunction in HIV-1 infection (reviewed in (49)) and with the development of autoimmunity (reviewed in (50)). Thus, we measured the level of PD-1 on circulating CD25⁺ Foxp3⁺ CD4⁺ Treg cells, and found that in the A.bnAb group Treg cells expressed significantly higher levels of the inhibitory receptor PD-1 than Tregs in A.Control individuals ($p < 0.0001$, t -test) or in HIV-1-seronegative controls ($p < 0.0001$, t -test; **Figure 3D; Table S18 online**). Importantly, the differences in mTfh and Treg frequencies and PD-1 expression on Tregs in the A.bnAb and A.Control groups were independent of their differing viral loads (**Tables S21-22 online**).

Recent studies have identified a subpopulation of CD25⁺ Foxp3⁺ CD4⁺ Treg cells that shares some of the phenotypic characteristics of CD4⁺ T follicular helper (Tfh) cells including expression of Bcl6, CXCR5, PD-1 and ICOS; these CD4⁺ T follicular regulatory (Tfr) cells can home into germinal centers, and regulate the germinal center response by limiting Tfh numbers and function and via direct effects on B cells (35, 37-42, 51, 52). Germinal center B cell responses are thought to be determined by the relative proportions of Tfr and Tfh cells, rather than the number of Tfr cells (41). Memory Tfr populations circulate in peripheral blood (41). We therefore measured the proportion of CD25⁺ Foxp3⁺

regulatory cells in the circulating CD4⁺ T follicular-phenotype cell population, defined as CXCR5⁺ CD4⁺ T cells. In both Cohort A groups of HIV-1-infected individuals, the proportion of Tfr cells within the circulating CXCR5⁺ CD4⁺ T cell population (**Figure 3E; Table S18 online**) and the Tfr/Tfh ratio (ie, ratio of CD25⁺ Foxp3⁺ to non-CD25⁺ Foxp3⁺ cells in the circulating CXCR5⁺ CD4⁺ T cell population) (**Figure 3F; Table S18 online**) did not differ significantly in the A.bnAb and the A.Control groups, although the level of PD-1 expression on Tfr cells was significantly higher in the former group ($p = 0.004$, t -test; **Figure 3G; Table S18 online**). Given the current lack of consensus about the phenotypic definition of circulating CD4⁺ Tfr cells in humans (41, 53-55), we also considered two other definitions for this population (CD25⁺ Foxp3⁺ cells within CXCR3⁻ PD-1⁺ CXCR5⁺ CD4⁺ T cells, and CD25⁺ Foxp3⁺ cells within ICOS⁺ PD-1⁺ CXCR5⁺ CD4⁺ T cells). Similar results were obtained regardless of the definition used, with no significant difference being observed in circulating Tfr frequencies or the Tfr/Tfh ratio in the A.bnAb and the A.Control groups, and PD-1 on Tfr being significantly higher or showing a trend towards higher expression in the A.bnAb group (**Figure S6; Table S23 online**). Interestingly, when we divided the Cohort A subjects into groups on the basis of generation of autoantibodies rather than bnAbs, we found that autoantibody-positive subjects exhibited similar alterations in T cell subsets, including expression of higher levels of PD-1 on CD4⁺ Treg and Tfr populations, to that seen between the A.bnAb and A.Control groups, although this difference was less pronounced and did not reach statistical significance (data not shown).

The higher levels of PD-1 expression on CD4⁺ Treg and Tfr cells in the A.bnAb group raised the hypothesis that regulatory CD4⁺ T cell populations in the A.bnAb group are more activated and may be more dysfunctional than those in the A.Control group. We thus

205 compared the expression of HLA-DR (another marker associated with CD4⁺ T cell
206 activation) and CTLA-4 and LAG-3 (both of which are markers of CD4⁺ T cell exhaustion
207 (56), but are also involved in CD4⁺ Treg cell effector function (57, 58)) on CD4⁺ Treg cells
208 in the Cohort A bnAb and non-bnAb groups and matched HIV-1-seronegative controls. The
209 percentage of CD4⁺ Treg cells expressing HLA-DR was significantly higher in the A.bnAb
210 than the A.control group ($p = 0.0003$, t -test; **Figure 4A; Table S24 online**), and the level of
211 PD-1 expression on Tregs was also significantly higher in the former group (not shown).
212 Similar observations were also made for CTLA-4 ($p = 0.01$, t -test; **Figure 4B; Table S24**
213 **online**); and although there was no difference between groups in the percentage of CD4⁺
214 Treg cells expressing LAG-3 (**Figure 4C; Table S24 online**), the level of LAG-3 expression
215 on CD4⁺ Tregs was again significantly higher in the A.bnAb than the A.control group (not
216 shown). Notably, HLA-DR, CTLA-4 and LAG-3 were all expressed on a significantly higher
217 proportion of PD-1^{high} CD4⁺ Treg cells than PD-1^{low} or PD-1^{negative} CD4⁺ Tregs in both
218 HIV-1-infected (data for the A.bnAb group shown in **Figure 4D-F; Table S25 online**) and
219 HIV-1 seronegative control subjects (**Figure 4G-I; Table S26 online**). To explore the
220 functional capacity of the PD-1^{high} subset of CD4⁺ Treg cells, CD25^{high} CD127^{low} CD4⁺ Treg
221 cells from HIV-1-seronegative donors were sorted into PD-1^{high}, PD-1^{low} and PD-1^{negative}
222 subpopulations and their ability to suppress the proliferation of conventional (CD25^{low}
223 CD127^{high}) CD4⁺ T cells assessed. Whereas PD-1^{low} and PD-1^{negative} CD4⁺ Treg
224 subpopulations mediated significant suppression of conventional CD4⁺ T cell proliferation
225 ($p = 0.01$, sign test; **Figure 4J, Table S27 online**), this was not the case for PD-1^{high} CD4⁺
226 Treg cells—the PD-1^{high} CD4⁺ Treg subpopulation from some donors had a highly impaired
227 suppressive capacity (**Figure 4J**). Together, these results suggested that high PD-1

expression on regulatory CD4⁺ T cells, as observed in the A.bnAb group, is indicative of activation and development of an impaired functional capacity.

The higher frequency of blood autoantibodies, higher frequency of circulating CD4⁺ mTfh cells, lower frequency of CD4⁺ Treg cells, and higher levels of PD-1 expression on CD4⁺ Treg and Tfr cells observed in the A.bnAb as compared to the A.control group may have been present prior to HIV-1 infection, and/or may have developed or been accentuated during the course of infection. The Cohort A subjects had not been sampled prior to or during the early stages of HIV-1 infection and we were unable to address the sequence of events preceding bnAb development during the course of infection. However, to gain insight into whether some healthy individuals have a pre-existing immunological profile that could potentially predispose them to bnAb induction following HIV acquisition, we analyzed CD4⁺ T cell subsets in healthy HIV-1-seronegative individuals with and without plasma autoantibodies. None of the 48 HIV-1-seronegative control individuals studied in parallel to the HIV-1-infected groups had plasma autoantibodies (data not shown). However, when we screened for the presence of autoantibodies in 118 predominantly African HIV-1-seronegative individuals, we identified 12 individuals who did have plasma autoantibodies. Analysis of total and regulatory CD4⁺ T cell populations in these individuals and a control group of 23 age, sex, and location-matched HIV-1-seronegative individuals without plasma autoantibodies revealed that there was no difference between groups in the frequency of total CD4⁺ T cells within lymphocytes or circulating frequency of mTfh cells (**Figures 5A and 5B; Table S28 online**); but that the frequency of CD25⁺ Foxp3⁺ CD4⁺ Treg cells in the HIV-1-uninfected individuals with autoantibodies was lower than that in those without autoantibodies, although not statistically significant ($p = 0.06$, t -test; **Figure**

5C; Table S28 online). The level of PD-1 expression on CD4⁺ Treg cells in some of the HIV-1-uninfected individuals with autoantibodies was also higher than that in those without autoantibodies, although there was not a significant difference between groups in PD-1 expression on CD4⁺ Treg cells overall ($p = 0.63$, t -test; **Figure 5D; Table S28 online).**

Since HLA allotypes have been associated with the development of autoimmune disease (59), we performed HLA typing on all individuals in Cohort A and found no significant differences in distribution between bnAb versus control groups for HLA class I (**Tables S29-30 online**) or class II allotypes (**Tables S31-32 online**) (Cochran-Mantel-Haenszel tests).

Finally, to look for evidence of genes that predisposed HIV-1-infected individuals to make bnAbs, we performed full exome sequencing on the 51 bnAb individuals and on the 51 control HIV-1-infected individuals without bnAbs. We found no genome-wide significant mutations in either group, although we did identify 20 single nucleotide variants or small indels in the association study of HIV-1 broad neutralization before genome-wide statistical correction (**Table S33 online**). To focus the analysis, we compared only those bnAb individuals that also expressed plasma autoantibody reactivity to individuals in the non-bnAb group that showed no autoantibody activity. Again no significant genome-wide associations were found, however a number of candidate genes were identified that are known to be relevant to control of the immune system (**Table S34 online**).

Discussion

A major conundrum in the HIV-1 vaccine development field is why 50% of HIV-1-infected individuals make bnAbs after years of infection, but vaccination of uninfected individuals with antigenic HIV-1 envelopes has, as yet, not induced bnAbs. While structural integrity of the native envelope immunogen is a critical component for induction of bnAbs (3), multiple envelope trimer immunization studies have yet to induce bnAbs (60-66). Here we have defined the profile of immune perturbations found in those HIV-1-infected individuals with plasma bnAbs. HIV-1-infected individuals that make cross-reactive neutralizing antibodies have a higher viral load, lower total CD4⁺ T cells, higher frequency of blood autoantibodies, higher levels of circulating mTfh, a lower frequency of Treg cells and higher levels of PD-1 on Treg and Tfr cells compared to a group of HIV-1-infected individuals with no or low bnAb levels.

Early in the AIDS epidemic before anti-retroviral treatment, it was noted that HIV-1 infection induced host immunoregulatory abnormalities leading to plasma autoantibody production (27, 29, 31, 43), and a high incidence of autoantibody seropositivity (27-30, 32, 33). In an earlier pilot study of 16 HIV-1-infected individuals, we found anti-cardiolipin antibodies were frequently present in those with plasma neutralization breadth but no significant elevation of other autoantibodies (67). The findings in our current study provide evidence for the hypothesis that one reason that bnAbs are induced in some HIV-1-infected individuals is that HIV-1 infection perturbs their immune system by loss, activation, and/or exhaustion of CD25⁺ Foxp3⁺ regulatory CD4⁺ T cell populations in the setting of elevated CD4⁺ Tfh cells, thus facilitating the production of bnAbs. It would be of interest to prospectively recruit a new group of acutely HIV-1-infected individuals to determine the

mechanism and timing of these events rather than use retrospective samples. However, with evidence supporting the early initiation of antiretroviral therapy at the time of diagnosis (68), it is no longer ethical to perform natural history studies of HIV-1 infection without offering antiretroviral therapy.

In HIV-1 infection, CD4⁺ T cells, including CD25⁺ Foxp3⁺ CD4⁺ Treg cells, are lost as a consequence of infection with HIV-1 and bystander apoptosis (69, 70). The Cohort A HIV-1-infected individuals producing bnAbs had higher viral loads than those subjects not producing bnAbs, and higher viral loads have also been associated with bnAb production in other HIV-1-infected cohorts (reviewed in (71)). However, although the high viral loads in bnAb individuals may have been among the factors contributing to the greater depletion of both total CD4⁺ T cells and CD4⁺ Tregs in the subjects producing bnAbs in our study, all the differences observed in CD4⁺ T cell subsets in the groups of subjects producing or not producing bnAbs were independent of viral load, indicating that they were primarily driven by other factors.

Tfh cell differentiation is a multistep process regulated by numerous signals; however, cytokines play an important role in regulation of early Tfh differentiation, with signaling via IL-6 promoting and via IL-2 inhibiting Tfh differentiation (72). Tfh cells are thus expanded in a number of chronic viral infections including HIV-1 where IL-6 is induced and IL-2 is limited (34, 73-77). In a previous study of an HIV-1-infected cohort, chronically-infected individuals generating bnAbs were found to have higher circulating frequencies of mTfh than matched individuals not generating bnAbs (34). Locci et al. further showed that mTfh frequencies during early HIV-1 infection were higher in subjects who subsequently developed bnAbs;

likewise Cohen et al. reported an association between early preservation of PD1⁺ CXCR5⁺ CD4⁺ Tfh cells and bnAb development (78).

A recent study proposed that the expansion of germinal centre Tfh cells during SIV infection may be facilitated by a decline in the Tfr/Tfh ratio (79). However others have reported an increase in the frequency of Tfr in lymph nodes and spleen during SIV/HIV infection, which suggests that the lymph node Tfr/Tfh ratio may not be perturbed (80, 81). Here, we studied circulating CD4⁺ Treg and Tfr cell subsets. We found that compared to subjects without bnAbs, subjects with bnAbs had a lower frequency of CD4⁺ Treg cells within lymphocytes; but although CD4⁺ Tfr largely differentiate from Tregs (37-39, 82), the circulating frequency of Tfr did not differ significantly between groups. Notably, PD-1 was expressed at significantly higher levels on both CD4⁺ Treg and CD4⁺ Tfr cells in subjects with bnAbs. Elevated PD-1 expression in the bnAb group likely reflects higher levels of immune activation in these subjects, consistent with which CD4⁺ Treg cells also expressed higher levels of the activation marker HLA-DR. PD-1 is an inhibitory receptor, ligation of which has been shown to inhibit Tfr function in mice (41). PD-L1 expression on lymph node B cells is increased during HIV-1 infection (77), hence the function of Tfr in subjects producing bnAbs may be inhibited as a consequence of their elevated expression of PD-1. PD-1 expression can also reflect T cell exhaustion as a consequence of sustained activation, and CD4⁺ Treg cells from subjects producing bnAbs expressed elevated levels of CTLA-4 and LAG-3, markers indicative of CD4⁺ T cell exhaustion (56). Despite the fact that CTLA-4 and LAG-3 are also involved in Treg and Tfr function (40, 57, 58), we found that PD-1^{high} CD4⁺ Treg cells exhibited an impaired ability to suppress the proliferation of conventional CD4⁺ T cells in vitro, supporting the hypothesis that elevated PD-1 expression

on regulatory CD4⁺ T cell subsets may reflect cellular exhaustion and an impaired suppressive capacity.

Our data suggest that by the time of chronic HIV-1 infection, the majority of viremic individuals develop alterations in the CD4⁺ T cell subsets that mediate control of germinal center B-cell responses. High viral loads, immune activation, dysregulation of cytokine production and alterations in lymphoid tissue microenvironments may drive the development of particularly profound abnormalities in regulatory CD4⁺ T cell subsets in some subjects, creating an environment permissive to generation of both autoantibodies and bnAbs that then emerge in a subset of these individuals. However, since some HIV-1-infected individuals with bnAbs did not have autoantibodies, the propensity to make autoantibodies may be a surrogate marker for an as yet undiscovered perturbation induced by HIV-1 that leads to bnAb induction. Moreover, we cannot rule out that those HIV-1-infected individuals without plasma bnAbs but with autoantibodies may eventually go on to develop bnAbs, but had not done so at the time of study.

Some individuals may also be predisposed to generate bnAbs following infection with HIV-1 due to pre-existing abnormalities in host tolerance controls. Increased Tfh frequencies and loss or functional impairment of regulatory CD4⁺ T cell subsets have been associated with autoantibody production in subjects with autoimmune disease (35, 44-48). There may be a spectrum of tolerance controls in healthy individuals, with subjects at the lower end being more likely to develop autoantibodies, and potentially also to produce bnAbs in the context of HIV-1 infection.

We previously demonstrated that two bnAbs (2F5, 4E10) directed at the HIV-1 Env gp41 neutralizing site near the viral membrane are autoreactive (13, 83), and in bnAb

antibody heavy and light chain knock-in mice, both bnAbs were shown to be controlled by multiple immune tolerance mechanisms (21, 22, 24, 84, 85). The observations of bnAb autoreactivity prompted the hypothesis that patients with systemic lupus erythematosus (SLE) will be able to make bnAbs more readily than others during chronic HIV-1 infection (15). We recently described an individual with both HIV-1 infection and SLE who had serum anti-dsDNA and bnAb activity (86), and remarkably, an isolated CD4 binding site bnAb (CH98) from this individual cross-reacted with dsDNA—thus, providing direct evidence that bnAbs and SLE autoantibodies can be derived from similar autoreactive pools of B cells and may be similarly regulated (86). Regardless of the mechanisms involved, the presence of autoantibodies in plasma is an indication of HIV-1-associated breaks in immune tolerance, and our finding of decreased frequency of CD25⁺ Foxp3⁺ regulatory CD4⁺ T cell subsets in HIV-1-infected individuals who make bnAbs, together with increased expression of PD-1 on regulatory CD4⁺ T cell populations, suggests a mechanism of release of peripheral immune tolerance controls (35).

The studies presented here raise several hypotheses. First, our data suggest that continued immunization of animals and humans with HIV-1 envelopes in the absence of modifying host immune tolerance mechanisms or mimicking other HIV-1-induced immune perturbations will be unlikely to induce mature bnAbs. New vaccination strategies for amplifying antibody responses by limiting immune tolerance controls of antibody responses to bnAb Env epitopes will likely be needed. Such vaccination strategies are already being tested in the setting of cancer vaccines to augment host anti-cancer T cell responses (87). Temporary breaks in tolerance may be mediated by strong adjuvants, since we have shown that peripheral anergy of bnAb-producing B cells can be broken in bnAb V_HDJ_H/V_LJ_L

knock-in mice by immunization with an Env subunit with a TLR4 agonist (23). Furthermore, TLR9 agonists can boost Tfh differentiation while blocking Tfr, thereby skewing the Tfr/Tfh ratio in favor of Tfh (88, 89).

Second, based on the continuum of bnAb responses made after HIV-1 infection ((7) and the present study), it is possible that a strategy that succeeds in transiently breaking immune tolerance in the setting of HIV-1 Env immunization may only induce bnAbs in some individuals. Some bnAbs are restricted during early B-cell development at the first tolerance checkpoint in bone marrow due to germline B-cell receptor (BCR) autoreactivity, resulting in fewer bnAb precursors before vaccination (21, 22, 24, 84, 85), while other bnAb germline BCRs are not autoreactive, and autoreactivity is only acquired in the periphery during affinity maturation (90). BnAbs with long third heavy chain complementarity determining regions that do emerge in HIV-1 infection appear to be rare by virtue of tolerance mechanisms that reduce their precursor frequency (12, 26, 91). Recent data have demonstrated that one form of immune tolerance is continued accumulation of somatic mutations in autoantibody (92) and bnAb B cell lineages (23) that can lead to reduction in BCR antibody autoreactivity and, in the case of bnAb development, can reduce bnAb activity. It is important to note that not all bnAbs that eventually are made in HIV-1-infected individuals are autoreactive (93, 94), and immunization strategies are being developed to select and drive such subdominant B-cell lineages (12, 16, 95).

Finally, low affinity BCR autoreactivity can be a normal component of the human B-cell response (96, 97). Thus, transient manipulation of the germinal center response to augment persistent responses of normal autoreactive pools of B cells without permanently

breaking systemic immune tolerance to induce desired bnAb B-cell clonal lineages is plausible.

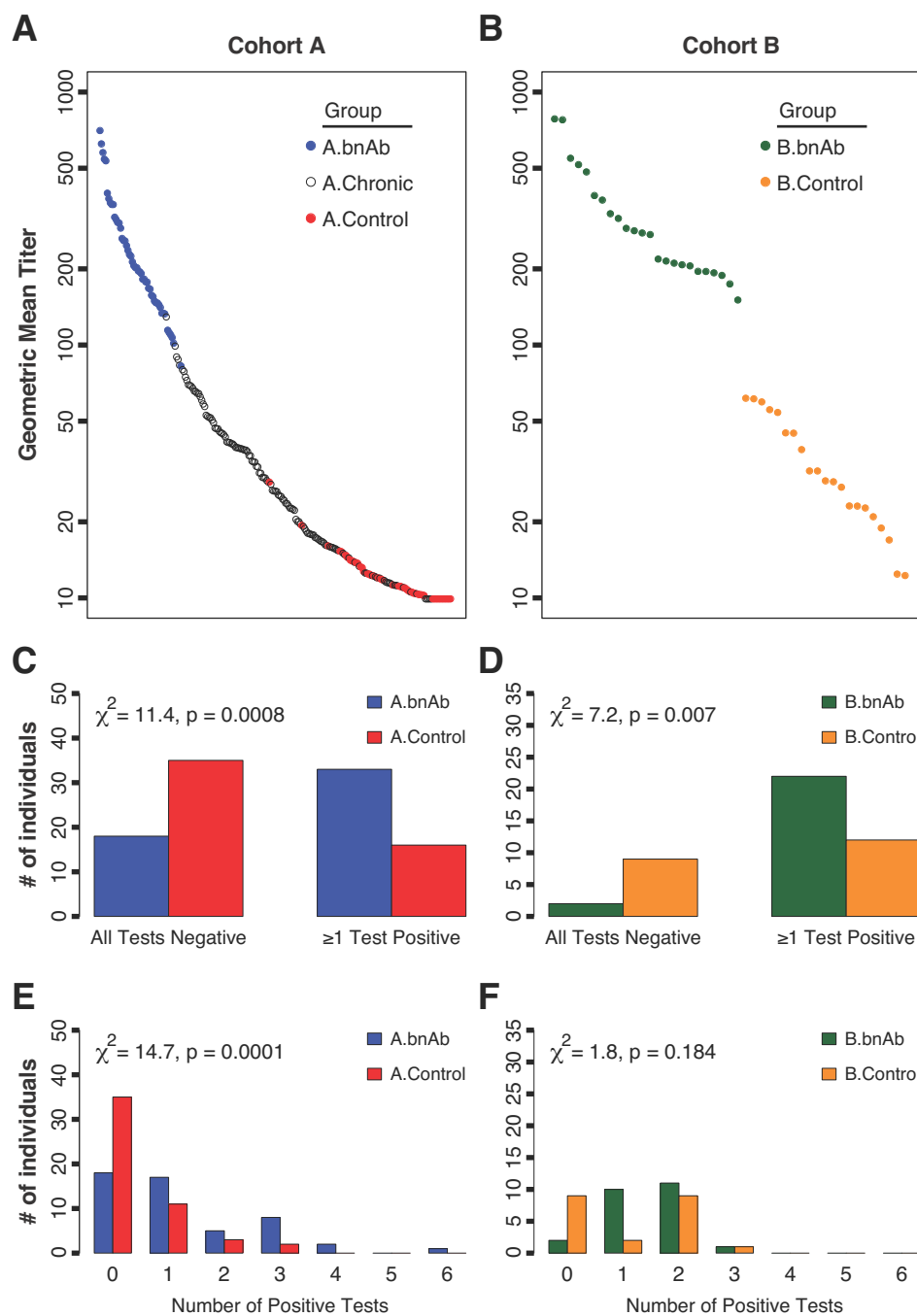
Acknowledgments

The authors acknowledge the contributions of the Center for HIV/AIDS Vaccine Immunology (CHAVI) Clinical Core Team for recruiting study participants and carrying out all aspects of the CHAVI001 and CHAVI008 protocols at University of North Carolina at Chapel Hill, North Carolina (Joseph Eron); Duke University, Durham, NC (Charles Hicks); Blantyre, Malawi (Johnstone Kumwenda, Taha Taha); University of North Carolina Center at Lilongwe, Malawi (Irving Hoffman, Gift Kaminga); University of the Witwatersrand, Johannesburg, South Africa (Helen Rees); University of KwaZulu-Natal, Durban, South Africa (Salim Abdool Karim); Kilimanjaro Christian Medical Center, Moshi, Tanzania (Sam Noel, Saidi Kapiga, John Crump); Imperial College, London, UK (Sarah Fidler); and also of the team at the Mortimer Market Center, London, UK (Ian Williams, Pierre Pellegrino) who recruited additional HIV-1-infected individuals. We thank Fangping Cai for expert technical support. Support for this work was provided by grants from the NIH, NIAID, Division of AIDS, UM-1 grant for the Duke Center for HIV/AIDS Vaccine Immunology-Immunogen Discovery AI100645, National Institutes of Health grants R21-AI100696, CHAVI-AI0678501 and MRC Programme grant MR/K012037.

Author Contributions

BFH conceived and designed the study, oversaw and directed autoreactivity and plasma protein binding assays, evaluated all data, wrote the paper; IPP developed methods for and

performed flow analysis of CD4⁺ T cell subsets, contributed to data analysis; NAV performed all statistical analysis in the paper, edited the paper; CC developed methods for and performed flow analysis of CD4⁺ T cell subsets; KEL performed autoreactivity and plasma protein binding assays; RP performed autoreactivity and plasma protein binding assays; KAS managed programmatic aspects of the study including sample annotation and cohort analysis; MSC led the team that acquired the samples in Cohort A; HXL provided recombinant protein reagents for plasma binding assays; FG performed clade typing of HIV-1; AJM designed experiments and evaluated CD4⁺ T cell flow data; DCM performed neutralization assays; LV designed experiments and evaluated data; GK designed experiments, evaluated data, and edited the paper; JH screened, recruited, and performed neutralization assays on Cohort B; PRS performed the exome sequencing study and association analysis; MC provided samples for Cohort B, wrote and edited the paper; PB designed and directed the CD4⁺ T cell subset analyses, evaluated all data, wrote and edited the paper; and MAM designed the study, wrote and edited the paper, and analyzed all data.



447

448 **Figure 1.** Neutralization and autoantibody testing of HIV-1-infected individuals. HIV-1
 449 neutralization data are shown as geometric mean titer for a panel of isolates for Cohort A
 450 (A) and B (B). Individuals with the highest (bnAb) and lowest (Control) HIV-1 neutralization
 451 for each cohort were tested in autoantibody assays. **Panels C and D** compare the

452 frequency of individuals in the bnAb and control groups with any positive result for
453 Cohorts A and B, respectively. The number of positive autoantibody results is shown for
454 Cohort A (**panel E**) and B (**panel F**).

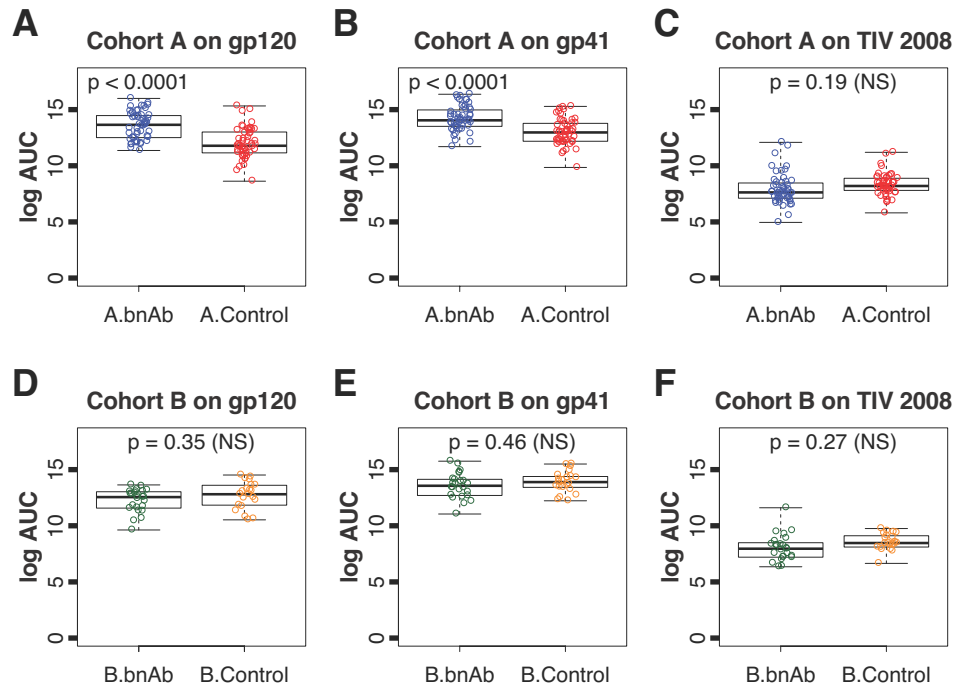


Figure 2. Comparison of plasma antibody responses. When compared with the A.Control group, the A.bnAb group had higher binding to HIV-1 Env gp120 (A) and gp41 (B) but similar binding (C) to trivalent inactivated influenza vaccine for 2008 (TIV 2008). Binding was similar between the B.bnAb and B.Control groups for the same three antigens (D – F). Each symbol represents data from an individual subject; group medians, range, and quartiles are shown.

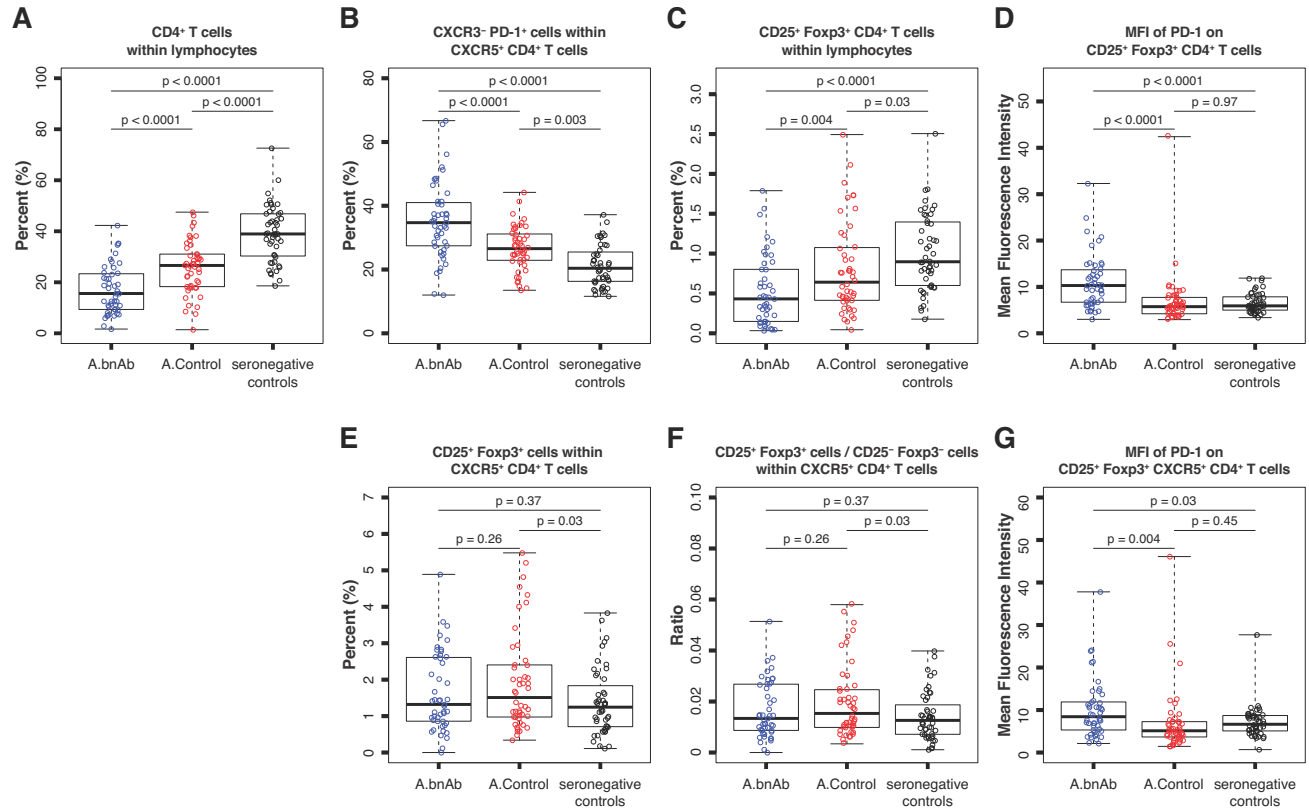


Figure 3. T cell subsets in Cohort A subjects with and without bnAbs and matched HIV-1-seronegative controls. Total CD4⁺ T cell frequency within lymphocytes was lower in Cohort A HIV-1-infected individuals vs. HIV-1-seronegative controls and was lowest in the A.bnAb group (A). Resting memory T follicular helper (mTfh) cells were elevated in Cohort A HIV-1-infected individuals vs. HIV-seronegative controls, and were highest in the A.bnAb group (B). CD4⁺ Treg cell frequency was lowest in the A.bnAb group (C). PD-1 MFI on CD4⁺ Treg cells was highest in the A.bnAb group (D). The proportion of Tfr cells within circulating CD4⁺ follicular-phenotype T cells in the A.bnAb group did not differ significantly from that in the A.Control or seronegative groups (E). The Tfr/Tfh ratio, defined as

$$\text{Tfr} / \text{Tfh} = \frac{\% \text{ CD25}^+ \text{ Foxp3}^+ \text{ cells within CXCR5}^+ \text{ CD4}^+ \text{ T cells}}{\% \text{ non-CD25}^+ \text{ Foxp3}^+ \text{ cells within CXCR5}^+ \text{ CD4}^+ \text{ T cells}}$$

in the A.bnAb group did not differ significantly from that in the A.Control or seronegative groups (F). The MFI of PD-1 staining on CD4⁺ Tfr cells was highest in the A.bnAb group (G). Each symbol represents data from an individual subject; group medians, range, and quartiles are shown.

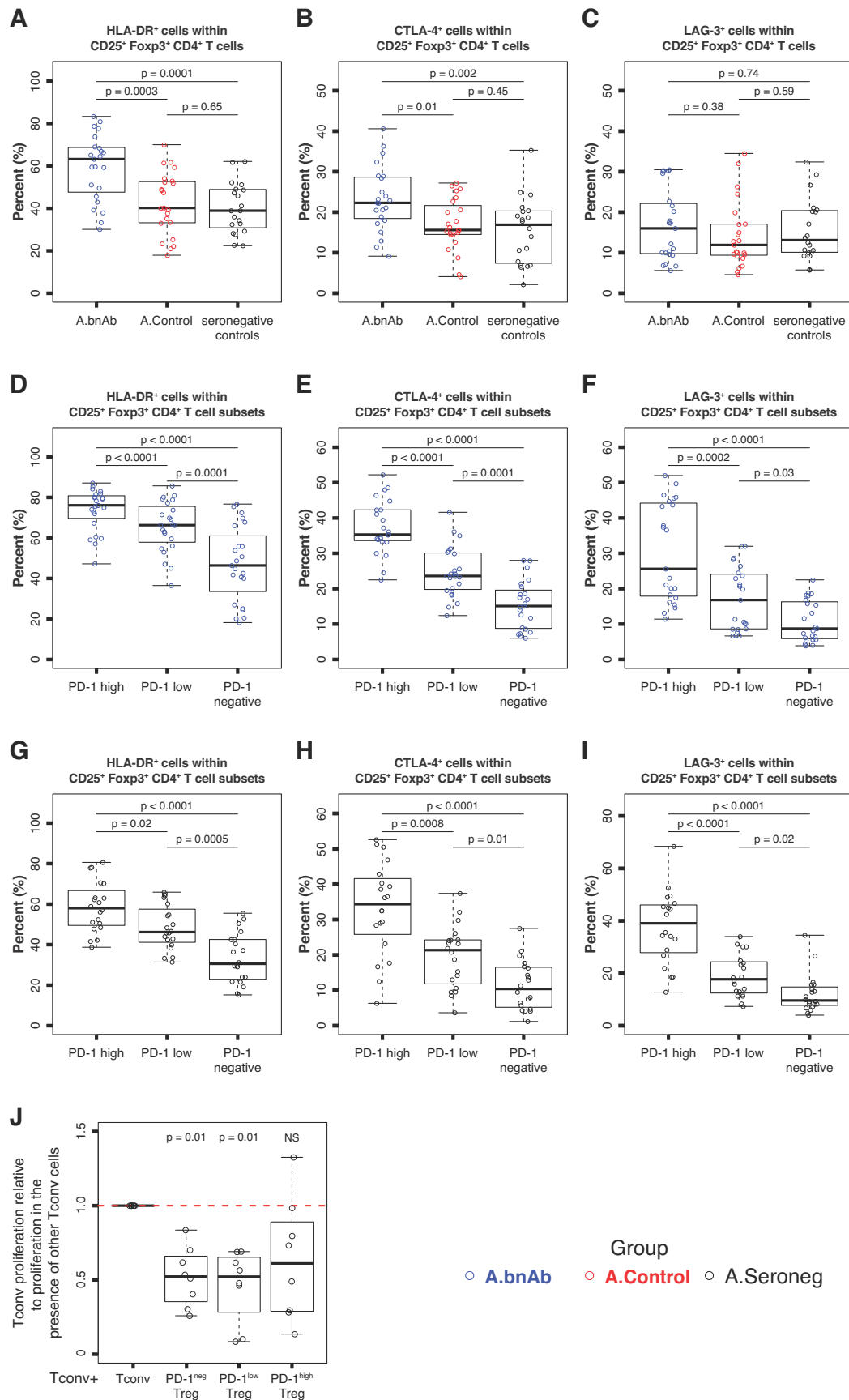


Figure 4. Phenotypic and functional analysis of CD4⁺ Treg cells. CD4⁺ Treg cells expressing HLA-DR were higher in the A.bnAb group vs. the A.Control or seronegative groups (**A**). Total CD4⁺ Treg cells expressing CTLA-4 were also higher in the A.bnAb group vs. the A.Control or seronegative groups (**B**); no difference between groups was found for CD4⁺ Treg cells expressing LAG-3 (**C**). In the A.bnAb group, the PD-1^{high} subset of CD4⁺ Treg cells expressed higher levels of HLA-DR (**D**), CTLA-4 (**E**) and LAG-3 (**F**) than the PD-1^{low} or PD-1 negative subsets of CD4⁺ Treg cells. The results were similar for the HIV-1 seronegative control group (**G**, **H** and **I**). In panels **A-I**, symbols represent individual subjects; group medians, range, and quartiles are shown. In experiments performed with samples from healthy HIV-1-seronegative UK donors, PD-1 negative and PD-1^{low} CD4⁺ Treg cells suppressed the proliferation of conventional CD4⁺ T cells (Tconv) compared to that observed in the presence of other conventional CD4⁺ T cells, whereas PD-1^{high} CD4⁺ Treg cells did not do so (**J**). In panel **J**, the symbols represent individual subjects; group medians, range and quartiles are shown; and the horizontal dashed red line indicates the level of proliferation of conventional CD4⁺ T cells in the presence of other conventional CD4⁺ T cells to which other values were normalized.

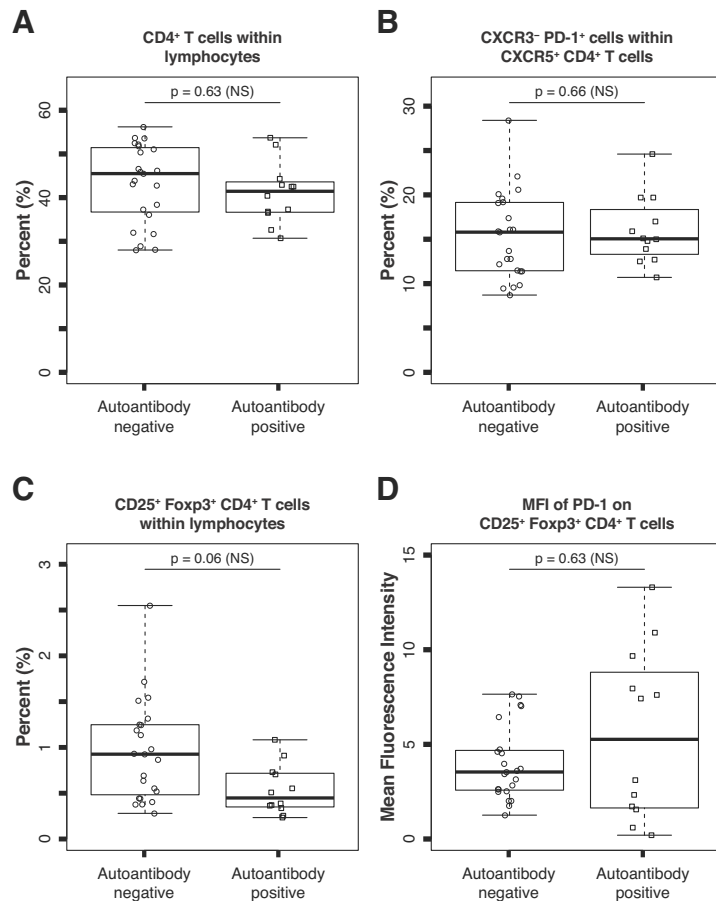


Figure 5. T cell subsets in healthy, HIV-1-seronegative African individuals with and without autoantibodies. HIV-1-seronegative subjects with and without autoantibodies had similar frequencies of total CD4⁺ T cells within lymphocytes (**A**). The circulating frequency of resting memory T follicular helper (mTfh) cells was similar in HIV-1-seronegative individuals with and without autoantibodies (**B**). CD4⁺ Treg cell frequency within lymphocytes in HIV-1-seronegative individuals with autoantibodies did not differ significantly from that in those without autoantibodies (**C**). PD-1 MFI on CD4⁺ Treg cells in HIV-1-seronegative individuals with autoantibodies did not differ significantly from that in those without autoantibodies (**D**). In all panels, each symbol represents data from an individual subject; group medians, range, and quartiles are shown.

References

1. A. S. Fauci, H. D. Marston, Ending AIDS--is an HIV vaccine necessary? *N Engl J Med* **370**, 495–498 (2014).
2. J. R. Mascola, B. F. Haynes, HIV-1 neutralizing antibodies: understanding nature's pathways, *Immunol Rev* **254**, 225–244 (2013).
3. D. R. Burton, J. R. Mascola, Antibody responses to envelope glycoproteins in HIV-1 infection, *Nat Immunol* **16**, 571–576 (2015).
4. S. Rerks-Ngarm, P. Pitisuttithum, S. Nitayaphan, J. Kaewkungwal, J. Chiu, R. Paris, N. Premisri, C. Namwat, M. de Souza, E. Adams, M. Benenson, S. Gurunathan, J. Tartaglia, J. G. McNeil, D. P. Francis, D. Stablein, D. L. Birx, S. Chunsuttiwat, C. Khamboonruang, P. Thongcharoen, M. L. Robb, N. L. Michael, P. Kunasol, J. H. Kim, Vaccination with ALVAC and AIDSVAX to Prevent HIV-1 Infection in Thailand, *N Engl J Med* **361**, 2209–2220 (2009).
5. D. C. Montefiori, C. Karnasuta, Y. Huang, H. Ahmed, P. Gilbert, M. S. de Souza, R. mclinden, S. Tovanabutra, A. Laurence-Chenine, E. Sanders-Buell, M. A. Moody, M. Bonsignori, C. Ochsenbauer, J. Kappes, H. Tang, K. Greene, H. Gao, C. C. Labranche, C. Andrews, V. R. Polonis, S. Rerks-Ngarm, P. Pitisuttithum, S. Nitayaphan, J. Kaewkungwal, S. G. Self, P. W. Berman, D. Francis, F. Sinangil, C. Lee, J. Tartaglia, M. L. Robb, B. F. Haynes, N. L. Michael, J. H. Kim, Magnitude and breadth of the neutralizing antibody response in the RV144 and Vax003 HIV-1 vaccine efficacy trials, *Journal of Infectious Diseases* **206**, 431–441 (2012).
6. S. M. Hammer, M. E. Sobieszczyk, H. Janes, S. T. Karuna, M. J. Mulligan, D. Grove, B. A. Koblin, S. P. Buchbinder, M. C. Keefer, G. D. Tomaras, N. Frahm, J. Hural, C. Anude, B. S. Graham, M. E. Enama, E. Adams, E. DeJesus, R. M. Novak, I. Frank, C. Bentley, S. Ramirez, R. Fu, R. A. Koup, J. R. Mascola, G. J. Nabel, D. C. Montefiori, J. Kublin, M. J. McElrath, L. Corey, P. B. Gilbert, HVTN 505 Study Team, Efficacy trial of a DNA/rAd5 HIV-1 preventive vaccine, *N Engl J Med* **369**, 2083–2092 (2013).
7. P. Hraber, M. S. Seaman, R. T. Bailer, J. R. Mascola, D. C. Montefiori, B. T. Korber, Prevalence of broadly neutralizing antibody responses during chronic HIV-1 infection, *AIDS* **28**, 163–169 (2014).
8. N. A. Doria-Rose, R. M. Klein, M. G. Daniels, S. O'Dell, M. Nason, A. Lapedes, T. Bhattacharya, S. A. Migueles, R. T. Wyatt, B. T. Korber, J. R. Mascola, M. Connors, Breadth of human immunodeficiency virus-specific neutralizing activity in sera: clustering analysis and association with clinical variables, *J Virol* **84**, 1631–1636 (2010).
9. D. N. Sather, J. Armann, L. K. Ching, A. Mavrantoni, G. Sellhorn, Z. Caldwell, X. Yu, B. Wood, S. Self, S. Kalams, L. Stamatatos, Factors associated with the development of cross-reactive neutralizing antibodies during human immunodeficiency virus type 1

infection, *J Virol* **83**, 757–769 (2009).

10. L. M. Walker, M. D. Simek, F. Priddy, J. S. Gach, D. Wagner, M. B. Zwick, S. K. Phogat, P. Poignard, D. R. Burton, A limited number of antibody specificities mediate broad and potent serum neutralization in selected HIV-1 infected individuals, *PLoS Pathog* **6**, e1001028 (2010).

11. E. S. Gray, M. C. Madiga, T. Hermanus, P. L. Moore, C. K. Wibmer, N. L. Tumba, L. Werner, K. Mlisana, S. Sibeko, C. Williamson, S. S. Abdool Karim, L. Morris, and the CAPRISA002 Study Team, The Neutralization Breadth of HIV-1 Develops Incrementally over Four Years and Is Associated with CD4+ T Cell Decline and High Viral Load during Acute Infection, *J Virol* **85**, 4828–4840 (2011).

12. B. F. Haynes, L. Verkoczy, AIDS/HIV. Host controls of HIV neutralizing antibodies, *Science* **344**, 588–589 (2014).

13. B. F. Haynes, Cardiolipin Polyspecific Autoreactivity in Two Broadly Neutralizing HIV-1 Antibodies, *Science* **308**, 1906–1908 (2005).

14. H. Mouquet, J. F. Scheid, M. J. Zoller, M. Krogsgaard, R. G. Ott, S. Shukair, M. N. Artyomov, J. Pietzsch, M. Connors, F. Pereyra, B. D. Walker, D. D. Ho, P. C. Wilson, M. S. Seaman, H. N. Eisen, A. K. Chakraborty, T. J. Hope, J. V. Ravetch, H. Wardemann, M. C. Nussenzweig, Polyreactivity increases the apparent affinity of anti-HIV antibodies by heterologation, *Nature* **467**, 591–595 (2010).

15. B. F. Haynes, M. A. Moody, L. Verkoczy, G. Kelsoe, S. M. Alam, Antibody polyspecificity and neutralization of HIV-1: a hypothesis, *Hum Antibodies* **14**, 59–67 (2005).

16. B. F. Haynes, G. Kelsoe, S. C. Harrison, T. B. Kepler, B-cell-lineage immunogen design in vaccine development with HIV-1 as a case study, *Nat. Biotechnol.* **30**, 423–433 (2012).

17. F. D. Batista, M. S. Neuberger, Affinity dependence of the B cell response to antigen: a threshold, a ceiling, and the importance of off-rate, *Immunity* **8**, 751–759 (1998).

18. J. Zhang, E. I. Shakhnovich, A. K. Chakraborty, Ed. Optimality of mutation and selection in germinal centers, *PLoS Comput. Biol.* **6**, e1000800 (2010).

19. T. B. Kepler, A. S. Perelson, Somatic hypermutation in B cells: an optimal control treatment, *J Theor Biol* **164**, 37–64 (1993).

20. C. Chen, Z. Nagy, M. Z. Radic, R. R. Hardy, D. Huszar, S. A. Camper, M. Weigert, The site and stage of anti-DNA B-cell deletion, *Nature* **373**, 252–255 (1995).

21. L. Verkoczy, M. Diaz, T. M. Holl, Y.-B. Ouyang, H. Bouton-Verville, S. M. Alam, G. Kelsoe, B. F. Haynes, Autoreactivity in an HIV-1 broadly reactive neutralizing antibody variable region heavy chain induces immunologic tolerance, *Proceedings of the National Academy of Sciences* **107**, 181–186 (2010).

- 582 22. L. Verkoczy, Y. Chen, H. Bouton-Verville, J. Zhang, M. Diaz, J. Hutchinson, Y.-B.
583 Ouyang, S. M. Alam, T. M. Holl, K.-K. Hwang, G. Kelsoe, B. F. Haynes, Rescue of HIV-1
584 broad neutralizing antibody-expressing B cells in 2F5 VH x VL knockin mice reveals
585 multiple tolerance controls, **187**, 3785–3797 (2011).
- 586 23. L. Verkoczy, Y. Chen, J. Zhang, H. Bouton-Verville, A. Newman, B. Lockwood, R. M.
587 Scearce, D. C. Montefiori, S. M. Dennison, S.-M. Xia, K.-K. Hwang, S. M. Alam, B. F.
588 Haynes, Induction of HIV-1 broad neutralizing antibodies in 2F5 knock-in mice: selection
589 against membrane proximal external region-associated autoreactivity limits T-dependent
590 responses, **191**, 2538–2550 (2013).
- 591 24. Y. Chen, J. Zhang, K.-K. Hwang, H. Bouton-Verville, S.-M. Xia, A. Newman, Y.-B.
592 Ouyang, B. F. Haynes, L. Verkoczy, Common tolerance mechanisms, but distinct cross-
593 reactivities associated with gp41 and lipids, limit production of HIV-1 broad neutralizing
594 antibodies 2F5 and 4E10, *J. Immunol.* **191**, 1260–1275 (2013).
- 595 25. S. Shiokawa, F. Mortari, J. O. Lima, C. Nuñez, F. E. Bertrand, P. M. Kirkham, S. Zhu,
596 A. P. Dasanayake, H. W. Schroeder, IgM heavy chain complementarity-determining region
597 3 diversity is constrained by genetic and somatic mechanisms until two months after birth,
598 **162**, 6060–6070 (1999).
- 599 26. E. Meffre, M. Milili, C. Blanco-Betancourt, H. Antunes, M. C. Nussenzweig, C. Schiff,
600 Immunoglobulin heavy chain expression shapes the B cell receptor repertoire in human B
601 cell development, *J Clin Invest* **108**, 879–886 (2001).
- 602 27. R. T. Canoso, L. I. Zon, J. E. Groopman, Anticardiolipin antibodies associated with
603 HTLV-III infection, *Br. J. Haematol.* **65**, 495–498 (1987).
- 604 28. R. G. Kopelman, S. Zolla-Pazner, Association of human immunodeficiency virus
605 infection and autoimmune phenomena, *Am J Med* **84**, 82–88 (1988).
- 606 29. W. J. Morrow, D. A. Isenberg, R. E. Sobol, R. B. Stricker, T. Kieber-Emmons, AIDS
607 virus infection and autoimmunity: a perspective of the clinical, immunological, and
608 molecular origins of the autoallergic pathologies associated with HIV disease, *Clin.*
609 *Immunol. Immunopathol.* **58**, 163–180 (1991).
- 610 30. G. Zandman-Goddard, Y. Shoenfeld, HIV and autoimmunity, *Autoimmun Rev* **1**, 329–
611 337 (2002).
- 612 31. J. D. Reveille, The changing spectrum of rheumatic disease in human
613 immunodeficiency virus infection, *Semin Arthritis Rheum* **30**, 147–166 (2000).
- 614 32. D. Sène, J.-C. Piette, P. Cacoub, Antiphospholipid antibodies, antiphospholipid
615 syndrome and infections, *Autoimmun Rev* **7**, 272–277 (2008).
- 616 33. L. Iordache, O. Launay, O. Bouchaud, V. Jeantils, C. Goujard, F. Boue, P. Cacoub, T.
617 Hanslik, A. Mahr, O. Lambotte, O. Fain, Associated authors, Autoimmune diseases in HIV-
618 infected patients: 52 cases and literature review, *Autoimmun Rev* **13**, 850–857 (2014).

- 619 34. M. Locci, C. Havenar-Daughton, E. Landais, J. Wu, M. A. Kroenke, C. L. Arlehamn, L.
620 F. Su, R. Cubas, M. M. Davis, A. Sette, E. K. Haddad, A. V. I. P. C. P. I. International, P.
621 Poignard, S. Crotty, Human circulating PD-1+CXCR3-CXCR5+ memory Tfh cells are highly
622 functional and correlate with broadly neutralizing HIV antibody responses, *Immunity* **39**,
623 758–769 (2013).
- 624 35. J. B. Wing, S. Sakaguchi, Foxp3⁺ T(reg) cells in humoral immunity, *Int Immunol* **26**, 61–
625 69 (2014).
- 626 36. H. W. Lim, P. Hillsamer, C. H. Kim, Regulatory T cells can migrate to follicles upon T
627 cell activation and suppress GC-Th cells and GC-Th cell-driven B cell responses, *J Clin*
628 *Invest* **114**, 1640–1649 (2004).
- 629 37. Y. Chung, S. Tanaka, F. Chu, R. I. Nurieva, G. J. Martinez, S. Rawal, Y.-H. Wang, H.
630 Lim, J. M. Reynolds, X.-H. Zhou, H.-M. Fan, Z.-M. Liu, S. S. Neelapu, C. Dong, Follicular
631 regulatory T cells expressing Foxp3 and Bcl-6 suppress germinal center reactions, *Nat Med*
632 **17**, 983–988 (2011).
- 633 38. M. A. Linterman, W. Pierson, S. K. Lee, A. Kallies, S. Kawamoto, T. F. Rayner, M.
634 Srivastava, D. P. Divekar, L. Beaton, J. J. Hogan, S. Fagarasan, A. Liston, K. G. C. Smith,
635 C. G. Vinuesa, Foxp3⁺ follicular regulatory T cells control the germinal center response,
636 *Nat Med* **17**, 975–982 (2011).
- 637 39. I. Wollenberg, A. Agua-Doce, A. Hernández, C. Almeida, V. G. Oliveira, J. Faro, L.
638 Graca, Regulation of the germinal center reaction by Foxp3⁺ follicular regulatory T cells, *J.*
639 *Immunol.* **187**, 4553–4560 (2011).
- 640 40. P. T. Sage, A. M. Paterson, S. B. Lovitch, A. H. Sharpe, The coinhibitory receptor
641 CTLA-4 controls B cell responses by modulating T follicular helper, T follicular regulatory,
642 and T regulatory cells, *Immunity* **41**, 1026–1039 (2014).
- 643 41. P. T. Sage, L. M. Francisco, C. V. Carman, A. H. Sharpe, The receptor PD-1 controls
644 follicular regulatory T cells in the lymph nodes and blood, *Nat Immunol* **14**, 152–161 (2013).
- 645 42. J. B. Wing, W. Ise, T. Kurosaki, S. Sakaguchi, Regulatory T cells control antigen-
646 specific expansion of Tfh cell number and humoral immune responses via the coreceptor
647 CTLA-4, *Immunity* **41**, 1013–1025 (2014).
- 648 43. H. C. Lane, H. Masur, L. C. Edgar, G. Whalen, A. H. Rook, A. S. Fauci, Abnormalities
649 of B-cell activation and immunoregulation in patients with the acquired immunodeficiency
650 syndrome, *N Engl J Med* **309**, 453–458 (1983).
- 651 44. S. Sakaguchi, M. Ono, R. Setoguchi, H. Yagi, S. Hori, Z. Fehervari, J. Shimizu, T.
652 Takahashi, T. Nomura, Foxp3⁺ CD25⁺ CD4⁺ natural regulatory T cells in dominant self-
653 tolerance and autoimmune disease, *Immunol Rev* **212**, 8–27 (2006).
- 654 45. N. Ohkura, Y. Kitagawa, S. Sakaguchi, Development and maintenance of regulatory T
655 cells, *Immunity* **38**, 414–423 (2013).

656 46. R. Morita, N. Schmitt, S.-E. Bentebibel, R. Ranganathan, L. Bourdery, G. Zurawski, E.
657 Foucat, M. Dullaers, S. Oh, N. Sabzghabaei, E. M. Lavecchio, M. Punaro, V. Pascual, J.
658 Banachereau, H. Ueno, Human Blood CXCR5+CD4+ T Cells Are Counterparts of T
659 Follicular Cells and Contain Specific Subsets that Differentially Support Antibody Secretion,
660 *Immunity* **34**, 108–121 (2011).

661 47. C. S. Ma, E. K. Deenick, M. Batten, S. G. Tangye, The origins, function, and regulation
662 of T follicular helper cells, *Journal of Experimental Medicine* **209**, 1241–1253 (2012).

663 48. N. Simpson, P. A. Gatenby, A. Wilson, S. Malik, D. A. Fulcher, S. G. Tangye, H. Manku,
664 T. J. Vyse, G. Roncador, G. A. Huttley, C. C. Goodnow, C. G. Vinuesa, M. C. Cook,
665 Expansion of circulating T cells resembling follicular helper T cells is a fixed phenotype that
666 identifies a subset of severe systemic lupus erythematosus, *62*, 234–244 (2010).

667 49. V. Velu, R. D. Shetty, M. Larsson, E. M. Shankar, Role of PD-1 co-inhibitory pathway in
668 HIV infection and potential therapeutic options, *Retrovirology* **12**, 14 (2015).

669 50. E. Giancchetti, D. V. Delfino, A. Fierabracci, Recent insights into the role of the PD-
670 1/PD-L1 pathway in immunological tolerance and autoimmunity, *Autoimmun Rev* **12**, 1091–
671 1100 (2013).

672 51. J.-H. Chang, Y. Chung, Regulatory T cells in B cell follicles, *Immune Netw* **14**, 227–236
673 (2014).

674 52. P. T. Sage, A. H. Sharpe, T follicular regulatory cells in the regulation of B cell
675 responses, *Trends in Immunology* **36**, 410–418 (2015).

676 53. P. T. Sage, D. Alvarez, J. Godec, U. H. von Andrian, A. H. Sharpe, Circulating T
677 follicular regulatory and helper cells have memory-like properties, *J Clin Invest* **124**, 5191–
678 5204 (2014).

679 54. Y. Wei, J. Feng, Z. Hou, X. M. Wang, D. Yu, in *T follicular Helper Cells*, Methods in
680 Molecular Biology. (Springer New York, New York, NY, 2015), vol. 1291, pp. 199–207.

681 55. L. Wang, J. Qiu, L. Yu, X. Hu, P. Zhao, Y. Jiang, Increased numbers of
682 CD5+CD19+CD1dhighIL-10+ Bregs, CD4+Foxp3+ Tregs, CD4+CXCR5+Foxp3+ follicular
683 regulatory T (TFR) cells in CHB or CHC patients, *J Transl Med* **12**, 4178 (2014).

684 56. A. Crawford, J. M. Angelosanto, C. Kao, T. A. Doering, P. M. Odorizzi, B. E. Barnett, E.
685 J. Wherry, Molecular and transcriptional basis of CD4+ T cell dysfunction during chronic
686 infection, *Immunity* **40**, 289–302 (2014).

687 57. A. M. Thornton, C. A. Piccirillo, E. M. Shevach, Activation requirements for the induction
688 of CD4+CD25+ T cell suppressor function, *Eur J Immunol* **34**, 366–376 (2004).

689 58. C.-T. Huang, C. J. Workman, D. Flies, X. Pan, A. L. Marson, G. Zhou, E. L. Hipkiss, S.
690 Ravi, J. Kowalski, H. I. Levitsky, J. D. Powell, D. M. Pardoll, C. G. Drake, D. A. A. Vignali,
691 Role of LAG-3 in regulatory T cells, *Immunity* **21**, 503–513 (2004).

59. International MHC and Autoimmunity Genetics Network, J. D. Rioux, P. Goyette, T. J. Vyse, L. Hammarström, M. M. A. Fernando, T. Green, P. L. De Jager, S. Foisy, J. Wang, P. I. W. de Bakker, S. Leslie, G. McVean, L. Padyukov, L. Alfredsson, V. Annese, D. A. Hafler, Q. Pan-Hammarström, R. Matell, S. J. Sawcer, A. D. Compston, B. A. C. Cree, D. B. Mirel, M. J. Daly, T. W. Behrens, L. Klareskog, P. K. Gregersen, J. R. Oksenberg, S. L. Hauser, Mapping of multiple susceptibility variants within the MHC region for 7 immune-mediated diseases, *Proceedings of the National Academy of Sciences* **106**, 18680–18685 (2009).
60. J. D. Lifson, M. J. Piatak, J. L. Rossio, J. J. Bess, E. Chertova, D. Schneider, R. Kiser, V. Coalter, B. Poore, R. Imming, R. C. Desrosiers, L. E. Henderson, L. O. Arthur, Whole inactivated SIV virion vaccines with functional envelope glycoproteins: safety, immunogenicity, and activity against intrarectal challenge, *J. Med. Primatol.* **31**, 205–216 (2002).
61. J. D. Lifson, J. L. Rossio, M. Piatak, J. Bess, E. Chertova, D. K. Schneider, V. J. Coalter, B. Poore, R. F. Kiser, R. J. Imming, A. J. Scarzello, L. E. Henderson, W. G. Alvord, V. M. Hirsch, R. E. Benveniste, L. O. Arthur, Evaluation of the safety, immunogenicity, and protective efficacy of whole inactivated simian immunodeficiency virus (SIV) vaccines with conformationally and functionally intact envelope glycoproteins, *AIDS Res Hum Retroviruses* **20**, 772–787 (2004).
62. T. Tong, E. T. Crooks, K. Osawa, J. E. Robinson, M. Barnes, C. Apetrei, J. M. Binley, Multi-parameter exploration of HIV-1 virus-like particles as neutralizing antibody immunogens in guinea pigs, rabbits and macaques, *Virology* **456–457**, 55–69 (2014).
63. R. L. Willey, R. Byrum, M. Piatak, Y. B. Kim, M. W. Cho, J. L. Rossio, J. Bess, T. Igarashi, Y. Endo, L. O. Arthur, J. D. Lifson, M. A. Martin, Control of viremia and prevention of simian-human immunodeficiency virus-induced disease in rhesus macaques immunized with recombinant vaccinia viruses plus inactivated simian immunodeficiency virus and human immunodeficiency virus type 1 particles, *J Virol* **77**, 1163–1174 (2003).
64. J. M. Kovacs, J. P. Nkolola, H. Peng, A. Cheung, J. Perry, C. A. Miller, M. S. Seaman, D. H. Barouch, B. Chen, HIV-1 envelope trimer elicits more potent neutralizing antibody responses than monomeric gp120, *Proceedings of the National Academy of Sciences* **109**, 12111–12116 (2012).
65. C. A. Bricault, J. M. Kovacs, J. P. Nkolola, K. Yusim, E. E. Giorgi, J. L. Shields, J. Perry, C. L. Lavine, A. Cheung, K. Ellingson-Strouss, C. Rademeyer, G. E. Gray, C. Williamson, L. Stamatatos, M. S. Seaman, B. T. Korber, B. Chen, D. H. Barouch, G. Silvestri, Ed. A multivalent clade C HIV-1 Env trimer cocktail elicits a higher magnitude of neutralizing antibodies than any individual component, *J Virol* **89**, 2507–2519 (2015).
66. R. W. Sanders, M. J. van Gils, R. Derking, D. Sok, T. J. Ketas, J. A. Burger, G. Ozorowski, A. Cupo, C. Simonich, L. Goo, H. Arendt, H. J. Kim, J.-H. Lee, P. Pugach, M. Williams, G. Debnath, B. Moldt, M. J. van Breemen, G. Isik, M. Medina-Ramírez, J. W. Back, W. C. Koff, J.-P. Julien, E. G. Rakasz, M. S. Seaman, M. Guttman, K. K. Lee, P. J. Klasse, C. Labranche, W. R. Schief, I. A. Wilson, J. Overbaugh, D. R. Burton, A. B. Ward,

732 D. C. Montefiori, H. Dean, J. P. Moore, HIV-1 VACCINES. HIV-1 neutralizing antibodies
733 induced by native-like envelope trimers, *Science* **349**, aac4223–aac4223 (2015).

734 67. E. S. Gray, N. Taylor, D. Wycuff, P. L. Moore, G. D. Tomaras, C. K. Wibmer, A. Puren,
735 A. DeCamp, P. B. Gilbert, B. Wood, D. C. Montefiori, J. M. Binley, G. M. Shaw, B. F.
736 Haynes, J. R. Mascola, L. Morris, Antibody specificities associated with neutralization
737 breadth in plasma from human immunodeficiency virus type 1 subtype C-infected blood
738 donors, *J Virol* **83**, 8925–8937 (2009).

739 68. The INSIGHT START Study Group, Initiation of Antiretroviral Therapy in Early
740 Asymptomatic HIV Infection, *N Engl J Med* **373**, 795–807 (2015).

741 69. T. H. Finkel, G. Tudor-Williams, N. K. Banda, M. F. Cotton, T. Curiel, C. Monks, T. W.
742 Baba, R. M. Ruprecht, A. Kupfer, Apoptosis occurs predominantly in bystander cells and
743 not in productively infected cells of HIV- and SIV-infected lymph nodes, *Nat Med* **1**, 129–
744 134 (1995).

745 70. M. F. Chevalier, L. Weiss, The split personality of regulatory T cells in HIV infection,
746 *Blood* **121**, 29–37 (2013).

747 71. P. L. Moore, C. Williamson, L. Morris, Virological features associated with the
748 development of broadly neutralizing antibodies to HIV-1, *Trends Microbiol* **23**, 204–211
749 (2015).

750 72. S. Crotty, T follicular helper cell differentiation, function, and roles in disease, *Immunity*
751 **41**, 529–542 (2014).

752 73. J. A. Harker, G. M. Lewis, L. Mack, E. I. Zuniga, Late interleukin-6 escalates T follicular
753 helper cell responses and controls a chronic viral infection, *Science* **334**, 825–829 (2011).

754 74. L. M. Fahey, E. B. Wilson, H. Elsaesser, C. D. Fistonich, D. B. McGavern, D. G.
755 Brooks, Viral persistence redirects CD4 T cell differentiation toward T follicular helper cells,
756 *J Exp Med* **208**, 987–999 (2011).

757 75. M. Lindqvist, J. van Lunzen, D. Z. Soghoian, B. D. Kuhl, S. Ranasinghe, G. Kranias, M.
758 D. Flanders, S. Cutler, N. Yudanin, M. I. Muller, I. Davis, D. Farber, P. Hartjen, F. Haag, G.
759 Alter, J. Schulze zur Wiesch, H. Streeck, Expansion of HIV-specific T follicular helper cells
760 in chronic HIV infection, *J Clin Invest* **122**, 3271–3280 (2012).

761 76. M. Perreau, A.-L. Savoye, E. De Crignis, J.-M. Corpataux, R. Cubas, E. K. Haddad, L.
762 De Leval, C. Graziosi, G. Pantaleo, Follicular helper T cells serve as the major CD4 T cell
763 compartment for HIV-1 infection, replication, and production, *Journal of Experimental*
764 *Medicine* **210**, 143–156 (2013).

765 77. R. A. Cubas, J. C. Mudd, A.-L. Savoye, M. Perreau, J. van Grevenynghe, T. Metcalf, E.
766 Connick, A. Meditz, G. J. Freeman, G. Abesada-Terk, J. M. Jacobson, A. D. Brooks, S.
767 Crotty, J. D. Estes, G. Pantaleo, M. M. Lederman, E. K. Haddad, Inadequate T follicular cell
768 help impairs B cell immunity during HIV infection, *Nat Med* **19**, 494–499 (2013).

769 78. K. Cohen, M. Altfeld, G. Alter, L. Stamatatos, Early preservation of CXCR5+ PD-1+
770 helper T cells and B cell activation predict the breadth of neutralizing antibody responses in
771 chronic HIV-1 infection, *J Virol* **88**, 13310–13321 (2014).

772 79. A. Chowdhury, P. M. Del Rio Estrada, P. M. E. Del Rio, G. K. Tharp, R. P. Tribble, R. R.
773 Amara, A. Chahroudi, G. Reyes-Teran, S. E. Bosinger, G. Silvestri, Decreased T Follicular
774 Regulatory Cell/T Follicular Helper Cell (TFH) in Simian Immunodeficiency Virus-Infected
775 Rhesus Macaques May Contribute to Accumulation of TFH in Chronic Infection, *J.*
776 *Immunol.* **195**, 3237–3247 (2015).

777 80. B. Miles, S. M. Miller, J. M. Folkvord, A. Kimball, M. Chamanian, A. L. Meditz, T.
778 Arends, M. D. McCarter, D. N. Levy, E. G. Rakasz, P. J. Skinner, E. Connick, Follicular
779 regulatory T cells impair follicular T helper cells in HIV and SIV infection, *Nat Commun* **6**,
780 8608 (2015).

781 81. L. Colineau, A. Rouers, T. Yamamoto, Y. Xu, A. Urrutia, H.-P. Pham, S. Cardinaud, A.
782 Samri, K. Dorgham, P.-G. Coulon, R. Cheynier, A. Hosmalin, E. Oksenhendler, A. Six, A.
783 D. Kelleher, J. Zaunders, R. A. Koup, B. Autran, A. Moris, S. Graff-Dubois, D. Unutmaz, Ed.
784 HIV-Infected Spleens Present Altered Follicular Helper T Cell (Tfh) Subsets and Skewed B
785 Cell Maturation, *PLoS ONE* **10**, e0140978 (2015).

786 82. M. Aloulou, E. J. Carr, M. Gador, A. Bignon, R. S. Liblau, N. Fazilleau, M. A. Linterman,
787 Follicular regulatory T cells can be specific for the immunizing antigen and derive from
788 naive T cells, *Nat Commun* **7**, 10579 (2016).

789 83. G. Yang, T. M. Holl, Y. Liu, Y. Li, X. Lu, N. I. Nicely, T. B. Kepler, S. M. Alam, D. W.
790 Cain, L. Spicer, J. L. VandeBerg, B. F. Haynes, G. Kelsoe, Identification of autoantigens
791 recognized by the 2F5 and 4E10 broadly neutralizing HIV-1 antibodies, *Journal of*
792 *Experimental Medicine* **210**, 241–256 (2013).

793 84. L. Verkoczy, M. A. Moody, T. M. Holl, H. Bouton-Verville, R. M. Searce, J. Hutchinson,
794 S. M. Alam, G. Kelsoe, B. F. Haynes, D. Unutmaz, Ed. Functional, non-clonal IgMa-
795 restricted B cell receptor interactions with the HIV-1 envelope gp41 membrane proximal
796 external region, *PLoS ONE* **4**, e7215 (2009).

797 85. C. Doyle-Cooper, K. E. Hudson, A. B. Cooper, T. Ota, P. Skog, P. E. Dawson, M. B.
798 Zwick, W. R. Schief, D. R. Burton, D. Nemazee, Immune tolerance negatively regulates B
799 cells in knock-in mice expressing broadly neutralizing HIV antibody 4E10, *J. Immunol.* **191**,
800 3186–3191 (2013).

801 86. M. Bonsignori, K. Wiehe, S. K. Grimm, R. Lynch, G. Yang, D. M. Kozink, F. Perrin, A. J.
802 Cooper, K.-K. Hwang, X. Chen, M. Liu, K. McKee, R. J. Parks, J. Eudailey, M. Wang, M.
803 Clowse, L. G. Criscione-Schreiber, M. A. Moody, M. E. Ackerman, S. D. Boyd, F. Gao, G.
804 Kelsoe, L. Verkoczy, G. D. Tomaras, T. B. Kepler, D. C. Montefiori, J. R. Mascola, B. F.
805 Haynes, An autoreactive antibody from an SLE/HIV-1 individual broadly neutralizes HIV-1,
806 *J Clin Invest* **124**, 1835–1843 (2014).

807 87. P. Sharma, J. P. Allison, The future of immune checkpoint therapy, *Science* **348**, 56–61

808 (2015).

- 809 88. S. Chakarov, N. Fazilleau, Monocyte-derived dendritic cells promote T follicular helper
810 cell differentiation, *EMBO Mol Med* **6**, 590–603 (2014).
- 811 89. D. C. Rookhuizen, A. L. DeFranco, Toll-like receptor 9 signaling acts on multiple
812 elements of the germinal center to enhance antibody responses, *Proceedings of the*
813 *National Academy of Sciences* **111**, E3224–33 (2014).
- 814 90. H.-X. Liao, R. Lynch, T. Zhou, F. Gao, S. M. Alam, S. D. Boyd, A. Z. Fire, K. M. Roskin,
815 C. A. Schramm, Z. Zhang, J. Zhu, L. Shapiro, NISC Comparative Sequencing Program, J.
816 C. Mullikin, S. Gnanakaran, P. Hraber, K. Wiehe, G. Kelsoe, G. Yang, S.-M. Xia, D. C.
817 Montefiori, R. Parks, K. E. Lloyd, R. M. Searce, K. A. Soderberg, M. Cohen, G. Kamanga,
818 M. K. Louder, L. M. Tran, Y. Chen, F. Cai, S. Chen, S. Moquin, X. Du, M. G. Joyce, S.
819 Srivatsan, B. Zhang, A. Zheng, G. M. Shaw, B. H. Hahn, T. B. Kepler, B. T. M. Korber, P.
820 D. Kwong, J. R. Mascola, B. F. Haynes, Co-evolution of a broadly neutralizing HIV-1
821 antibody and founder virus, *Nature* **496**, 469–476 (2013).
- 822 91. B. S. Briney, J. R. Willis, J. E. Crowe, Y. Hoshino, Ed. Human peripheral blood
823 antibodies with long HCDR3s are established primarily at original recombination using a
824 limited subset of germline genes, *PLoS ONE* **7**, e36750 (2012).
- 825 92. Z. Sabouri, P. Schofield, K. Horikawa, E. Spierings, D. Kipling, K. L. Randall, D.
826 Langley, B. Roome, R. Vazquez-Lombardi, R. Rouet, J. Hermes, T. D. Chan, R. Brink, D.
827 K. Dunn-Walters, D. Christ, C. C. Goodnow, Redemption of autoantibodies on anergic B
828 cells by variable-region glycosylation and mutation away from self-reactivity, *Proceedings*
829 *of the National Academy of Sciences* **111**, E2567–75 (2014).
- 830 93. L. M. Walker, S. K. Phogat, P.-Y. Chan-Hui, D. Wagner, P. Phung, J. L. Goss, T. Wrin,
831 M. D. Simek, S. Fling, J. L. Mitcham, J. K. Lehrman, F. H. Priddy, O. A. Olsen, S. M. Frey,
832 P. W. Hammond, Protocol G Principal Investigators, S. Kaminsky, T. Zamb, M. Moyle, W.
833 C. Koff, P. Poignard, D. R. Burton, Broad and potent neutralizing antibodies from an African
834 donor reveal a new HIV-1 vaccine target, *Science* **326**, 285–289 (2009).
- 835 94. M. Bonsignori, K.-K. Hwang, X. Chen, C.-Y. Tsao, L. Morris, E. Gray, D. J. Marshall, J.
836 A. Crump, S. H. Kapiga, N. E. Sam, F. Sinangil, M. Pancera, Y. Yongping, B. Zhang, J.
837 Zhu, P. D. Kwong, S. O'Dell, J. R. Mascola, L. Wu, G. J. Nabel, S. Phogat, M. S. Seaman,
838 J. F. Whitesides, M. A. Moody, G. Kelsoe, X. Yang, J. Sodroski, G. M. Shaw, D. C.
839 Montefiori, T. B. Kepler, G. D. Tomaras, S. M. Alam, B. F. Haynes, Analysis of a clonal
840 lineage of HIV-1 envelope V2/V3 conformational epitope-specific broadly neutralizing
841 antibodies and their inferred unmutated common ancestors, *J Virol* **85**, 9998–10009 (2011).
- 842 95. A. T. McGuire, A. M. Dreyer, S. Carbonetti, A. Lippy, J. Glenn, J. F. Scheid, H.
843 Mouquet, L. Stamatatos, HIV antibodies. Antigen modification regulates competition of
844 broad and narrow neutralizing HIV antibodies, *Science* **346**, 1380–1383 (2014).
- 845 96. H. Wardemann, S. Yurasov, A. Schaefer, J. W. Young, E. Meffre, M. C. Nussenzweig,
846 Predominant autoantibody production by early human B cell precursors, *Science* **301**,

847 1374–1377 (2003).

848 97. T. Tiller, M. Tsuiji, S. Yurasov, K. Velinzon, M. C. Nussenzweig, H. Wardemann,
849 Autoreactivity in human IgG⁺ memory B cells, *Immunity* **26**, 205–213 (2007).

850

Immune perturbations in HIV-1-infected individuals who make broadly reactive neutralizing antibodies

by

M. Anthony Moody^{1,2,3,#*}, Isabela Pedroza-Pacheco^{4,#}, Nathan A. Vandergrift^{1,5}, Cecilia Chui⁴,
Krissey E. Lloyd¹, Robert Parks¹, Kelly A. Soderberg¹, Ane T. Ogbe⁴, Myron S. Cohen⁶,
Hua-Xin Liao^{1,5}, Feng Gao^{1,5}, Andrew J. McMichael⁴, David C. Montefiori⁷, Laurent Verkoczy^{1,5,8},
Garnett Kelsoe^{1,2}, Jinghe Huang⁹, Patrick R. Shea¹⁰, Mark Connors⁹,
Persephone Borrow^{4*} and Barton F. Haynes^{1,2,5*}

¹Duke University Human Vaccine Institute, Duke University School of Medicine, Durham, NC 27710.

²Department of Immunology, Duke University School of Medicine, Durham, NC 27710.

³Department of Pediatrics, Duke University School of Medicine, Durham, NC 27710.

⁴Nuffield Dept. of Clinical Medicine, University of Oxford, Oxford OX3 7FZ, United Kingdom.

⁵Department of Medicine, Duke University School of Medicine, Durham, NC 27710.

⁶University of North Carolina at Chapel Hill, 27599.

⁷Department of Surgery, Duke University School of Medicine, Durham, NC 27710.

⁸Department of Pathology, Duke University School of Medicine, Durham, NC 27710.

⁹Laboratory of Immunoregulation, NIAID, NIH, Bethesda, MD 20814.

¹⁰Institute for Genomic Medicine, Columbia University, New York, NY 10032.

#co-first authors

Table of Contents

1. Methods	4
1.1. Study Populations	4
1.1.1. African CHAVI Cohort A Selection	4
1.1.1.1. Description of CHAVI Cohort	4
1.1.1.2. Threshold for bnAb Status	5
1.1.1.3. Matching Non-Neutralizers	5
1.1.1.4. Principal Components Analysis of Neutralization Panel	5
1.1.1.5. Distribution of Neutralization Breadth	6
1.1.2. US NIH Cohort B Selection	6
1.2. Antibody Assays	7
1.3. Analysis of CD4 ⁺ T cell subsets	7
1.4. CD4 ⁺ Treg Cell Suppression Assay	9
1.5. HLA Typing	10
1.6. Exome Sequencing	10
1.7. Statistical Analysis	11
1.7.1. Statistical Analyses of Reported Tests	11
1.7.2. Pre-Determined Statistical Plan	12
1.7.3. Analysis Excluding US and UK patients	13
2. Supporting Figures	14
2.1. Figure S1. Eigenvalues and amount of variance explained up to principal component six	14
2.2. Figure S2. Cohort A PC1 scores in descending order	15
2.3. Figure S3. Plots of individual autoantibody assay results	17
2.4. Figure S4. Gating strategy for flow cytometric analysis of T cell subsets	20
2.5. Figure S5. Comparison of Helios expression in CD4 ⁺ Treg cells in Cohort A subjects with and without bnAbs and matched HIV-1-seronegative controls	21
2.6. Figure S6. Comparison of Tfr subsets (as defined using alternative phenotyping strategies) in Cohort A subjects with and without bnAbs and matched HIV-1-seronegative controls	22
3. Supporting Tables	24
3.1. Table S1. Country of origin for Cohort A individuals	24
3.2. Table S2. Cohort A individuals included and excluded from principal components analysis and control group	24
3.3. Table S3. Cohort A bnAb group reciprocal dilution ID50 neutralization results	25
3.4. Table S4. Cohort A Control group reciprocal dilution ID50 neutralization results	26
3.5. Table S5. Cohort A differences between bnAb and Control groups for biological sex	27
3.6. Table S6. Cohort A differences between bnAb and Control groups for country of origin	27
3.7. Table S7. Cohort A differences between bnAb and Control groups	27
3.8. Table S8. Cohort A mean duration individuals were followed	27
3.9. Table S9. Cohort A clade of HIV-1 infection	28
3.10. Table S10. General linear model results for the effect of clade of HIV-1 infection in Cohort A on PC1 score	29
3.11. Table S11. Logistic model results for the effect of clade of HIV-1 infection in Cohort A on the presence of autoantibodies	29

3.12.	Table S12. Poisson model results for the effect of clade of HIV-1 infection in Cohort A on the presence of autoantibodies.	29
3.13.	Table S13. Cohort B bnAb individuals reciprocal dilution ID50 neutralization results.	30
3.14.	Table S14. Cohort B Control individuals reciprocal dilution ID50 neutralization results.	31
3.15.	Table S15. Cohort B differences between bnAb and Control groups for biological sex.	32
3.16.	Table S16. Cohort B differences between bnAb and Control groups.	32
3.17.	Table S17. General linear model results for the difference between Cohort A and B, bnAb and Control groups for binding to additional antigens.	33
3.18.	Table S18. General linear model results for the difference in T cell subsets between Cohort A bnAb and Control groups and African seronegative individuals.	34
3.19.	Table S19. Logistic model results for the effect of viral load in Cohort A on the presence of autoantibodies.	35
3.20.	Table S20. Poisson model results for the effect of viral load in Cohort A on the presence of autoantibodies.	35
3.21.	Table S21. General linear model results for Cohort A bnAb and Control groups with covariates for group, viral load, and as an interaction term.	36
3.22.	Table S22. General linear model results for Cohort A bnAb and Control groups with viral load as a main effect.	37
3.23.	Table S23. General linear model results for the difference in alternatively defined Tfr subsets between Cohort A bnAb and Control groups and African seronegative individuals.	38
3.24.	Table S24. General linear model results for Treg activation/exhaustion marker expression between Cohort A bnAb and Control groups and African seronegative individuals.	39
3.25.	Table S25. General linear model results for Treg marker expression levels on Treg subsets defined by PD-1 expression levels for the Cohort A bnAb group.	39
3.26.	Table S26. General linear model results for Treg marker expression levels on Treg subsets defined by PD-1 expression levels for the African seronegative individuals.	40
3.27.	Table S27. Sign test results for suppression of T cell proliferation by subsets of Treg cells with differing levels of PD-1 expression, normalized to Tconv + Tconv.	40
3.28.	Table S28. General linear model results for the difference in T cell subsets within Cohort A HIV-1-seronegative individuals who were autoantibody positive and autoantibody negative.	41
3.29.	Table S29. Cohort A bnAb group two-digit HLA Class I types.	42
3.30.	Table S30. Cohort A Control group two-digit HLA Class I types.	43
3.31.	Table S31. Cohort A bnAb group two-digit HLA Class II types.	44
3.32.	Table S32. Cohort A Control group two-digit HLA Class II types.	45
3.33.	Table S33. Top 20 most highly associated functional variants in exome sequencing of bnAbs vs non-bnAbs (dominant genetic model).	46
3.34.	Table S34. Top 20 most highly associated functional variants in exome sequencing of autoimmune-bnAbs vs non-bnAbs (dominant genetic model).	47
4.	References	48

1. Methods

1.1. Study Populations

1.1.1. African CHAVI Cohort A Selection

1.1.1.1. Description of CHAVI Cohort

The individuals in Cohort A were drawn from two studies conducted by the Center for HIV/AIDS Vaccine Immunology (CHAVI). CHAVI 001 was a multisite study of acute and chronic HIV-1 infection that included an uninfected control arm (1). CHAVI 008 was a single-site study conducted at King's College (London, UK) that recruited chronically infected individuals from an international population (1). Both studies were approved by the Duke Medicine Institutional Review Board as well as the ethics boards of the local sites. Individuals included in this study were followed on average > 400 days (**Table S8**).

From these studies, we began with a cohort of N = 389 individuals with a full neutralization panel for at least 1 visit (see **Table S2**). We excluded N = 34 individuals because they were clinically defined as virus controllers. From the remaining sample of N = 351, we found N = 51 individuals that exceeded our definitional threshold for bnAb status (described in 1.1.1.2 below). Prior to selecting the matching non-neutralizers (Controls), we excluded N = 20 individuals who had re-enrolled in the study. We excluded a further N = 92 individuals who only had one visit, so their neutralization status could not be confirmed with a second visit. We excluded N = 4 individuals because they were suspected of being on anti-retroviral therapy (ART). The final dataset had N = 239 individuals.

Cohort A was derived from these 239 chronically HIV-1-infected individuals, of whom 90% were African (**Table S1**). Neutralizing antibody assays were performed for all subjects; a panel of 12 HIV-1 isolates (6 from Clade B and 6 from Clade C) was used (**Tables S3** and **S4**). From the neutralization panel we chose the top 51 neutralizers (defined as those with bnAbs; see section 1.1.1.2 below) and matched them with 51 individuals from the same cohort (see section 1.1.1.3 below). The final country of origin distribution for Cohort A is shown in **Table S6**. HLA typing for the individuals in this cohort is shown in **Tables S19-22**.

Infecting HIV-1 clade information for Cohort A is shown in **Table S9**; 1/102 assays was not informative. Group A.bnAb had 7/50 (14%) of individuals infected with clade A, 4/50 (8%) infected with clade B, and 33/50 (66%) infected with clade C; 2/50 (4%) were infected with A1C, 1/50 (2%) with A1D, and 3/50 (6%) with CD. Group A.Control had 6/51 (12%) infected with clade A, 5/51 (10%) infected with clade B, 37/51 (73%) infected with clade C, 1/51 (2%) infected with clade D, and 1/51 (2%) infected with clade F; 1/51 (2%) were infected with A1C. 48 HIV-1-seronegative control subjects, matched to the HIV-1-infected individuals in Cohort A, were also included as a comparator group in the T cell studies.

In a follow-on study, 118 HIV-1-seronegative subjects, again predominantly African individuals recruited in parallel to the Cohort A HIV-1-infected subjects, were screened for the presence of autoantibodies. Twelve individuals with autoantibodies (but no clinical autoimmune disease) were identified, and T cell analyses were performed on these individuals and 23 matched HIV-1-seronegative subjects without autoantibodies.

1.1.1.2. Threshold for bnAb Status

We defined broad neutralizers (bnAbs) by requiring that the individual have exceeded two thresholds. First, an individual must have had a PC1 score (see 1.1.1.4) of > 3 . Second, an individual must have met or exceeded an ID50 threshold of 95 on 7 of the 12 isolates in the panel. Setting a threshold for the PC1 > 3 selected the top 14% of neutralizers. Of note, no individual who had an ID50 > 95 for 7 of 12 isolates had a PC1 value less than 3.

1.1.1.3. Matching Non-Neutralizers

In order to ensure the greatest possible power for the study, we used propensity score matching (2, 3) to find controls that best matched the selected bnAb individuals using a covariate set. We used age, sex, and country of origin as our matching covariates. Thus, the control group was balanced on these variables so that they would not bias any study where those variables could play a role.

As described above, the final dataset had $N = 239$ individuals with $N = 51$ bnAbs and $N = 188$ individuals that could be potential Controls. Using propensity score matching, we selected $N = 51$ Controls matched on age, sex, and country of origin restricting them to have a PC1 score less than 0.1 and no isolates exceeding the ID50 threshold of 95 described above. The resulting matched data set of bnAbs and Controls were not significantly different on age, sex distribution, or country of origin distribution (see **Tables S4, S5 and S6**). There was a small but significant difference between the groups for viral load geometric mean over the available data (**Table S7**). Geometric mean viral load and country of origin could not be used in the same matching algorithm; country of origin was used as a proxy for infectious clade because it was deemed to be more important.

1.1.1.4. Principal Components Analysis of Neutralization Panel

Principal Components Analysis [PCA; (4, 5)] is a method commonly used to reduce the dimensionality of a data set. PCA uses Eigen Vector Decomposition of the correlation matrix of the variables to be reduced in dimension, in our case, viral isolates. By definition, the first principal component (PC1) is the vector that explains the most shared variance of the correlations of the measured variables. The second principal component is a vector orthogonal to the first that explains the residual variance from PC1. Each following principal component is orthogonal to all preceding it, up to the total number of variables. If the data are highly correlated, PC1 will explain a lot of variance

and the rest of the PCs (here, 12 are possible) will explain very little. When selecting the number of PCs to keep, the first criterion is that the PC has an Eigenvalue of at least 1. Ideally, you would want to explain 70% of the variance, but not at the expense of adding principal components with an Eigenvalue less than 1 (6).

We used a neutralization panel of 12 HIV isolates (**Tables S3 and S4**); thus, our data set has 12 dimensions. Neutralization was measured as a reciprocal inhibitory dilution giving 50% reduction of infection (ID50) calculated from a dilution curve for each viral isolate in the TZM-bl pseudovirus neutralization assay (7). In our analysis, only PC1 had an Eigenvalue greater than 1. PC1 explained 64% of the variance in the isolate panel (**Figure S1**), which is substantial. Each PC after PC1 accounted for a small (6% or less) amount of variance. This implies that they are mostly random variation and do not explain common variability in the data. The first principal component is analogous to a weighted average of the 12 isolates that includes magnitude of response as well as correlation (6). That is, we can interpret PC1 as a proxy for neutralization breadth taking into account magnitude: a higher PC1 means more breadth and a lower PC1 score means less breadth.

To facilitate comparison with Cohort B (section 1.1.2), we computed a geometric mean titer (GMT) of the neutralization data (**Figure 1A main text**), and found that PC1 score and GMT were highly correlated.

1.1.1.5. Distribution of Neutralization Breadth

For this study, we selected bnAbs and Controls from two ends of a continuum of neutralization breadth, as measured by PC1, in order to maximize the probability that we could find differences between the groups. Neutralization breadth is a continuum with the bnAbs at the top and the Controls at the bottom, but with overlapping levels of neutralization with patients that were not selected (see **Figure S2**). **Figure 1A** in the main text shows that the same distribution holds if the geometric mean titer is used as a metric of breadth rather than PC1. The propensity matching eliminated other potential sources of confounding from the two groups further increasing the power to find a statistically significant difference between the two groups.

1.1.2. US NIH Cohort B Selection

A second group of bnAb-producing individuals (Cohort B) served as a confirmation cohort and was comprised of HIV-1-infected individuals in the US (8) that were derived from 290 total infected individuals not receiving ART, and were screened in a manner similar to Cohort A using a 5-pseudovirus mini-panel (8) in the TZM-bl neutralization assay. Based on these preliminary results, a

subset of individuals was then tested with a larger panel of 20 pseudoviruses. From the original 290 individuals, 24 individuals with high bnAb scores (neutralizing ≥ 10 of 20 pseudoviruses at an ID₅₀ ≥ 100) (B.bnAb group) and 21 with the lowest bnAb scores (neutralizing ≤ 9 of 20 pseudoviruses at an ID₅₀ ≥ 100) (B.Control group) were selected for study. All individuals in this US-based cohort were presumed to be infected with clade B viruses.

1.2. Antibody Assays

The AtheNA MultiLyte Test assays (Alere, Inc.; Princeton, NJ) were performed as described (9) for measures of plasma antibodies against ribonucleoprotein (RNP), SSA (Ro), SSB (La), ScL-70, Smith (Sm), double-stranded deoxyribonucleic acid (dsDNA), histones, Jo-1, and Centromere B. Assays for antibody to cardiolipin were performed as described (9) using the Quanta lite ACA IgGIII kit (Inova Diagnostic; San Diego, CA). Plasma antibody assays to HIV-1 C.CH505 Env gp120 (10), gp120 resurfaced core (RSC3) (11), HIV-1 Env gp41 B.MN (12), and trivalent inactivated influenza vaccine 2008 (TIV 2008) (Sanofi-pasteur Inc; Swiftwater, PA) (13) were performed as described. For assays using RSC3 proteins, ELISAs were performed using captured streptavidin and biotinylated proteins in order to minimize the effects of plate binding on antigen configuration.

1.3. Analysis of CD4⁺ T cell subsets

Multiparameter flow cytometry panels were used to analyse samples from subjects in cohort A and HIV-1-seronegative individuals with and without autoantibodies recruited in parallel to the cohort A HIV-1-infected subjects.

For analysis of the circulating frequency of resting memory follicular helper CD4⁺ T cells, defined as the PD-1⁺ CXCR3⁻ subset of CXCR5⁺ CD4⁺ T cells (14), peripheral blood mononuclear cells (PBMCs) were surface stained with directly fluorescent-labeled antibodies to CXCR3 allophycocyanin (APC) (1C6) and CXCR5 Alexa Fluor® (AF)488 (RF8B2) (both from BD Biosciences) at 37°C for 10 minutes, then washed and surface stained with directly labelled antibodies to CD3 phycoerythrin (PE)-Texas Red (S4.1; Life Technologies); CD4 APC-H7 (SK3), CD45RO PE-Cy7 (UCHL1), CCR6 PE (11A9) and PD-1 Brilliant Violet™ (BV)421 (EH12.1) (all from BD Biosciences), plus a biotinylated antibody to ICOS (ISA-3; eBioscience) at room temperature for 15 minutes; then washed and stained with fluorescent-conjugated streptavidin Peridinin chlorophyll protein (PerCP) (BD Biosciences) and Live/Dead Fixable Aqua Dead Cell Stain (Life Technologies) at room temperature for 10 minutes, prior to washing and fixation with 4% paraformaldehyde for 15 minutes. Flow cytometry data were acquired with a Cyan ADP Analyzer (Beckman Coulter) and were analyzed using FlowJo software

(v8.8.6; Treestar). The gating strategy for identification of resting memory Tfh is illustrated in **Figure S4A**; the gate for PD-1 staining was set using a fluorescence minus one (FMO) control.

For analysis of circulating CD4⁺ T cells and regulatory subsets thereof, PBMCs were surface stained with directly fluorescent-labeled antibodies to CD3 PE-Texas Red (S4.1; Life Technologies); CD4 APC-H7 (SK3), CD25 PE-Cy7 (2A3), CXCR5 AF488 (RF8B2), PD-1 BV421 (EH12.1) (all from BD Biosciences); and ICOS PE (ISA-3; eBioscience) at 37°C for 15 minutes; then washed and stained with Live/Dead Fixable Aqua Dead Cell Stain (Life Technologies) at room temperature for 10 minutes. Cells were then fixed and permeabilized at room temperature for 15 minutes using the Foxp3 Fix/Perm Kit (eBioscience) and stained in permeabilization buffer with a directly labeled antibody to Foxp3 APC (PCH101; eBioscience) at room temperature for 45 minutes, prior to two washes with permeabilization buffer. Flow cytometry data were acquired with a Cyan ADP Analyzer (Beckman Coulter) with standard filter sets and data were analyzed as described above.

The gating strategy for identification of total CD4⁺ T cells, and regulatory subsets thereof is illustrated in **Figure S4B**; gates for CD25 and Foxp3 were set using a FMO control and an internal negative population (non-CD3) within the sample, respectively. The frequencies of total CD4⁺ T cells (defined as CD3⁺ CD4⁺ cells) and regulatory CD4⁺ T cells (defined as CD3⁺ CD4⁺ CD25⁺ Foxp3⁺ cells) within live lymphocytes; and the proportions and relative ratios of regulatory (defined as CD25⁺ Foxp3⁺) and helper (non-CD25/Foxp3 double positive) cells within the circulating CD4⁺ T follicular-phenotype population (defined as CD3⁺ CD4⁺ CXCR5⁺ cells) were determined. As there is a lack of consensus as to how blood T follicular regulatory (Tfr) populations should be defined, we also performed comparative analyses using two alternative definitions for Tfr: CD25⁺ Foxp3⁺ CXCR3⁻ PD-1⁺ CXCR5⁺ CD4⁺ CD3⁺ cells (**Figure S4C**) or CD25⁺ Foxp3⁺ ICOS⁺ PD-1⁺ CXCR5⁺ CD4⁺ CD3⁺ cells (**Figure S4D**). It was possible to define the latter population when PBMC were stained as detailed above: the proportions and relative ratios of regulatory (defined as CD25⁺ Foxp3⁺) and helper (non-CD25/Foxp3 double positive) cells within the circulating CD4⁺ T follicular-phenotype population (defined as CD3⁺ CD4⁺ CXCR5⁺ ICOS⁺ PD-1⁺ cells) were determined (**Figure S4D**).

To enable definition of the former population of cells and to evaluate the expression of exhaustion and activation markers, PBMCs were instead surface stained with directly fluorescent-labeled antibodies to CD3 PE-Texas Red (S4.1; Life Technologies); CD4 APC-H7 (SK3), CD25 PE-Cy7 (2A3), CXCR5 AF488 (RF8B2), PD-1 BV421 (EH12.1), ICOS BV711 (DX29), CXCR3 PE (1C6) (all from BD Biosciences); CD8 BV650 (RPA-T8) or HLA-DR BV650 (L243), CD127 BV785 (A019D5), (from BioLegend) and LAG-3 biotin (polyclonal) (R&D Systems) at 37°C for 15 minutes; then washed and stained with CCR6 BV605 (11A9) or streptavidin BV605 (BD Biosciences); and CD45RO AF700 (UCHL1) or CD27 AF700 (O323) (both from BioLegend) at room temperature for 15 min. Cells were then washed and stained with Live/Dead Fixable Aqua Dead Cell Stain (Life Technologies) at room

temperature for 10 minutes. After the surface staining, cells were fixed and permeabilized at room temperature for 15 minutes using the Foxp3 Fix/Perm Kit (eBioscience) and stained in permeabilization buffer with a directly labeled antibody to Foxp3 APC (PCH101) and Helios PerCP-eFluor710 (22F6) or CTLA-4 PerCP-eFluor710 (14D3) (all from eBiosciences) at room temperature for 45 minutes, prior to two washes with permeabilization buffer. Flow cytometry data were acquired with an LSR Fortessa X-20 Analyzer (BD Biosciences) with standard filter sets and data were analyzed as described above. Rainbow beads (BioLegend) were used in all acquisitions.

The gating strategy used to evaluate expression of HLA-DR, CTLA-4 and LAG-3 on CD4⁺ Treg cells and subsets thereof expressing different levels of PD-1 is illustrated in **Figure S4E**. Gates for HLA-DR and LAG-3 were set using a FMO control; a FMO + isotype control was used for CTLA-4. Gates for CD25 and Foxp3 were set using a FMO control and an internal negative population (non-CD3) within the sample, respectively. The frequency of regulatory CD4⁺ T cells (defined as CD3⁺ CD4⁺ CD25⁺ Foxp3⁺ cells) expressing HLA-DR, CTLA-4 or LAG-3 was determined; and the mean fluorescence intensity (MFI) of expression of each of these markers on subsets of CD3⁺ CD4⁺ CD25⁺ Foxp3⁺ cells expressing high levels, low levels or no PD-1 was also evaluated.

To confirm that activation-associated increases in CD4⁺ T cell expression of CD25 and Foxp3 (15) in HIV-1-infected subjects were not resulting in inclusion of non-regulatory CD4⁺ T cells in the CD25⁺ Foxp3⁺ gate, the proportion of CD25⁺ Foxp3⁺ CD4⁺ Treg cells expressing Helios, a marker distinguishing a subset of thymus-derived natural CD4⁺ Treg cells (16), was assessed, and was shown not to differ significantly in HIV-1-seronegative and HIV-1-seropositive donors (**Figure S5**; all comparisons non-significant, t-test).

1.4. CD4⁺ Treg Cell Suppression Assay

The *in vitro* functional capacity of CD4⁺ Treg subsets was assessed based on their capacity to suppress the proliferation of autologous conventional CD4⁺ T cells (Tconv). PBMCs freshly isolated from the blood of healthy, HIV-1-seronegative volunteers were incubated at 37°C overnight in RPMI-1640 (Gibco) supplemented with 10% AB serum (Sigma), 1% penicillin-streptomycin (Gibco), 1 mM Sodium Pyruvate (Sigma), 1× MEM-NEAA (Gibco), 1× Glutamax-I (Gibco) and 50 µM β-mercaptoethanol (Gibco). CD4⁺ T cells were isolated using the CD4 negative selection kit from Miltenyi and stained with directly fluorescent-labeled antibodies to CD3 PE-Texas Red (S4.1; Life Technologies), CD4 APC-H7 (SK3), CD127 FITC (HIL-7R-M21), CD25 PE-Cy7 (2A3), PD-1 PE (EH12.1) (all from BD Biosciences) and Live/Dead Fixable Far Red Dead Cell Stain (Life Technologies) for 15 min at 37°C. CD4⁺ Tconv cells (CD3⁺ CD4⁺ CD25^{low} CD127^{high}) and CD4⁺ CD25^{high} CD127^{low} Treg subsets with different levels of expression of PD-1 (PD-1^{neg}, PD-1^{low} or PD-1^{high}) were sorted using a MoFlo cell sorter (Beckman Coulter). CD4⁺ Tconv cells were washed

and resuspended in 1 mL PBS and CFSE was added at a final concentration of 4 μ M (Life Technologies). The mixture was vortexed for 15 s and incubated at room temperature for 10 min. Labeling was quenched with 3 times the staining volume of ice-cold FBS. Cells were then washed twice with complete media. 2.5×10^4 CFSE-labeled target Tconv cells were co-cultured in 96-well round-bottom plates at a 2 to 1 target-to-effector ratio with Tconv cells or Treg subsets in the presence of anti-CD2/CD3/CD28 beads (1 to 2 bead-to-cell ratio; Miltenyi). Unstimulated CFSE-labeled cells and unlabeled stimulated Tconv cells were used as controls. When possible, co-cultures were set up in duplicate. At day 6 post-activation, cells were collected, stained with Live/Dead Far Red Dead Cell stain and fixed with 4% paraformaldehyde for 15 min. Flow cytometry data were acquired with a Cyan ADP Analyzer (Beckman Coulter) and were analyzed using FlowJo software (v8.8.6; Treestar).

1.5. HLA Typing

DNA was isolated from PBMC samples using standard extraction kits (Qiagen) per the manufacturer's instructions. Class I and II HLA typing to 2-digit allele resolution was performed by PCR on these DNA samples by ProImmune (Oxford, UK).

1.6. Exome Sequencing

High molecular weight genomic DNA was purified from 101 samples falling in the extremes of the PC1 distribution using the Gentra Autopure system and 5 μ g was used to prepare next-generation sequencing (NGS) libraries using the Illumina TruSeq reagent kit. Coding regions of the genome were then enriched using Illumina TruSeq 37Mb, 50Mb or 65Mb exome capture kits and high-throughput, short-read sequencing was performed using Illumina 2000 or 2500 DNA sequencers. Samples were sequenced to an average depth of 74-fold autosomal coverage and quality was evaluated by comparing concordance with previously generated genotype array data. Sequencing reads passing standard Illumina quality filters were trimmed and aligned to the 1000 genomes phase 2 (build37) human genome reference sequence using BWA version 0.5.10. PCR duplicates were removed using picard-tools-1.59. Single nucleotide variants and short insertions/deletions were called using GATK-1.6-11. Variants were then annotated with SnpEff-3.3 using the Ensembl GRCh37.73 database.

An initial association analysis was then conducted to determine whether any variants were enriched among either the HIV-1 broad-neutralizer group or controls. Common variation with a minor allele frequency (MAF) of greater than 5% was tested for associations with the phenotype groups using the Fisher's Exact test (FET) adjusted for multiple testing using a Bonferroni correction. Rare variants were examined using a gene-based method, which collapsed rare variants (MAF < 5%) with a predicted functional role (non-synonymous, start-loss, stop-gain, frameshift, or disrupted essential

splice sites) down to a binomial value that was then summed across all subjects in each of the broad-neutralizer or control groups. Enrichment of rare, functional variants was then evaluated using a Bonferroni-corrected FET. A second analysis was then conducted as above after removing subjects with no evidence of autoimmune serology from the broad-neutralizer group and non-broad neutralizer controls positive for autoimmune serology. All association analyses were performed using the Analysis Tool for Annotated Variants (ATAV) software package.

1.7. Statistical Analysis

1.7.1. Statistical Analyses of Reported Tests

Statistical analysis of the autoantibody results followed a pre-determined statistical analysis plan (see 1.7.2 below). Each individual received a score of 1 if the assay exceeded the clinical threshold according to the manufacturer, and a 0 if it did not. An individual was defined as autoantibody positive if they had one or more positive autoantibody result and negative if they did not. A contingency table analysis with a Chi-square statistic was used to determine whether the bnAb individuals were more likely to be positive than Controls. The number of positive results was also of interest. A Poisson regression was used to determine whether the bnAb individuals were more likely to have a higher positive count than Controls.

Analyses of antibody binding data were performed using the general linear model (PROC GLM) with the bnAb group as a predictor. The Benjamini-Hochberg (17) false discovery rate correction was applied to these results. The T cell subsets were analyzed using a combination of methods. When the data were expressed as a percentage, the arcsine transformation of the data was performed before analysis. If the data were MFI, then the natural log transformation was performed before analysis. The data were then analyzed using the general linear model and pairwise comparisons between groups were made resulting in a t-statistic for the mean difference. For the analysis of PD-1 subsets in **Figure 4** within group, a linear mixed model was used to account for the within subjects nature of the data. For the analysis of expression within PD-1 type, a non-parametric sign test was used to account for the within subject nature of the data. The Benjamini-Hochberg (17) false discovery rate correction was applied to these results.

To assess whether the T cell subsets were affected not just by group but by Viral Load, the natural log of the mean Viral Load was added to the general linear models as a covariate in models with A.bnAb and A.Control groups (**Table S18**). It was included as a main effect and as an interaction with bnAb group to predict T cell subset. None of the interactions were statistically significant; therefore, the models were run again with Viral Load only as a main effect (**Table S19**). In this case all of the observed effects remained significant and Viral Load was non-significant except for the CD4- T cells within lymphocytes (**Table S19**, $p = 0.04$). However, the Group effect remained significant ($p = 0.02$)

showing explicitly that the Group effect is independent of Viral Load. Thus, we concluded that the effects we observe for T cell subsets are statistically independent of Viral Load. We reported statistical results for the full model including A.SeroNegs and without Viral Load (since SeroNegs by definition have no Viral Load and would not be able to be assessed in the same model).

To test differences in frequency distributions between bnAb individuals and Controls for HLA haplotypes, we used Cochran-Mantel-Haenszel test statistics.

All statistical analyses were performed using SAS v9.4 (SAS Institute, Inc., Cary, NC).

1.7.2. Pre-Determined Statistical Plan

HIV-1 Broadly Neutralizing Antibody-Auto-antibody Study Statistical Plan

Groups

N = 51 bnAb individuals with highest PC1 score

N = 51 Control (no-nAb) individuals with low PC1 score, Heckman matched by age, sex, and country of origin.

Assays

1. AtheNA Multilyte
 - a. 9 autoantibody assays with a clinical positive defined as > 120 luminex AtheNA Units.
 - b. Potential alternate threshold at the highest dilution if HIV+ status causes high background noise for auto antibody.
2. ELISA
 - a. Cardiolipin assay with a positive value defined by plate controls as a GLU threshold.

Question 1

Is there a difference between the groups on whether the number of patients with any positive reactivity?

1. AtheNA positive on any of the 9.
2. ELISA: positive for cardiolipin.

Statistical method: contingency table logistic regression. If necessary, we will analyze with both categorization methods.

Question 2

Is there a difference between the groups on the amount of positive responses in the patients?

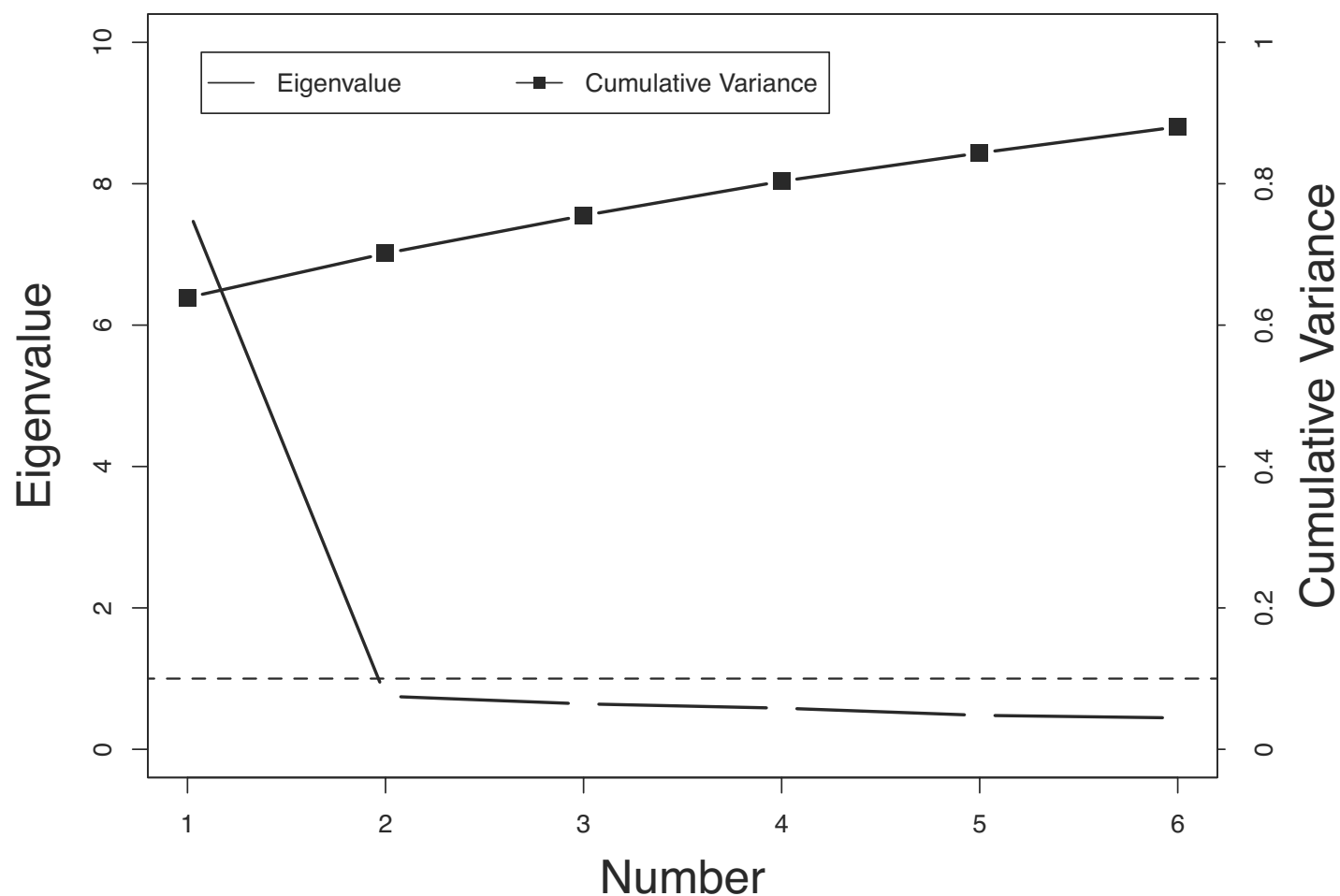
1. AtheNA positive count out of 9.
2. All positive count out of 10.

Statistical method: Poisson regression (zero-inflated Poisson if the data require it). If necessary, we will analyze with both categorization methods.

1.7.3. Analysis Excluding US and UK patients

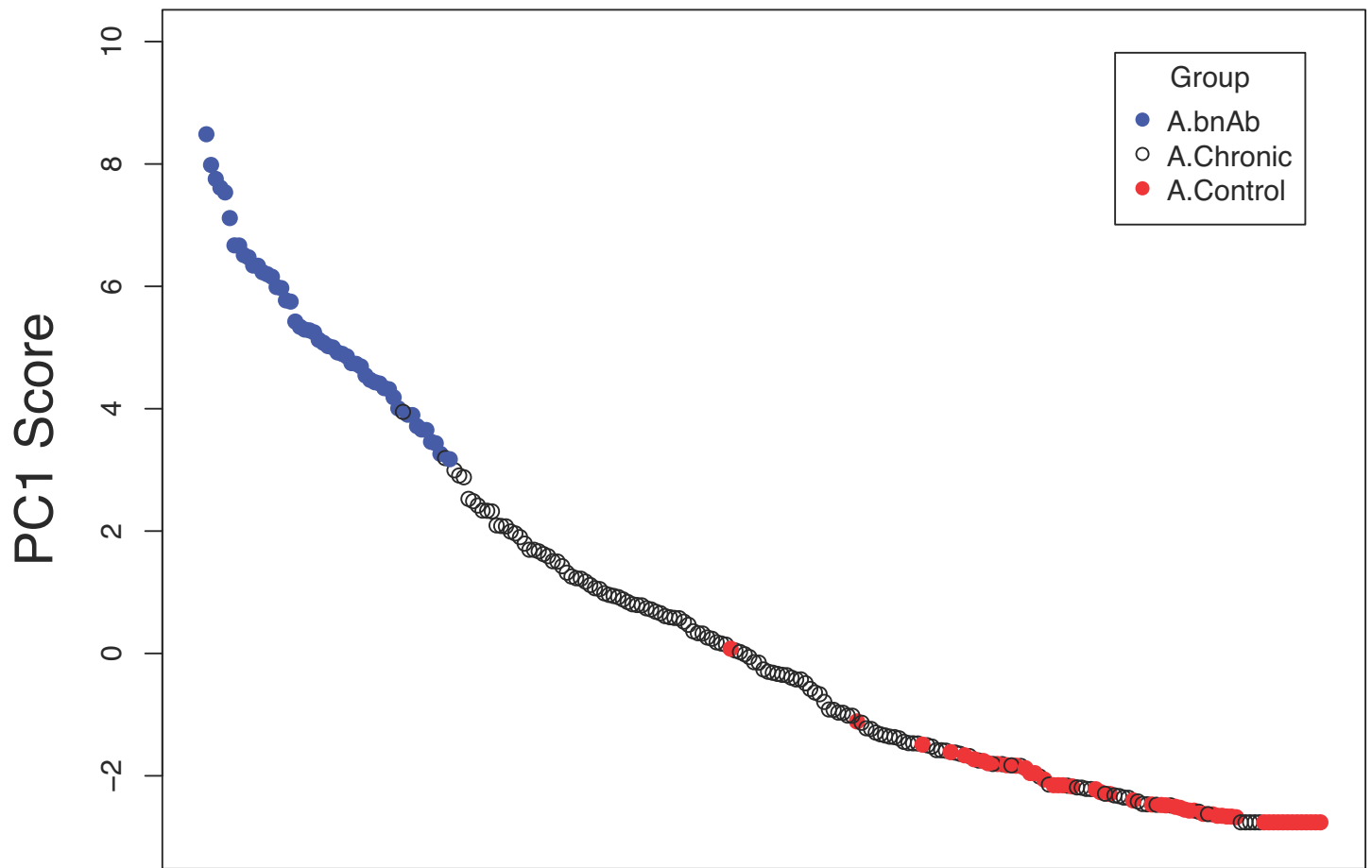
We wanted to make sure that there was no sample bias related to African versus Anglo individual origin in Cohort A (see **Table S6**). Thirty out of 46 (65%) A.bnAbs and 15 out of 44 (33%) A.Controls were positive for autoantibodies. As in the full study, this difference was statistically significant ($\chi^2 = 9.3$, $p = 0.002$). We also re-ran the Poisson regression with similar results, it showed the A.bnAb individuals to have had a higher number of positives than the A.Controls ($\chi^2 = 12.7$, $p = 0.0004$).

2. Supporting Figures



2.1. Figure S1. Eigenvalues and amount of variance explained up to principal component six.

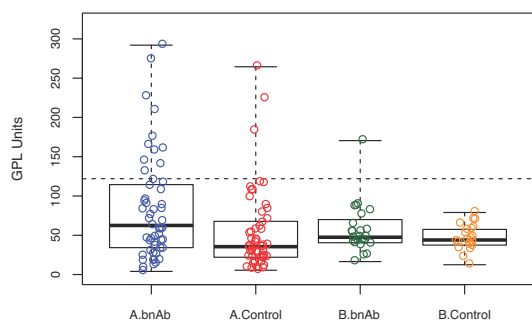
The principal components analysis of neutralization for Cohort A resulted in only one Eigenvalue > 1. PC1 explained 64% of the variance and each subsequent Eigenvalue was < 1 and explained a small amount of the variance.



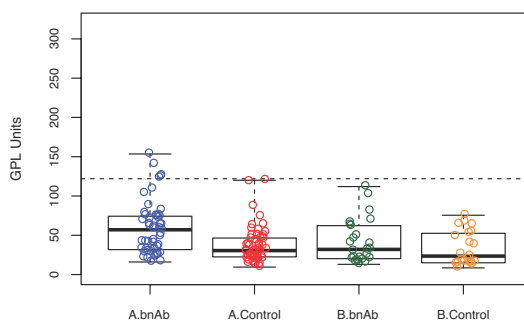
2.2. Figure S2. Cohort A PC1 scores in descending order.

The 239 individuals in Cohort A are shown in descending order of PC1 score. Individuals in the bnAb group are closed blue circles, matched controls are closed red circles, and those not selected for either group are open black circles.

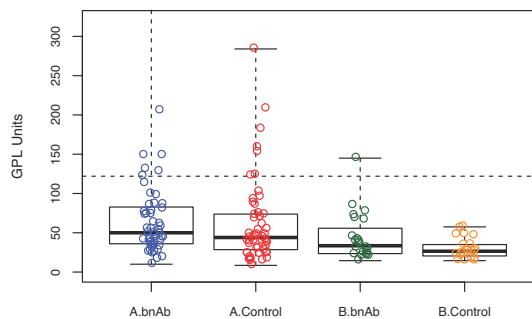
A: Centromere B



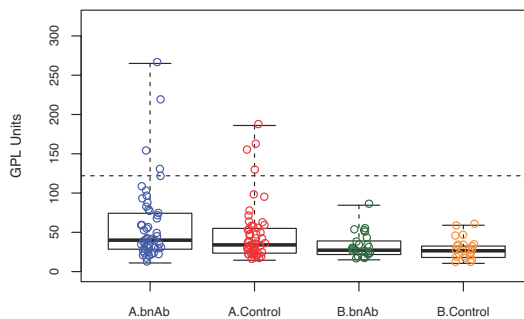
B: Histone



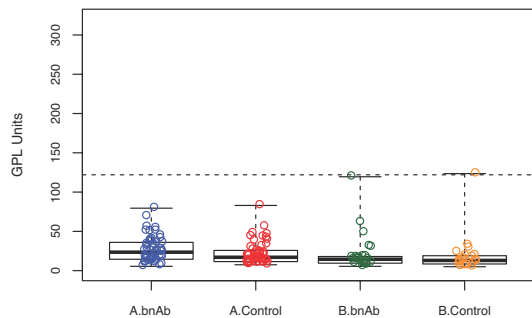
C: Jo-1



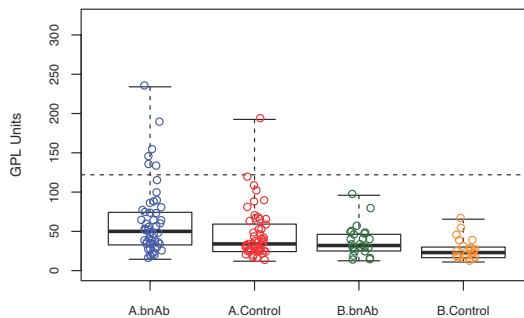
D: RNP



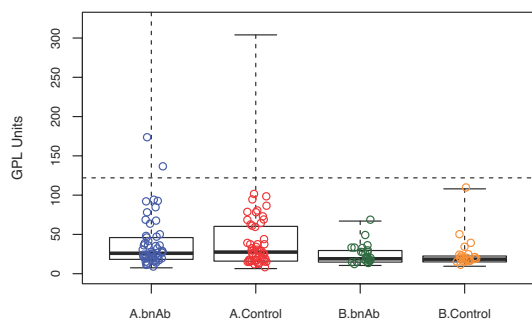
E: SSA (Ro)



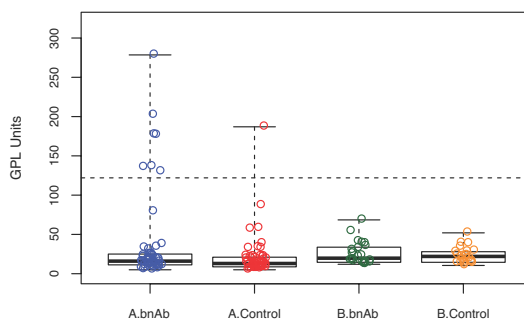
F: SSB (La)



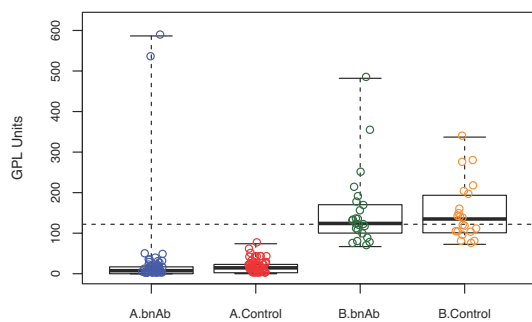
G: Scl-70



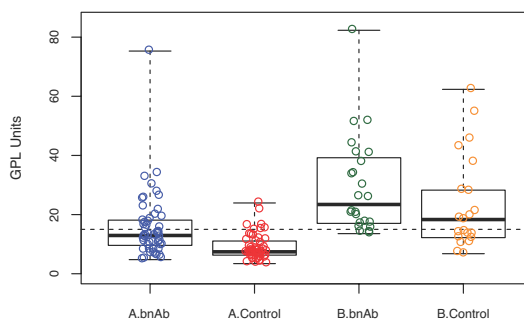
H: Smith (Sm)



I: dsDNA

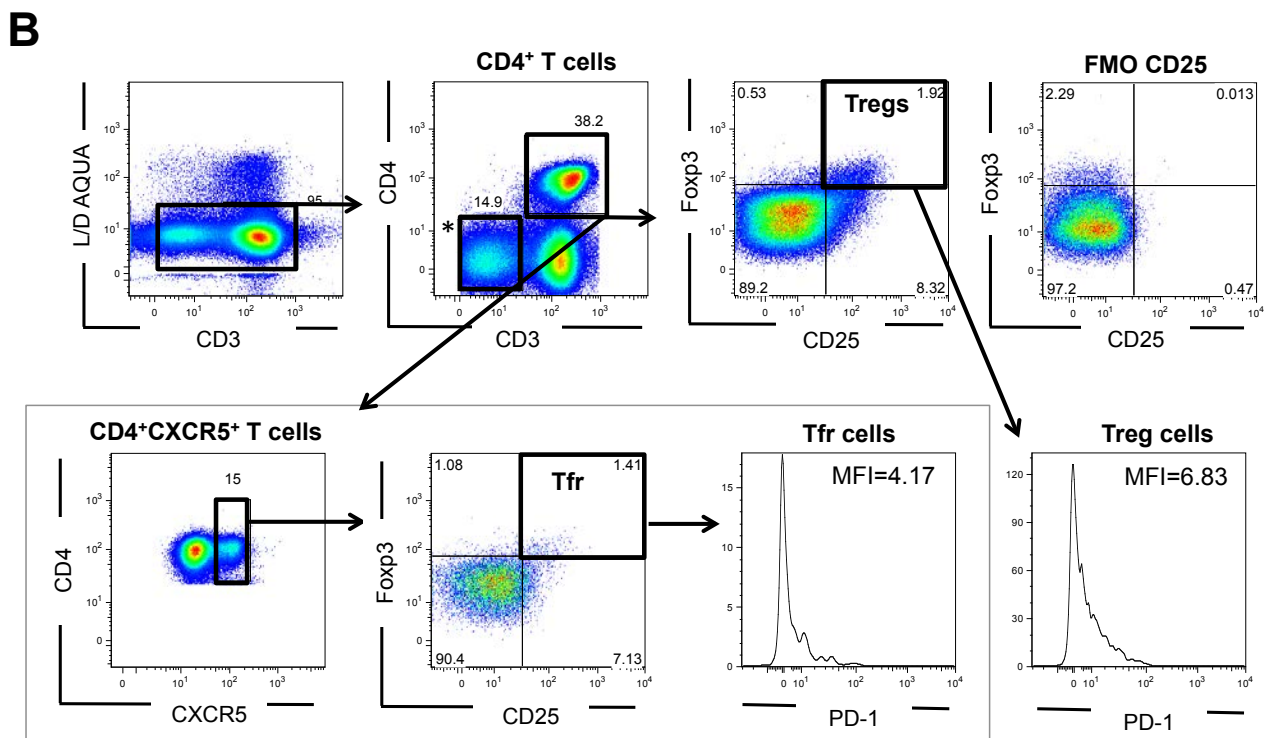
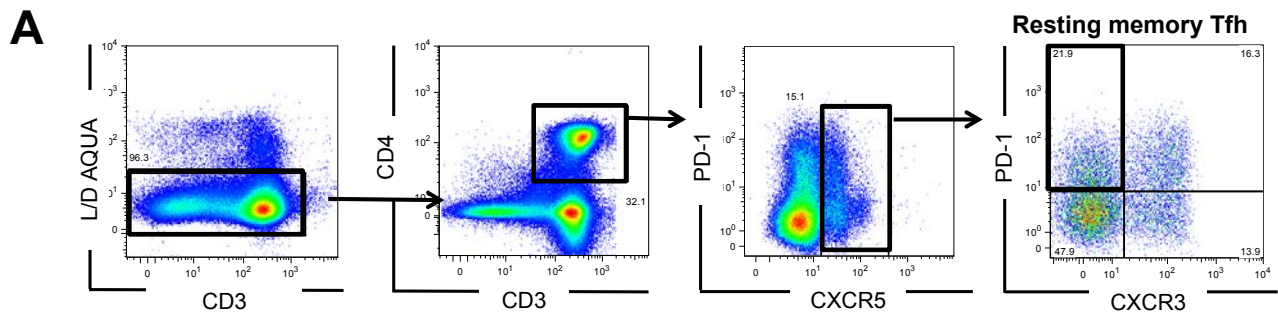


J: Cardiolipin

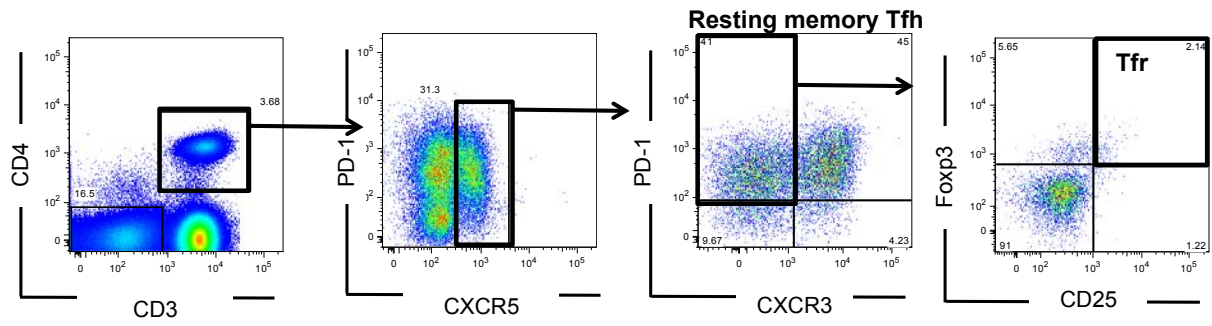


2.3. **Figure S3.** *Plots of individual autoantibody assay results.*

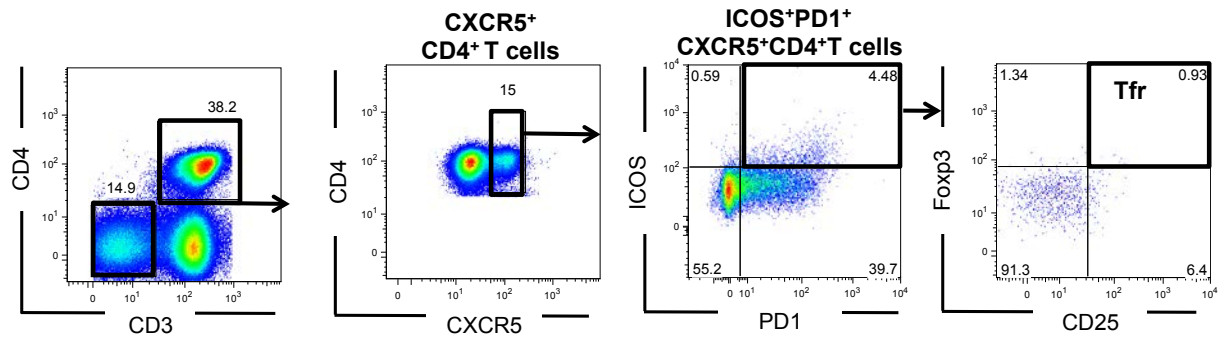
Data for each of the 10 autoantibody tests are shown for the cohorts studied. Dashed horizontal lines show the cutoff level for positivity in this clinical assay.



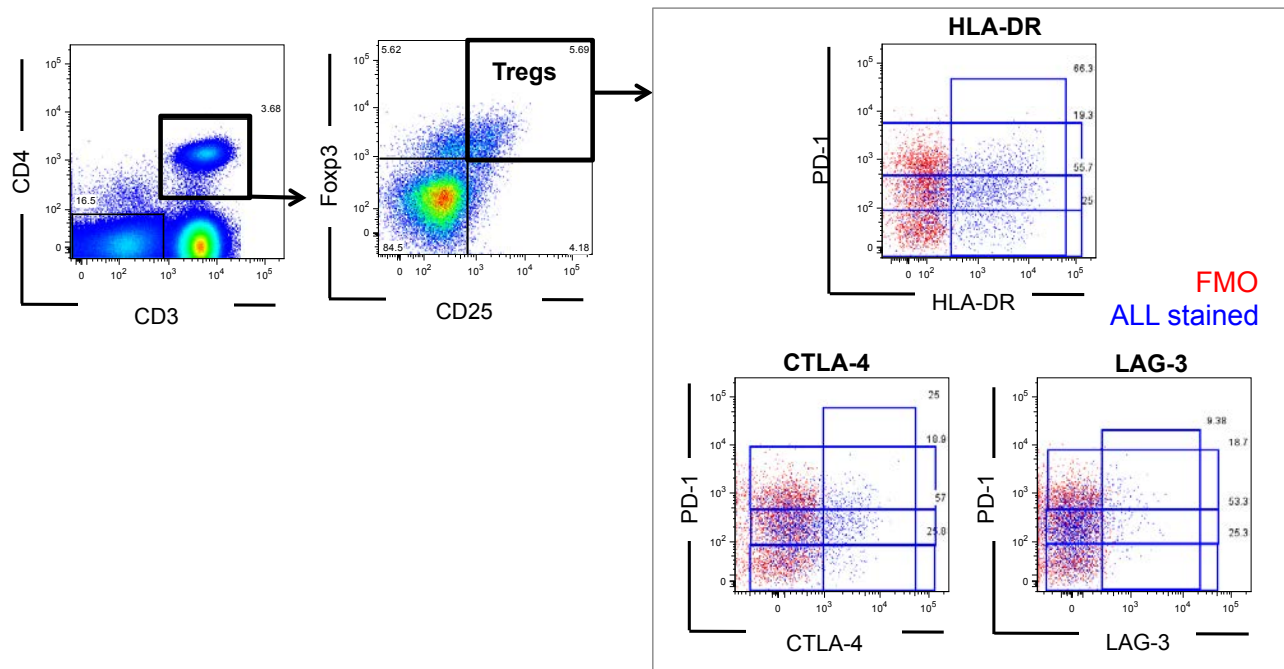
C



D



E



2.4. Figure S4. Gating strategy for flow cytometric analysis of T cell subsets.

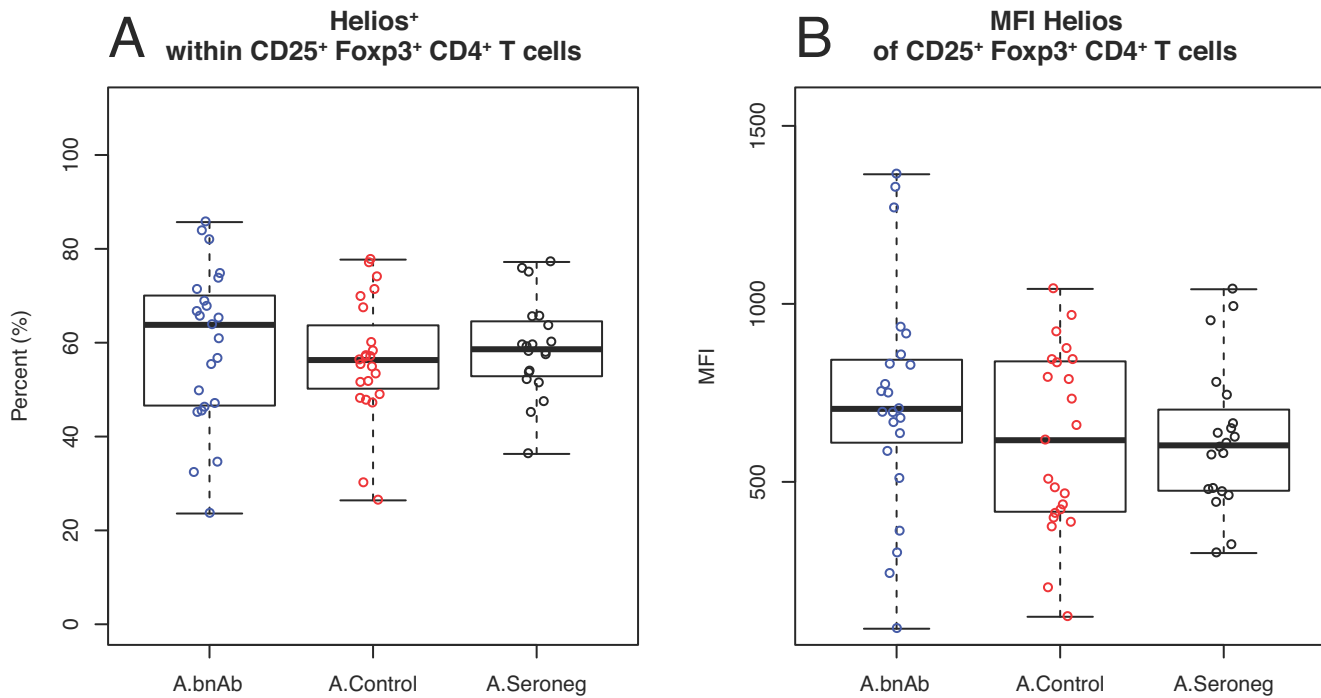
A. Gating strategy for analysis of resting memory Tfh. The gate for PD-1 was set using a FMO control. The frequency of PD-1⁺ CXCR3⁻ cells within the circulating CD3⁺ CD4⁺ CXCR5⁺ population was quantified as shown. The staining shown is from a representative subject in the Cohort A bnAb HIV-1-infected group.

B. Gating strategy for analysis of total CD4⁺ T cells and regulatory subsets thereof. Gates for CD25 and Foxp3 were set using an FMO control and an internal negative population (non-CD3) within the sample, respectively. The frequencies of total CD4⁺ T cells (defined as CD3⁺ CD4⁺ cells) and regulatory CD4⁺ T cells (defined as CD3⁺ CD4⁺ CD25⁺ Foxp3⁺ cells) within live lymphocytes; the proportions and relative ratios of regulatory (defined as CD25⁺ Foxp3⁺) and helper (non-CD25/Foxp3 double positive) cells within the circulating CD4⁺ T follicular-phenotype population (defined as CD3⁺ CD4⁺ CXCR5⁺ cells); and the MFI of PD-1 expression on regulatory CD4⁺ T cells (CD3⁺ CD4⁺ CD25⁺ Foxp3⁺ cells) and follicular regulatory CD4⁺ T cells (CD3⁺ CD4⁺ CXCR5⁺ CD25⁺ Foxp3⁺ cells) were quantified as shown. The staining shown is from a representative subject in the Cohort A bnAb HIV-1-infected group.

C. Gating strategy for analysis of the proportions and relative ratios of regulatory (defined as CD25⁺ Foxp3⁺) and helper (non-CD25/Foxp3 double positive) cells within the circulating CD4⁺ CXCR5⁺ PD-1⁺ CXCR3⁻ T cell subset. Gates for CD25 and Foxp3 were set as in (B). The staining shown is from a representative subject in the Cohort A bnAb HIV-1-infected group.

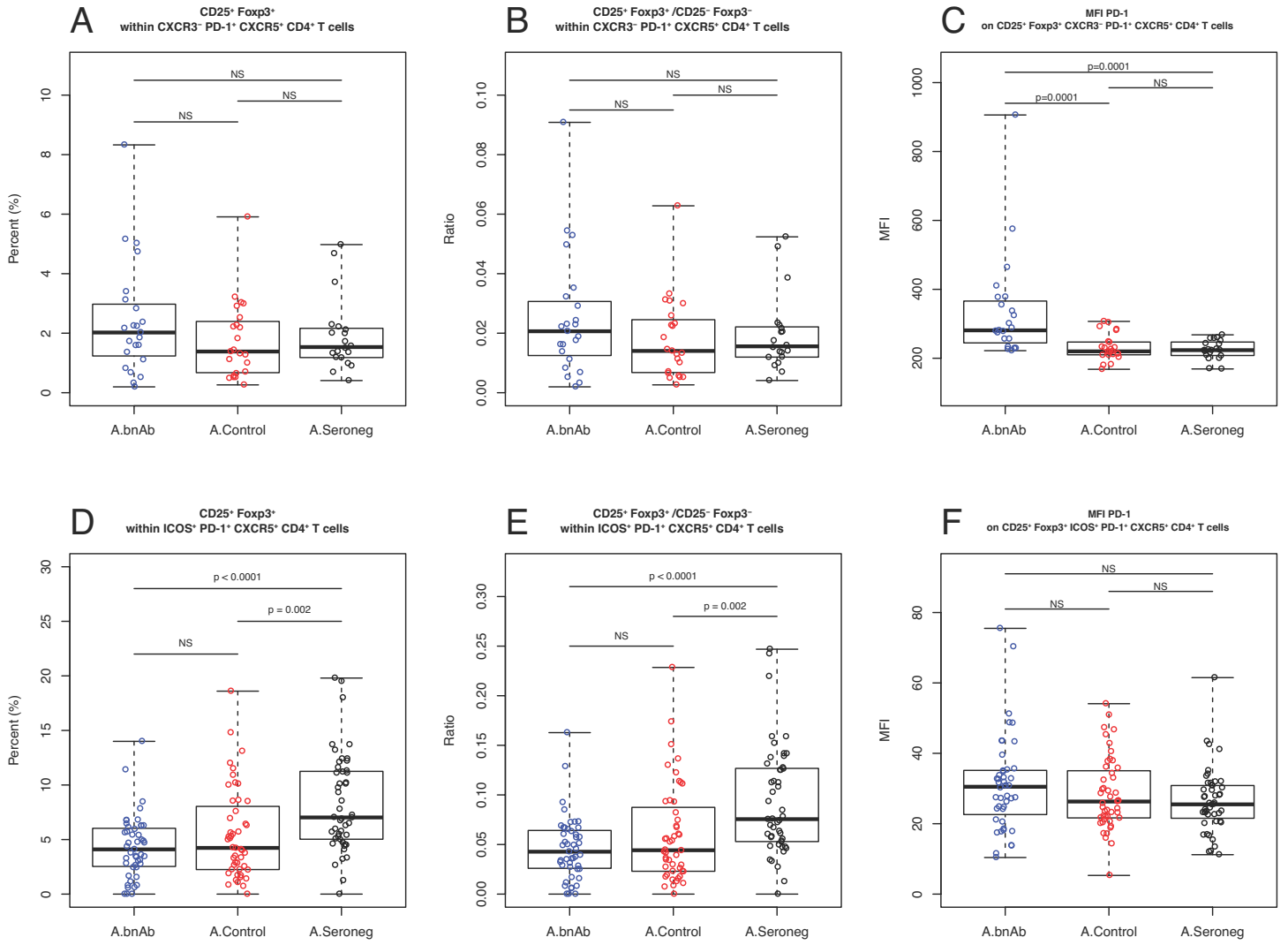
D. Gating strategy for analysis of the proportions and relative ratios of regulatory (defined as CD25⁺ Foxp3⁺) and helper (non-CD25/Foxp3 double positive) cells within the circulating CD4⁺ CXCR5⁺ PD-1⁺ ICOS⁺ T cell subset. Gates for CD25 and Foxp3 were set as in (B). The staining shown is from a representative subject in the Cohort A bnAb HIV-1-infected group.

E. Gating strategy for analysis of the proportion of regulatory CD4⁺ T cells (defined as CD3⁺ CD4⁺ CD25⁺ Foxp3⁺ cells) expressing HLA-DR, CTLA-4 and LAG-3 and assessment of the MFI of expression of each of these markers on total regulatory CD4⁺ T cells and subsets thereof expressing high or low levels of PD-1 and PD-1 negative cells. Gates for CD25 and Foxp3 were set as in (B). The staining shown is from a representative subject in the Cohort A bnAb HIV-1-infected group.



2.5. Figure S5. Comparison of Helios expression in CD4⁺ Treg cells in Cohort A subjects with and without bnAbs and matched HIV-1-seronegative controls.

Comparison of the proportion of Helios⁺ cells within CD25⁺ Foxp3⁺ CD4⁺ Treg cells (**A**) and the MFI of Helios expression in CD25⁺ Foxp3⁺ CD4⁺ Treg cells (**B**) in Cohort A chronic HIV-1-infected subjects and HIV-1-seronegative controls. In both panels, each symbol represents data from an individual subject; group medians, range, and quartiles are shown.



2.6. Figure S6. Comparison of Tfr subsets (as defined using alternative phenotyping strategies) in Cohort A subjects with and without bnAbs and matched HIV-1-seronegative controls.

The proportion of Tfr cells within the circulating CXCR3⁻ PD-1⁺ CXCR5⁺ CD4⁺ T cell pool (% CD25⁺ Foxp3⁺ cells within CXCR3⁻ PD-1⁺ CXCR5⁺ CD4⁺ T cells) in the A.bnAb group did not differ significantly from that in the A.Control or seronegative groups (**A**). The Tfr/Tfh ratio, defined as

$$\frac{\text{Tfr}}{\text{Tfh}} = \frac{\% \text{ CD25}^+ \text{ Foxp3}^+ \text{ cells within CXCR3}^- \text{ PD-1}^+ \text{ CXCR5}^+ \text{ CD4}^+ \text{ T cells}}{\% \text{ non-CD25}^+ \text{ Foxp3}^+ \text{ cells within CXCR3}^- \text{ PD-1}^+ \text{ CXCR5}^+ \text{ CD4}^+ \text{ T cells}} \quad (\text{Eq. 1})$$

in the A.bnAb group also did not differ significantly from that in the A.Control or seronegative groups (**B**). The MFI of PD-1 staining on CD4⁺ Tfr cells (CD25⁺ Foxp3⁺ CXCR3⁻ PD-1⁺ CXCR5⁺ CD4⁺ T cells) was highest in the A.bnAb group (**C**). The proportion of Tfr cells within the circulating ICOS⁺ PD-1⁺ CXCR5⁺ CD4⁺ T cell pool (% CD25⁺ Foxp3⁺ cells within ICOS⁺ PD-1⁺ CXCR5⁺ CD4⁺ T cells) in the A.bnAb group did not differ significantly from that in the A.Control group (although was higher than that in the HIV-1-seronegative group) (**D**). The Tfr/Tfh ratio, defined as

$$\frac{\text{Tfr}}{\text{Tfh}} = \frac{\% \text{ CD25}^+ \text{ Foxp3}^+ \text{ cells within ICOS}^+ \text{ PD-1}^+ \text{ CXCR5}^+ \text{ CD4}^+ \text{ T cells}}{\% \text{ non-CD25}^+ \text{ Foxp3}^+ \text{ cells within ICOS}^+ \text{ PD-1}^+ \text{ CXCR5}^+ \text{ CD4}^+ \text{ T cells}} \quad (\text{Eq. 2})$$

in the A.bnAb group also did not differ significantly from that in the A.Control group (although was higher than that in the HIV-1-seronegative control group). (**E**). The MFI of PD-1 staining on CD4⁺ Tfr cells (CD25⁺ Foxp3⁺ ICOS⁺ PD-1⁺ CXCR5⁺ CD4⁺ T cells) was highest in the A.bnAb group, although this did not reach statistical significance (**F**). In all panels, each symbol represents data from an individual subject; group medians, range, and quartiles are shown.

3. Supporting Tables

3.1. **Table S1.** Country of origin for Cohort A individuals.

Country	Frequency	%
Malawi	74	31.0
South Africa	82	34.3
Tanzania	58	24.3
UK	3	1.3
USA	22	9.2
239		

3.2. **Table S2.** Cohort A individuals included and excluded from principal components analysis and control group.

Potential						Excluded	
In PCA	Control	# Visits	Patient Type	N	%	N	%
0	0	1	Controller	13	3.3		
0	0	2	Controller	20	5.1		
0	0	3	Controller	1	0.3	34	8.7
0	0	1	Re-Enroll	10	2.6		
0	0	2	Re-Enroll	10	2.6	20	5.1
1	0	1	Established	92	23.7		
0	0	2	Established	2	0.5		
0	0	3	Established	2	0.5	96	24.7
Total Excluded						150	38.6
Potential						Included	
In PCA	Control	# Visits	Patient Type	N	%	N	%
1	1	1	Established	48	12.3		
1	1	2	Established	182	46.8		
1	1	3	Established	9	2.3		
Total Included						239	61.4
Total PTIDs				389			

3.3. Table S3. Cohort A bnAb group reciprocal dilution ID50 neutralization results.

PTID	Group	B.6535.3	B.AC10.0.29	B.PVO.4	B.QH0692.42	B.RHPA4259.7	B.SC422661.8	C.CAP45.2.00.G3	C.Du156.12	C.Du172.17	C.Du422.1	C.ZM197M.PB7	C.ZM214M.PL15	GeoMean	PC1
0457	A.bnAb	239	99	1369	215	3309	754	3131	771	970	829	399	1963	710.6	8.5
1852	A.bnAb	1811	1444	169	77	768	500	1312	2767	233	1513	198	1164	628.9	8.0
0219	A.bnAb	507	438	358	204	1049	1405	2336	1810	338	258	424	342	547.5	7.8
1749	A.bnAb	1461	577	76	126	1004	403	521	2205	1798	529	271	727	539.3	7.6
0534	A.bnAb	160	322	60	196	2745	696	13204	10748	303	224	277	1865	581.1	7.5
0536	A.bnAb	158	909	405	218	184	733	1860	859	101	612	804	211	401.8	7.1
0581	A.bnAb	347	253	548	43	1793	382	289	436	1006	356	190	693	362.4	6.7
0547	A.bnAb	1052	560	136	100	781	302	1447	1150	125	606	225	892	382.5	6.7
0401	A.bnAb	212	228	108	31	1056	76	1049	663	1043	808	787	857	362.6	6.5
0763	A.bnAb	1769	1204	188	83	871	329	7695	1911	97	817	106	10	368.2	6.5
0210	A.bnAb	246	243	34	337	123	159	242	2333	378	106	1646	1431	307.8	6.3
0510	A.bnAb	1265	1184	441	71	810	267	50	1438	131	398	64	275	306.2	6.3
0175	A.bnAb	541	120	141	478	3860	587	1714	245	161	187	196	286	322.9	6.2
0258	A.bnAb	296	69	196	187	269	429	603	265	131	408	636	820	292.1	6.2
0782	A.bnAb	704	601	65	62	137	130	2636	915	485	486	182	451	315.6	6.2
1477	A.bnAb	3001	1074	236	70	2479	159	10	1402	642	1462	303	10	266.1	6.0
0269	A.bnAb	601	246	189	269	436	190	144	575	255	108	504	279	261.1	6.0
0440	A.bnAb	289	117	160	175	295	371	309	790	265	296	201	344	249.2	5.8
0259	A.bnAb	626	147	87	206	236	156	1118	658	361	179	201	264	260.0	5.7
0540	A.bnAb	175	22	589	69	1309	280	1148	219	190	171	136	342	229.7	5.4
0564	A.bnAb	256	77	251	439	178	437	211	123	53	153	455	222	198.0	5.3
0741	A.bnAb	463	43	26	47	451	605	1137	430	749	222	145	435	238.7	5.3
0141	A.bnAb	231	83	108	200	156	565	514	300	183	88	209	346	207.9	5.3
0090	A.bnAb	234	239	44	30	110	514	2178	226	169	5459	93	232	226.4	5.2
0619	A.bnAb	276	46	81	127	1333	55	1441	180	185	217	521	191	215.1	5.1
0596	A.bnAb	725	149	54	282	535	446	154	211	67	56	496	140	196.3	5.1
0343	A.bnAb	1361	174	223	224	807	380	50	173	94	235	63	46	183.7	5.0
0765	A.bnAb	1079	228	136	135	772	339	10	1027	320	267	10	183	183.7	5.0
0585	A.bnAb	201	127	166	153	33	577	216	357	405	69	363	128	167.8	4.9
0432	A.bnAb	319	525	35	33	1607	288	404	430	247	103	146	113	204.2	4.9
0598	A.bnAb	208	542	41	67	130	136	101	838	593	265	174	458	178.9	4.9
0957	A.bnAb	312	221	10	106	347	193	597	876	103	308	64	521	193.3	4.7
0277	A.bnAb	122	24	90	70	627	265	330	666	226	234	160	757	179.2	4.7
0461	A.bnAb	685	31	70	25	4016	149	2629	463	251	242	113	86	203.9	4.7
0874	A.bnAb	595	172	39	93	694	10	151	252	186	410	275	265	169.1	4.5
0293	A.bnAb	1274	342	17	167	256	38	30	587	288	170	246	180	156.7	4.5
0073	A.bnAb	94	210	10	72	28	97	701	740	349	251	571	253	158.6	4.4
0232	A.bnAb	216	176	51	179	95	288	181	384	132	226	298	164	148.1	4.4
0211	A.bnAb	179	280	40	353	639	228	164	493	104	183	164	10	145.3	4.3
0468	A.bnAb	333	476	68	160	463	91	376	102	77	52	247	96	150.4	4.3
0333	A.bnAb	351	65	55	33	98	178	379	191	100	73	181	1599	147.8	4.2
0537	A.bnAb	735	71	10	77	215	174	36	241	124	603	173	588	134.8	4.0
0060	A.bnAb	179	106	43	36	323	243	164	198	83	366	60	641	134.7	3.9
0314	A.bnAb	252	92	10	70	2033	10	124	131	831	111	128	1054	141.9	3.9
0562	A.bnAb	401	41	97	70	1087	257	2427	344	259	90	58	169	133.9	3.7
0111	A.bnAb	99	285	46	84	195	1113	460	195	39	80	341	99	115.3	3.7
0191	A.bnAb	184	77	101	272	340	357	10	209	118	94	544	10	102.6	3.6
0476	A.bnAb	795	182	30	56	66	197	997	127	85	263	96	10	112.8	3.5
0028	A.bnAb	123	24	45	24	25	56	1473	243	234	211	449	308	110.6	3.4
0383	A.bnAb	123	30	22	54	138	100	1302	327	120	238	68	209	108.0	3.3
0134	A.bnAb	173	158	224	91	41	204	10	143	37	49	131	1299	83.4	3.2

3.4. Table S4. Cohort A Control group reciprocal dilution ID50 neutralization results.

PTID	Group	B.6535.3	B.AC10.0.29	B.PVO.4	B.QH0692.42	B.RHPA4259.7	B.SC422661.8	C.CAP45.2.00.G3	C.Du156.12	C.Du172.17	C.Du422.1	C.ZM197M.PB7	C.ZM214M.PL15	GeoMean	PC1
0501	A.Control	70	17	16	88	63	23	17	88	25	18	68	10	29.0	0.1
0118	A.Control	36	10	10	10	23	10	23	93	40	25	19	84	19.5	-1.1
0391	A.Control	37	10	10	10	10	10	10	55	24	52	70	10	16.2	-1.5
0038	A.Control	81	10	10	25	10	10	10	21	37	10	23	10	15.4	-1.6
0260	A.Control	69	10	10	10	10	28	10	21	10	30	20	10	15.4	-1.7
0486	A.Control	47	10	10	15	10	10	10	23	16	10	92	10	14.6	-1.7
0516	A.Control	15	10	10	71	10	10	10	20	21	18	10	10	13.9	-1.8
0632	A.Control	10	10	10	27	10	10	25	28	10	39	28	10	14.2	-1.8
0350	A.Control	68	10	10	10	10	10	50	20	32	16	21	10	14.8	-1.8
0375	A.Control	18	16	10	10	10	10	10	29	58	18	32	10	14.1	-1.8
0750	A.Control	21	10	10	20	10	10	10	43	46	10	10	10	14.1	-1.8
0133	A.Control	18	10	10	17	10	10	10	27	17	60	10	10	13.8	-1.9
0183	A.Control	21	10	10	27	10	10	10	10	10	81	10	10	13.3	-2.0
0207	A.Control	41	10	10	40	10	10	10	31	10	25	10	10	13.4	-2.0
0171	A.Control	10	10	10	10	10	10	10	10	67	30	36	10	12.8	-2.1
0523	A.Control	16	10	10	29	10	10	10	16	10	10	38	10	12.3	-2.2
0630	A.Control	10	10	10	19	10	10	10	28	28	10	10	10	12.4	-2.2
0167	A.Control	31	10	10	10	10	10	10	10	24	10	64	10	12.5	-2.2
0403	A.Control	32	10	10	10	10	10	10	20	16	10	36	10	12.5	-2.2
0234	A.Control	10	10	10	10	10	10	10	10	22	18	37	10	12.1	-2.2
0169	A.Control	16	10	10	16	10	10	10	22	15	10	16	10	12.0	-2.3
0835	A.Control	10	10	10	10	10	10	10	23	49	10	10	10	11.9	-2.3
0381	A.Control	10	10	10	10	10	10	10	10	29	10	26	10	11.3	-2.4
0156	A.Control	18	10	10	10	10	10	10	19	10	10	16	10	11.2	-2.5
0413	A.Control	10	10	10	10	10	10	10	10	29	10	16	10	11.1	-2.5
0392	A.Control	25	10	10	10	10	10	10	10	18	10	10	10	11.2	-2.5
0329	A.Control	10	10	10	10	10	10	10	10	15	10	26	10	10.9	-2.5
0339	A.Control	36	10	10	10	10	10	10	10	10	10	10	10	11.1	-2.5
0474	A.Control	10	10	10	10	10	10	10	18	18	10	10	10	10.8	-2.6
0539	A.Control	10	10	10	18	10	10	10	10	10	15	10	10	10.6	-2.6
0789	A.Control	10	15	10	10	10	10	10	10	10	18	10	10	10.7	-2.6
0453	A.Control	10	10	10	10	10	10	10	10	22	10	10	10	10.5	-2.6
0614	A.Control	10	10	10	10	10	10	10	22	10	10	10	10	10.5	-2.6
0303	A.Control	10	10	10	10	10	10	10	10	18	10	10	10	10.4	-2.7
0322	A.Control	10	10	10	10	10	10	10	10	18	10	10	10	10.4	-2.7
0408	A.Control	10	10	10	10	10	10	10	10	16	10	10	10	10.3	-2.7
0699	A.Control	19	10	10	10	10	10	10	10	10	10	10	10	10.4	-2.7
0566	A.Control	10	10	10	10	10	10	10	10	15	10	10	10	10.3	-2.7
0094	A.Control	10	10	10	10	10	10	10	10	10	10	10	10	10.0	-2.8
0514	A.Control	10	10	10	10	10	10	10	10	10	10	10	10	10.0	-2.8
0675	A.Control	10	10	10	10	10	10	10	10	10	10	10	10	10.0	-2.8
1871	A.Control	10	10	10	10	10	10	10	10	10	10	10	10	10.0	-2.8
0532	A.Control	10	10	10	10	10	10	10	10	10	10	10	10	10.0	-2.8
0715	A.Control	10	10	10	10	10	10	10	10	10	10	10	10	10.0	-2.8
0366	A.Control	10	10	10	10	10	10	10	10	10	10	10	10	10.0	-2.8
0645	A.Control	10	10	10	10	10	10	10	10	10	10	10	10	10.0	-2.8
0661	A.Control	10	10	10	10	10	10	10	10	10	10	10	10	10.0	-2.8
0801	A.Control	10	10	10	10	10	10	10	10	10	10	10	10	10.0	-2.8
0830	A.Control	10	10	10	10	10	10	10	10	10	10	10	10	10.0	-2.8
0142	A.Control	10	10	10	10	10	10	10	10	10	10	10	10	10.0	-2.8
0225	A.Control	10	10	10	10	10	10	10	10	10	10	10	10	10.0	-2.8

3.5. Table S5. Cohort A differences between bnAb and Control groups for biological sex.

Biological sex at birth	bnAb	Control
Female	34	32
Male	17	19
Chi-Sq	0.17	
p-value	0.68	

3.6. Table S6. Cohort A differences between bnAb and Control groups for country of origin.

Country	bnAb	Control
Malawi	20	14
South Africa	12	22
Tanzania	14	9
UK	2	1
USA	3	5
Chi-Sq	5.92	
p-value	0.21	

3.7. Table S7. Cohort A differences between bnAb and Control groups.

Variable	A.bnAb		A.Control		t-Test		
	N	Mean	N	Mean	t	DF	p-value
Age at screening	51	34.1	51	31.5	1.36	100	0.177
VL Geomean	51	91953	51	50567	2.17	99	0.032
VL Set Point	30	94550	37	41220	2.55	40	0.015
PC1	51	5.29	51	-2.29	38.11	67	5.9E-47

3.8. Table S8. Cohort A mean duration individuals were followed.

Group	N	Mean	SD
bnAb	51	408.8	226.9
Control	50	450.1	211.1

3.9. Table S9. Cohort A clade of HIV-1 infection.

PTID	Group	HIV-1 clade		PTID	Group	HIV-1 clade
0457	A.bnAb	C		0501	A.Control	B
1852	A.bnAb	C		0118	A.Control	C
0219	A.bnAb	A		0391	A.Control	C
1749	A.bnAb	*		0038	A.Control	A1C
0534	A.bnAb	C		0260	A.Control	B
0536	A.bnAb	A		0486	A.Control	C
0581	A.bnAb	C		0516	A.Control	B
0547	A.bnAb	C		0632	A.Control	C
0401	A.bnAb	C		0350	A.Control	C
0763	A.bnAb	A		0375	A.Control	C
0210	A.bnAb	C		0750	A.Control	A1
0510	A.bnAb	A		0133	A.Control	C
0175	A.bnAb	A		0183	A.Control	A1
0258	A.bnAb	B		0207	A.Control	C
0782	A.bnAb	C		0171	A.Control	C
1477	A.bnAb	C		0523	A.Control	C
0269	A.bnAb	C		0630	A.Control	C
0440	A.bnAb	C		0167	A.Control	C
0259	A.bnAb	C		0403	A.Control	C
0540	A.bnAb	C		0234	A.Control	C
0564	A.bnAb	C		0169	A.Control	A1
0741	A.bnAb	C		0835	A.Control	C
0141	A.bnAb	C		0381	A.Control	C
0090	A.bnAb	C		0156	A.Control	A1
0619	A.bnAb	C		0413	A.Control	C
0596	A.bnAb	C		0392	A.Control	C
0343	A.bnAb	C		0329	A.Control	B
0765	A.bnAb	C		0339	A.Control	F
0585	A.bnAb	A1C		0474	A.Control	C
0432	A.bnAb	C		0539	A.Control	C
0598	A.bnAb	CD		0789	A.Control	A1
0957	A.bnAb	C		0453	A.Control	C
0277	A.bnAb	A1C		0614	A.Control	C
0461	A.bnAb	C		0303	A.Control	C
0874	A.bnAb	C		0322	A.Control	C
0293	A.bnAb	C		0408	A.Control	C
0073	A.bnAb	C		0699	A.Control	C
0232	A.bnAb	A1		0566	A.Control	C
0211	A.bnAb	B		0094	A.Control	B
0468	A.bnAb	C		0514	A.Control	C
0333	A.bnAb	B		0675	A.Control	C
0537	A.bnAb	C		1871	A.Control	C
0060	A.bnAb	A1		0532	A.Control	C
0314	A.bnAb	C		0715	A.Control	C
0562	A.bnAb	C		0366	A.Control	C
0111	A.bnAb	B		0645	A.Control	C
0191	A.bnAb	CD		0661	A.Control	C
0476	A.bnAb	A1D		0801	A.Control	C
0028	A.bnAb	C		0830	A.Control	C
0383	A.bnAb	C		0142	A.Control	A1
0134	A.bnAb	CD		0225	A.Control	D

* PCR nonproductive, no clade could be assigned.

3.10. **Table S10.** General linear model results for the effect of clade of HIV-1 infection in Cohort A on PC1 score.

Model	Effect	F value	p
Clade Interaction	Cohort Group	1197	<0.0001
	Clade	0.02	0.87
	Clade*Group	1.15	0.29

3.11. **Table S11.** Logistic model results for the effect of clade of HIV-1 infection in Cohort A on the presence of autoantibodies.

Model	Effect	ChiSq	p
Clade Interaction	Cohort Group	11.03	0.0009
	Clade	2.21	0.14
	Clade*Group	1.04	0.31
Clade Covariate	Group3	11.56	0.0007
	Clade	1.88	0.17

3.12. **Table S12.** Poisson model results for the effect of clade of HIV-1 infection in Cohort A on the presence of autoantibodies.

Model	Effect	ChiSq	p
Clade Interaction	Cohort Group	17.46	<0.0001
	Clade	3.69	0.055
	Clade*Group	2.36	0.12
Clade Covariate	Group	15.68	<0.0001
	Clade	1.51	0.22

3.13. **Table S13.** Cohort B bnAb individuals reciprocal dilution ID50 neutralization results.

Group	PTID	KER2018	RWO20.2	Q168.a2	Q769.d22	Q769.h5	JRFL	BaL.01	YU2.DG	PVO.04	TRO.11	CAAN.A2	TRJO.58	THRO.18	BG1168.1	.101.1	ZA012.29	DU156.12	DU422.01	ZM106.9	ZM55.28a	GeoMean
B.bnAb	127/C	160	956	628	1233	3032	3750	1308	320	496	940	93	749	189	152	267	734	1185	309	166	178	503.9
B.bnAb	35/N14	259	334	213	231	891	413	961	78	224	406	105	409	305	117	31	43	169	157	52	32	177.4
B.bnAb	N6	63	865	93	165	44	2097	397	210	245	413	226	68	270	87	141	205	461	166	327	105	205.3
B.bnAb	N17	105	566	175	1517	978	810	469	134	617	1321	130	75	163	228	125	290	69	272	139	133	265.0
B.bnAb	N18	153	352	206	401	64	552	799	130	184	205	187	181	263	55	69	113	241	156	156	197	186.9
B.bnAb	N21	65	696	253	1356	122	2126	7045	129	4369	583	65	47	53	81	82	410	292	133	223	104	268.2
B.bnAb	N22	89	374	121	87	5	2702	1277	211	87	416	119	95	158	69	166	160	232	617	135	260	175.5
B.bnAb	N26	449	173	667	991	359	3666	1532	309	1875	1701	631	150	166	119	298	100	139	418	431	42	387.9
B.bnAb	N27	45	2122	97	413	106	558	2011	93	126	1386	491	153	346	50	192	53	227	418	340	21	219.0
B.bnAb	N37	218	1041	126	60	5	9605	394	120	488	375	276	101	141	64	117	52	344	198	487	131	192.2
B.bnAb	N44	143	361	152	1605	309	2040	727	24	304	2326	107	173	276	541	40	268	302	443	5	5	199.0
B.bnAb	N55	145	3072	319	72	15	8602	667	96	624	824	611	114	235	108	473	105	510	124	1702	35	287.0
B.bnAb	N90	358	408	347	759	55	2147	521	125	183	177	215	53	112	204	76	110	113	129	358	115	201.7
B.bnAb	N102	493	501	411	638	375	637	790	447	716	234	293	506	397	563	219	396	421	646	573	626	468.2
B.bnAb	N116	301	1921	680	686	162	1060	608	292	396	418	209	128	463	327	662	137	101	340	99	330	344.7
B.bnAb	N123	354	182	192	308	178	1063	1699	188	185	615	258	149	69	279	39	123	505	745	246	304	263.8
B.bnAb	N162	342	338	329	519	641	1067	1205	370	705	688	400	198	413	130	48	116	307	123	121	57	290.3
B.bnAb	N170	56	368	32	142	1476	415	725	238	254	329	103	47	131	72	45	131	605	122	174	309	176.9
B.bnAb	N208	471	1090	1900	888	472	1908	11602	1005	170	1304	675	392	2089	226	459	252	974	490	1679	224	769.0
B.bnAb	Z237	748	1069	619	2875	4057	3403	3223	446	1147	1322	290	242	203	188	160	1002	754	319	331	1070	724.0
B.bnAb	Z258	494	553	1170	665	431	8299	1369	595	603	383	338	235	283	215	442	260	944	154	1164	411	545.9
B.bnAb	44	115	237	81	264	144	6121	275	217	182	1423	164	236	264	176	57	89	79	142	49	148	194.3
B.bnAb	45	88	207	251	1033	732	18000	1578	767	172	806	222	262	69	79	870	301	794	97	298	393	393.2
B.bnAb	107	87	418	481	671	254	76	815	67	293	314	166	25	230	127	125	100	272	131	14	41	150.4

3.14. **Table S14.** Cohort B Control individuals reciprocal dilution ID50 neutralization results.

Group	PTID	KER2018	RWO20.2	Q168.a2	Q769.d22	Q769.h5	JRFL	BaL.01	YU2.DG	PVO.04	TRO.11	CAAN.A2	TRJO.58	THRO.18	BG1168.1	.101.1	ZA012.29	DU156.12	DU422.01	ZM106.9	ZM55.28a	GeoMean
B.Control	N9	5	18	11	5	5	95	36	11	28	20	27	5	21	15	5	17	5	16	5	5	12.0
B.Control	N12	75	219	62	17	18	317	198	31	103	166	28	70	57	31	25	5	5	65	30	17	44.0
B.Control	N23	144	150	67	18	266	99	413	66	85	391	91	52	56	81	19	5	5	121	31	5	56.7
B.Control	N29	19	64	21	21	69	50	99	5	42	76	35	5	67	10	5	5	5	35	40	5	21.2
B.Control	N36	52	33	172	47	11	317	518	26	54	59	153	50	224	5	5	20	125	190	24	5	48.4
B.Control	N40	58	43	101	109	107	536	296	14	533	164	67	18	71	5	5	24	23	84	29	5	49.6
B.Control	N48	40	28	90	53	34	127	260	5	170	91	95	5	112	12	5	5	5	58	20	5	29.2
B.Control	N77	10	35	14	29	5	3625	523	98	11	94	51	5	41	29	47	15	5	16	25	5	29.7
B.Control	N85	14	71	5	68	31	185	824	5	14	36	78	5	81	32	15	29	5	59	44	5	28.3
B.Control	N95	31	165	27	47	44	593	349	409	32	5	58	160	79	38	18	19	5	32	17	5	43.1
B.Control	N113	14	15	26	5	5	38	268	155	16	42	26	11	107	20	5	15	5	93	5	5	19.6
B.Control	N145	169	59	36	65	25	85	121	49	53	164	78	38	136	83	95	20	19	345	32	33	63.4
B.Control	N161	11	97	27	5	5	165	165	29	66	207	95	5	117	190	26	13	41	37	5	5	31.7
B.Control	24	14	74	14	22	17	48	84	5	35	78	49	5	5	13	5	22	5	20	5	5	16.1
B.Control	34	5	81	5	18	158	185	933	5	37	5	109	5	45	5	5	13	84	32	5	5	21.6
B.Control	36	5	5	14	17	5	317	20	5	5	22	27	31	26	11	5	5	5	39	5	5	11.8
B.Control	47	40	36	37	19	24	372	279	17	26	77	22	5	93	5	5	5	5	34	5	5	21.5
B.Control	50	61	215	66	168	119	95	226	15	443	222	88	20	154	18	5	17	5	118	22	19	54.5
B.Control	51	115	66	40	51	10	49	108	15	121	84	54	18	176	34	38	14	5	75	21	21	38.8
B.Control	54	11	56	22	5	32	5	199	15	167	246	60	58	82	101	12	5	5	103	5	5	26.5
B.Control	63	25	66	17	17	5	91	89	10	44	32	25	5	92	14	5	5	5	32	13	5	17.8

3.15. **Table S15.** Cohort B differences between bnAb and Control groups for biological sex.

Biological sex at birth	B.bnAb	B.Control
Female	6	8
Male	18	13
Chi-Sq	0.90	
p-value	0.34	

3.16. **Table S16.** Cohort B differences between bnAb and Control groups.

Variable	<u>B.bnAb</u>		<u>B.Control</u>		<u>t-Test</u>		
	N	Mean	N	Mean	t	DF	p-value
Age at screening	24	43.3	21	45.3	-0.86	43	0.396
VL	24	4628	21	1006	2.98	43	0.005

3.17. **Table S17.** General linear model results for the difference between Cohort A and B, bnAb and Control groups for binding to additional antigens.

Antigen	Group	Mean	A.bnAb	A.Control	B.bnAb	B.Control
CH0505 gp120	A.bnAb	13.58		5.8E-08	0.0002	0.0297
CH0505 gp120	A.Control	11.98	5.8E-08		0.5506	0.0848
CH0505 gp120	B.bnAb	12.24	0.0002	0.5506		0.3519
CH0505 gp120	B.Control	12.70	0.0297	0.0848	0.3519	
gp41	A.bnAb	14.21		2.1E-06	0.0569	0.3951
gp41	A.Control	12.99	2.1E-06		0.1205	0.0106
gp41	B.bnAb	13.55	0.0569	0.1205		0.4643
gp41	B.Control	13.88	0.3951	0.0106	0.4643	
TIV2008*	A.bnAb	7.91		0.1868	0.7449	0.0899
TIV2008	A.Control	8.31	0.1868		0.4812	0.5506
TIV2008	B.bnAb	8.04	0.7449	0.4812		0.2667
TIV2008	B.Control	8.55	0.0899	0.5506	0.2667	

Means for each group and the Benjamini-Hochberg (17) false discovery rate corrected p-value.

* TIV2008 = trivalent inactivated influenza vaccine for the 2008-09 season.

3.18. Table S18. General linear model results for the difference in T cell subsets between Cohort A bnAb and Control groups and African seronegative individuals.

Cell Type	Group	Mean	A.bnAb	A.Control	A.Seroneg
CD4 ⁺ T cells within lymphocytes (%)	A.bnAb	17.06		6.9E-05	5.1E-17
	A.Control	25.77	6.9E-05		2.5E-07
	A.Seronegative	39.08	5.1E-17	2.5E-07	
CXCR3 ⁻ PD-1 ⁺ within CXCR5 ⁺ CD4 ⁺ T cells (%)	A.bnAb	35.21		4.7E-05	3.0E-11
	A.Control	26.74	4.7E-05		0.0027
	A.Seronegative	21.24	3.0E-11	0.0027	
CD25 ⁺ Foxp3 ⁺ CD4 ⁺ T cells within lymphocytes (%)	A.bnAb	0.53		0.0044	1.7E-06
	A.Control	0.81	0.0044		0.0344
	A.Seronegative	1.01	1.7E-06	0.0344	
Mean Fluorescence Intensity of PD-1 on CD25 ⁺ Foxp3 ⁺ CD4 ⁺ T cells	A.bnAb	11.12		9.3E-06	1.0E-05
	A.Control	6.90	9.3E-06		0.9716
	A.Seronegative	6.59	1.0E-05	0.9716	
CD25 ⁺ Foxp3 ⁺ within CXCR5 ⁺ CD4 ⁺ T cells (%)	A.bnAb	1.63		0.2609	0.3753
	A.Control	1.92	0.2609		0.0344
	A.Seronegative	1.39	0.3753	0.0344	
Tfr/Tfh (ratio)	A.bnAb	0.0167		0.2609	0.3753
	A.Control	0.0198	0.2609		0.0344
	A.Seronegative	0.0142	0.3753	0.0344	
Mean Fluorescence Intensity of PD-1 on CD25 ⁺ Foxp3 ⁺ CXCR5 ⁺ CD4 ⁺ T cells	A.bnAb	10.08		0.0044	0.0344
	A.Control	6.93	0.0044		0.4545
	A.Seronegative	7.19	0.0344	0.4545	

Means for each group and the Benjamini-Hochberg (17) false discovery rate corrected p-value.

3.19. **Table S19.** Logistic model results for the effect of viral load in Cohort A on the presence of autoantibodies.

Model	Effect	ChiSq	p
Viral Load Interaction	Cohort Group	0.00	0.96
	ln_VL_Mean	0.18	0.67
	ln_VL_Mean*Group	0.09	0.76
Viral Load Covariate	Group	8.91	0.003
	ln_VL_Mean	0.14	0.71

3.20. **Table S20.** Poisson model results for the effect of viral load in Cohort A on the presence of autoantibodies.

Model	Effect	ChiSq	p
Viral Load Interaction	Cohort Group	0.55	0.46
	ln_VL_Mean	0.00	0.97
	ln_VL_Mean*Group	1.37	0.24
Viral Load Covariate	Group	11.88	0.001
	ln_VL_Mean	0.12	0.73

3.21. **Table S21.** General linear model results for Cohort A bnAb and Control groups with covariates for group, viral load, and as an interaction term.

Cell Type	Covariate	F statistic	uncorrected p-value	FDR p-value
CD4 ⁺ T cells within lymphocytes (%)	group	0.5073	0.4781	0.6679
	viral load	5.9424	0.01672	0.5017
	group and viral load	0.1233	0.7263	0.8204
CXCR3 ⁻ PD-1 ⁺ within CXCR5 ⁺ CD4 ⁺ T cells (%)	group	0.1123	0.7384	0.8204
	viral load	0.4809	0.4898	0.6679
	group and viral load	0.5965	0.4419	0.6679
CD25 ⁺ Foxp3 ⁺ CD4 ⁺ T cells within lymphocytes (%)	group	1.9206	0.1692	0.6679
	viral load	0.2321	0.6311	0.7721
	group and viral load	1.2275	0.2708	0.6679
Mean Fluorescence Intensity of PD-1 on CD25 ⁺ Foxp3 ⁺ CD4 ⁺ T cells	group	0.3190	0.5736	0.7482
	viral load	2.5891	0.1111	0.6679
	group and viral load	0.9580	0.3303	0.6679
CD25 ⁺ Foxp3 ⁺ within CXCR5 ⁺ CD4 ⁺ T cells (%)	group	0.9812	0.3245	0.6679
	viral load	0.7339	0.3939	0.6679
	group and viral load	0.6962	0.4063	0.6679
Tfr/Tfh (ratio)	group	0.9851	0.3236	0.6679
	viral load	0.7324	0.3944	0.6679
	group and viral load	0.6991	0.4053	0.6679
Mean Fluorescence Intensity of PD-1 on CD25 ⁺ Foxp3 ⁺ CXCR5 ⁺ CD4 ⁺ T cells	group	0.5587	0.4567	0.6679
	viral load	0.05159	0.8208	0.8795
	group and viral load	0.2158	0.6434	0.7721
HLA-DR ⁺ within CD25 ⁺ Foxp3 ⁺ CD4 ⁺ T cells (%)	group	1.3007	0.2606	0.6679
	viral load	2.1766	0.1476	0.6679
	group and viral load	2.3618	0.1318	0.6679
CTLA-4 ⁺ within CD25 ⁺ Foxp3 ⁺ CD4 ⁺ T cells (%)	group	0.5827	0.4495	0.6679
	viral load	2.0160	0.1630	0.6679
	group and viral load	1.0962	0.3011	0.6679
LAG-3 ⁺ within CD25 ⁺ Foxp3 ⁺ CD4 ⁺ T cells (%)	group	0.01663	0.8980	0.9290
	viral load	1.5990	0.2130	0.6679
	group and viral load	0.006446	0.9364	0.9364

FDR p-value = Benjamini-Hochberg (17) false discovery rate corrected p-value.

3.22. **Table S22.** General linear model results for Cohort A bnAb and Control groups with viral load as a main effect.

Cell Type	Covariate	F statistic	uncorrected p-value	FDR p-value
CD4 ⁺ T cells within lymphocytes (%)	group	9.36956	0.002892	0.01546
	viral load	6.7968	0.01065	0.04262
CXCR3 ⁻ PD-1 ⁺ within CXCR5 ⁺ CD4 ⁺ T cells (%)	group	13.1439	0.0004728	0.009456
	viral load	0.2774	0.5997	0.6663
CD25 ⁺ Foxp3 ⁺ CD4 ⁺ T cells within lymphocytes (%)	group	5.7225	0.01878	0.05366
	viral load	0.5850	0.4463	0.5875
Mean Fluorescence Intensity of PD-1 on CD25 ⁺ Foxp3 ⁺ CD4 ⁺ T cells	group	11.6309	0.0009650	0.009650
	viral load	2.0106	0.1596	0.3217
CD25 ⁺ Foxp3 ⁺ within CXCR5 ⁺ CD4 ⁺ T cells (%)	group	1.8515	0.1769	0.3217
	viral load	0.4618	0.4985	0.5875
Tfr/Tfh (ratio)	group	1.8564	0.1764	0.3217
	viral load	0.4600	0.4993	0.5875
Mean Fluorescence Intensity of PD-1 on CD25 ⁺ Foxp3 ⁺ CXCR5 ⁺ CD4 ⁺ T cells	group	5.7607	0.01843	0.05366
	viral load	0.1227	0.7269	0.7269
HLA-DR ⁺ within CD25 ⁺ Foxp3 ⁺ CD4 ⁺ T cells (%)	group	9.8298	0.003092	0.01546
	viral load	1.3824	0.2462	0.3517
CTLA-4 ⁺ within CD25 ⁺ Foxp3 ⁺ CD4 ⁺ T cells (%)	group	5.1983	0.02763	0.06907
	viral load	1.5262	0.2234	0.3437
LAG-3 ⁺ within CD25 ⁺ Foxp3 ⁺ CD4 ⁺ T cells (%)	group	0.1699	0.6823	0.7182
	viral load	1.7471	0.1932	0.3221

FDR p-value = Benjamini-Hochberg (17) false discovery rate corrected p-value.

3.23. Table S23. General linear model results for the difference in alternatively defined Tfr subsets between Cohort A bnAb and Control groups and African seronegative individuals.

Cell Type	Group	Mean	A.bnAb	A.Control	A.Seroneg
CD25 ⁺ Foxp3 ⁺ within CXCR3 ⁻ PD-1 ⁺ CXCR5 ⁺ CD4 ⁺ T cells (%)	A.bnAb	2.408		0.2852	0.5590
	A.Control	1.751	0.2852		0.6325
	A.Seronegative	1.910	0.5590	0.6325	
CD25 ⁺ Foxp3 ⁺ / CD25 ⁻ Foxp3 ⁻ within CXCR3 ⁻ PD-1 ⁺ CXCR5 ⁺ CD4 ⁺ T cells (ratio)	A.bnAb	0.0251		0.2852	0.5590
	A.Control	0.0180	0.2852		0.6325
	A.Seronegative	0.0196	0.5590	0.6325	
MFI of PD-1 on CD25 ⁺ Foxp3 ⁺ CXCR3 ⁻ PD-1 ⁺ CXCR5 ⁺ CD4 ⁺ T cells	A.bnAb	335.0		0.0001086	7.146E-05
	A.Control	231.6	0.0001086		0.7218
	A.Seronegative	224.6	7.146E-05	0.7218	
CD25 ⁺ Foxp3 ⁺ within ICOS ⁺ PD-1 ⁺ CXCR5 ⁺ CD4 ⁺ T cells (%)	A.bnAb	4.276		0.2824	2.135E-05
	A.Control	5.451	0.2824		0.002143
	A.Seronegative	8.283	2.135E-05	0.002143	
CD25 ⁺ Foxp3 ⁺ / CD25 ⁻ Foxp3 ⁻ within ICOS ⁺ PD-1 ⁺ CXCR5 ⁺ CD4 ⁺ T cells (ratio)	A.bnAb	0.04561		0.2824	2.135E-05
	A.Control	0.05972	0.2824		0.002143
	A.Seronegative	0.09292	2.135E-05	0.002143	
MFI of PD-1 on CD25 ⁺ Foxp3 ⁺ ICOS ⁺ PD-1 ⁺ CXCR5 ⁺ CD4 ⁺ T cells	A.bnAb	31.052		0.5590	0.2824
	A.Control	28.383	0.5590		0.5641
	A.Seronegative	26.394	0.2824	0.5641	

Means for each group and the Benjamini-Hochberg (17) false discovery rate corrected p-value.

3.24. Table S24. General linear model results for Treg activation/exhaustion marker expression between Cohort A bnAb and Control groups and African seronegative individuals.

Cell Type	Group	Mean	A.bnAb	A.Control	A.Seroneg
HLA-DR ⁺ cells within CD25 ⁺ Foxp3 ⁺ CD4 ⁺ T cells (%)	A.bnAb	59.39		0.0003025	0.0001045
	A.Control	42.47	0.0003025		0.6487
	A.Seronegative	40.14	0.0001045	0.6487	
CTLA-4 ⁺ cells within CD25 ⁺ Foxp3 ⁺ CD4 ⁺ T cells (%)	A.bnAb	23.25		0.01489	0.002222
	A.Control	16.91	0.01489		0.4545
	A.Seronegative	15.44	0.002222	0.4545	
LAG-3 ⁺ cells within CD25 ⁺ Foxp3 ⁺ CD4 ⁺ T cells (%)	A.bnAb	16.64		0.3753	0.7350
	A.Control	14.29	0.3753		0.5948
	A.Seronegative	15.56	0.7350	0.5948	

Means for each group and the Benjamini-Hochberg (17) false discovery rate corrected p-value.

3.25. Table S25. General linear model results for Treg marker expression levels on Treg subsets defined by PD-1 expression levels for the Cohort A bnAb group.

Cell Type	Group	Mean	PD-1 high	PD-1 low	PD-1 negative
HLA-DR ⁺ cells within CD25 ⁺ Foxp3 ⁺ CD4 ⁺ T cells (%)	PD-1 high	73.79		0.06557	6.5E-07
	PD-1 low	65.55	0.06557		0.0002307
	PD-1 negative	47.19	6.5E-07	0.0002307	
CTLA-4 ⁺ cells within CD25 ⁺ Foxp3 ⁺ CD4 ⁺ T cells (%)	PD-1 high	37.33		8.6E-06	8.5E-12
	PD-1 low	24.70	8.6E-06		6.4E-05
	PD-1 negative	15.40	8.5E-12	6.4E-05	
LAG-3 ⁺ cells within CD25 ⁺ Foxp3 ⁺ CD4 ⁺ T cells (%)	PD-1 high	30.43		0.0002281	2.7E-07
	PD-1 low	17.09	0.0002281		0.03343
	PD-1 negative	10.89	2.7E-07	0.03343	

Means for each group and the Benjamini-Hochberg (17) false discovery rate corrected p-value.

3.26. **Table S26.** General linear model results for Treg marker expression levels on Treg subsets defined by PD-1 expression levels for the African seronegative individuals.

Cell Type	Group	Mean	PD-1 high	PD-1 low	PD-1 negative
HLA-DR ⁺ cells within CD25 ⁺ Foxp3 ⁺ CD4 ⁺ T cells (%)	PD-1 high	58.59		0.01873	3.6E-07
	PD-1 low	48.49	0.01873		0.0005029
	PD-1 negative	33.28	3.6E-07	0.0005029	
CTLA-4 ⁺ cells within CD25 ⁺ Foxp3 ⁺ CD4 ⁺ T cells (%)	PD-1 high	33.17		0.0008366	3.1E-07
	PD-1 low	19.51	0.0008366		0.009874
	PD-1 negative	11.34	3.1E-07	0.009874	
LAG-3 ⁺ cells within CD25 ⁺ Foxp3 ⁺ CD4 ⁺ T cells (%)	PD-1 high	37.64		8.6E-06	8.2E-09
	PD-1 low	18.98	8.6E-06		0.02077
	PD-1 negative	12.10	8.2E-09	0.02077	

Means for each group and the Benjamini-Hochberg (17) false discovery rate corrected p-value.

3.27. **Table S27.** Sign test results for suppression of T cell proliferation by subsets of Treg cells with differing levels of PD-1 expression, normalized to Tconv + Tconv.

Cell Type	Sign test statistic	Raw p-value	FDR p-value
Tconv + Tconv compared with Tconv + PD-1 ^{neg} Tregs	-4	0.0078	0.01172
Tconv + Tconv compared with Tconv + PD-1 ^{low} Tregs	-4	0.0078	0.01172
Tconv + Tconv compared with Tconv + PD-1 ^{high} Tregs	-3	0.0703	0.07031

Raw sign test p-values and the Benjamini-Hochberg (17) false discovery rate corrected p-value.

3.28. **Table S28.** General linear model results for the difference in T cell subsets within Cohort A HIV-1-seronegative individuals who were autoantibody positive and autoantibody negative.

Cell Type	A.Seronegative AutoAbs negative	A.Seronegative AutoAbs positive	p
CD4 ⁺ T cells within lymphocytes (%)	43.30	41.02	0.63
CXCR3 ⁻ PD-1 ⁺ within CD4 ⁺ CXCR5 ⁺ T cells (%)	15.38	15.97	0.66
CD25 ⁺ Foxp3 ⁺ CD4 ⁺ T cells within lymphocytes (%)	0.952	0.536	0.06
MFI of PD-1 on CD25 ⁺ Foxp3 ⁺ CD4 ⁺ T cells	3.97	5.53	0.63

Means for each group and the Benjamini-Hochberg (17) false discovery rate corrected p-value.

3.29. **Table S29.** Cohort A bnAb group two-digit HLA Class I types.

PTID	Group	HLA A allele 1	HLA A allele 2	HLA B allele 1	HLA B allele 2	HLA C allele 1	HLA C allele 2
0457	A.bnAb	*02	*23	*42	*53	*04	*17
1852	A.bnAb	ND [†]	ND	ND	ND	ND	ND
0219	A.bnAb	*30	*33	*08	*15	*07	*17
1749	A.bnAb	*02	*32	*45	*81	*04	*16
0534	A.bnAb	*03	*68	*15	*08	*07	*08
0536	A.bnAb	*03	*30	*44	*18	*07	*07
0581	A.bnAb	*30	*30	*07	*15	*07	*02
0547	A.bnAb	*03	*30	*18	*44	*07	*07
0401	A.bnAb	*02	*74	*14	*58	*03	*08
0763	A.bnAb	*01	*02	*07	*15	*07	*02
0210	A.bnAb	*23	*30	*07	*58	*06	*07
0510	A.bnAb	ND	ND	ND	ND	ND	ND
0175	A.bnAb	*23	*34	*44	*44	*04	*06
0258	A.bnAb	ND	ND	ND	ND	ND	ND
0782	A.bnAb	*03	*30	*39	*58	*06	*12
1477	A.bnAb	*36		*53	*15	*04	
0269	A.bnAb	*29	*30	*07	*15	*07	*15
0440	A.bnAb	*23	*30	*08	*81	*07	*18
0259	A.bnAb	*29	*32	*44	*53	*04	*07
0540	A.bnAb	*29	*68	*15	*81	*03	*08
0564	A.bnAb	ND	ND	ND	ND	ND	ND
0741	A.bnAb	*23	*30	*42	*58	*06	*17
0141	A.bnAb	*02	*36	*53	*58	*04	*06
0090	A.bnAb	*30	*68	*42	*58	*06	*17
0619	A.bnAb	*23	*68	*14	*53	*08	
0596	A.bnAb	*03	*29	*15	*18		
0343	A.bnAb	*01	*43	*15	*15	*07	*18
0765	A.bnAb	*30	*43	*07	*58	*06	*07
0585	A.bnAb	*23	*68	*49	*42	*17	*07
0432	A.bnAb	*23	*26	*45	*57	*16	*18
0598	A.bnAb	*23	*80	*45	*40	*04	*16
0957	A.bnAb	*30	*30	*42	*45	*16	*17
0277	A.bnAb	*23	*36	*44	*53	*04	
0461	A.bnAb	*02	*68	*14	*15	*03	*08
0874	A.bnAb	*02	*23	*07	*53	*04	*07
0293	A.bnAb	*66	*74	*15	*57	*02	*07
0073	A.bnAb	*66	*74	*44	*15	*02	*04
0232	A.bnAb	*29	*30				
0211	A.bnAb	*11	*74	*51	*15	*15	*02
0468	A.bnAb	*02		*58	*15	*02	*06
0333	A.bnAb	*02	*69	*18	*35	*05	*12
0537	A.bnAb	*02	*30	*39	*45	*12	*16
0060	A.bnAb	*30	*68	*15	*57	*03	*18
0314	A.bnAb	*23	*68	*08	*15	*03	*07
0562	A.bnAb	*02	*03	*45	*57	*08	*16
0111	A.bnAb	*03		*07	*40	*02	*07
0191	A.bnAb	*33	*68	*39	*41	*17	*12
0476	A.bnAb	*03	*36	*58	*53	*04	*06
0028	A.bnAb	*68	*68	*14	*58	*06	*08
0383	A.bnAb	*01	*11	*35	*81	*04	*16
0134	A.bnAb	*03	*29	*58	*42	*17	*06

[†] ND = not done.

3.30. **Table S30.** Cohort A Control group two-digit HLA Class I types.

PTID	Group	HLA A allele 1	HLA A allele 2	HLA B allele 1	HLA B allele 2	HLA C allele 1	HLA C allele 2
0501	A.Control	*24	*03	*07	*53	*04	*07
0118	A.Control	*30	*68	*39	*44	*07	*12
0391	A.Control	*23	*26	*08	*81	*04	*07
0038	A.Control	*03	*68	*07	*42	*17	*07
0260	A.Control	*02	*68	*27	*35	*02	*04
0486	A.Control	*23	*34	*44	*44	*04	*06
0516	A.Control	*01	*32	*56	*57	*06	*01
0632	A.Control	*02	*29	*15	*45	*02	*07
0350	A.Control	*02	*30	*14	*45	*08	*16
0375	A.Control	*34	*68	*15	*44	*03	*04
0750	A.Control	*02	*02	*49	*41	*17	*07
0133	A.Control	*23	*68	*15	*42	*02	*17
0183	A.Control	*29	*30	*39	*41	*12	*07
0207	A.Control	*30	*34	*44	*45	*04	*18
0171	A.Control	*01	*34	*15	*81	*02	*18
0523	A.Control	*66	*68	*07	*67	*07	*12
0630	A.Control	ND	ND	ND	ND	ND	ND
0167	A.Control	*26	*74	*15	*41	*17	*02
0403	A.Control	*30	*74	*53	*57	*04	*18
0234	A.Control	*23	*66	*58	*15	*06	*02
0169	A.Control	*33	*68	*58	*53	*03	*04
0835	A.Control	*03	*66	*39	*57	*12	*18
0381	A.Control	*30	*34	*44	*39	*04	*12
0156	A.Control	*01	*03	*15	*35	*04	*14
0413	A.Control	*34	*74	*15	*42	*02	*17
0392	A.Control	*23	*34	*08	*18	*02	*07
0329	A.Control	*02	*03	*53	*15	*04	*03
0339	A.Control	ND	ND	ND	ND	ND	ND
0474	A.Control	*03	*29	*44	*58	*06	*07
0539	A.Control	*23	*29	*44	*45	*04	*06
0789	A.Control	*02	*30	*42	*42	*17	*17
0453	A.Control	*34	*66	*58	*58	*04	*07
0614	A.Control	*29	*30	*15	*42	*02	*17
0303	A.Control	*29	*34	*13	*08	*06	*07
0322	A.Control	*30	*30	*42	*42	*17	*17
0408	A.Control	*30	*30	*53	*57	*04	*18
0699	A.Control	*23	*74	*35	*58	*04	*06
0566	A.Control	*23	*33	*53	*58	*03	*06
0094	A.Control	*29	*03	*18	*49	*05	*07
0514	A.Control	*01	*30	*42	*81	*17	*18
0675	A.Control	*34	*36	*07	*57	*07	*18
1871	A.Control	ND	ND	ND	ND	ND	ND
0532	A.Control	*23	*32	*07		*01	*07
0715	A.Control	*68	*74	*15	*42	*03	*17
0366	A.Control	*30	*43	*15	*58	*06	*18
0645	A.Control	*29	*30	*42	*42	*17	*17
0661	A.Control	*29	*32	*13	*42	*06	*17
0801	A.Control	*68	*74	*14	*15	*02	*08
0830	A.Control	*30	*68	*42	*58	*06	*17
0142	A.Control	*03	*68	*18	*53	*03	*04
0225	A.Control	*30	*30				

† ND = not done.

3.31. **Table S31.** Cohort A bnAb group two-digit HLA Class II types.

PTID	Group	HLADRB1 allele 1	HLADRB1 allele 2	HLADRB3 allele 1	HLADRB3 allele 2	HLADRB4 allele 1	HLADRB4 allele 2	HLADRB5 allele 1	HLADRB5 allele 2	HLADQB1 allele 1	HLADQB1 allele 2	HLADPB1 allele 1	HLADPB1 allele 2	HLADQA1 allele 1	HLADQA1 allele 2
0457	A.bnAb	*15	*04			*01		*01		*06	*04	*01	*04	*01	*03
1852	A.bnAb	ND [†]													
0219	A.bnAb	*04	*07			*01				*03	*03	*04	*13	*02	*03
1749	A.bnAb	*03	*08	*01						*03	*04	*01	*04	*04	
0534	A.bnAb	*03	*08	*02						*02	*04	*02	*15	*04	*05
0536	A.bnAb	*15	*11	*02				*01		*06	*06	*04	*80	*01	
0581	A.bnAb	*15	*15					*01		*06		*02	*39	*01	
0547	A.bnAb	*03	*11	*03						*03	*04	*01	*13	*04	*05
0401	A.bnAb	ND													
0763	A.bnAb	*15	*03	*02				*01		*06	*02	*04	*39	*01	*05
0210	A.bnAb	*03	*11	*01	*02					*03	*04	*11	*17	*04	*05
0510	A.bnAb	ND													
0175	A.bnAb	*11	*13	*01	*03					*06	*06	*03	*04	*01	*01
0258	A.bnAb	ND													
0782	A.bnAb	*15	*13	*02				*01		*06	*06	*01	*11	*01	*01
1477	A.bnAb	*03	*11	*02						*02	*03	*04		*05	
0269	A.bnAb	*01	*03	*02						*05	*02	*01	*02	*01	*05
0440	A.bnAb	*15	*03	*02				*01		*06	*02	*01	*04	*01	*05
0259	A.bnAb	*01	*08							*05	*03	*01		*01	*04
0540	A.bnAb	*03	*12	*01	*02					*05	*02	*18		*01	*05
0564	A.bnAb	*15	*07			*01		*01						*01	*03
0741	A.bnAb	*13		*01	*03					*05	*06	*01	*02	*01	*01
0141	A.bnAb	ND													
0090	A.bnAb	*15	*12	*02				*01		*05	*06			*01	*01
0619	A.bnAb	*15	*07			*01		*01		*06	*02	*02	*04	*01	*03
0596	A.bnAb	*14	*07	*02		*01				*05	*02	*11	*39	*01	*02
0343	A.bnAb	*11	*10	*02						*05	*06	*01	*17	*01	*01
0765	A.bnAb	*15	*03	*02				*01		*06	*02	*01		*01	*05
0585	A.bnAb	*03	*13	*01	*03					*06	*04	*01	*30		
0432	A.bnAb	*07				*01				*02	*03	*04		*02	
0598	A.bnAb	*15	*13	*01				*01		*06	*06	*01	*04	*01	*01
0957	A.bnAb	*01								*05		*18		*01	
0277	A.bnAb	*03	*13	*01	*03					*06	*04	*01	*02	*01	*04
0461	A.bnAb	*15	*04			*01		*01		*06	*03	*18	*04	*01	*03
0874	A.bnAb	*11	*08	*03						*06	*03	*02	*17	*01	*04
0293	A.bnAb	*03	*13	*01	*03					*06	*04	*01		*01	*04
0073	A.bnAb	*15	*11	*02				*01		*06	*03	*01	*04	*01	*05
0232	A.bnAb	*15	*11	*02				*01		*06	*03	*01			
0211	A.bnAb	*03	*11	*02						*03		*01		*05	
0468	A.bnAb	ND													
0333	A.bnAb	*03	*11	*02						*02	*03	*04	*04	*05	
0537	A.bnAb	*01	*10							*05		*01	*04	*01	
0060	A.bnAb	*12	*13	*01	*03					*05	*06	*01		*01	*01
0314	A.bnAb	ND													
0562	A.bnAb	*03	*11	*01	*02					*03	*04	*01	*04	*04	*05
0111	A.bnAb	*15	*13	*02				*01		*06	*06	*04	*20	*01	*01
0191	A.bnAb	*13	*07	*03		*01				*06	*02	*02	*04	*01	*03
0476	A.bnAb	*11	*13	*02						*06	*06	*18	*04	*01	*01
0028	A.bnAb	ND													
0383	A.bnAb	ND													
0134	A.bnAb	*03	*13	*01						*03	*04	*01	*30	*03	*04

[†] ND = not done.

3.32. **Table S32.** Cohort A Control group two-digit HLA Class II types.

PTID	Group	HLADRB1 allele 1	HLADRB1 allele 2	HLADRB3 allele 1	HLADRB3 allele 2	HLADRB4 allele 1	HLADRB4 allele 2	HLADRB5 allele 1	HLADRB5 allele 2	HLADQB1 allele 1	HLADQB1 allele 2	HLADPB1 allele 1	HLADPB1 allele 2	HLADQA1 allele 1	HLADQA1 allele 2
0501	A.Control	*13	*07	*03		*01				*06	*03	*34	*04	*01	*02
0118	A.Control	ND [†]													
0391	A.Control	*11	*08	*03						*06	*04	*01	*02	*01	*04
0038	A.Control	*15	*11	*02				*01		*06	*03	*11	*18	*01	*05
0260	A.Control	*11		*02						*03		*02	*17	*05	
0486	A.Control	*03	*13	*02	*03					*02	*03	*03	*04	*05	*05
0516	A.Control	*04	*13	*03		*01				*06	*03	*04		*01	*03
0632	A.Control	ND													
0350	A.Control	*15	*13	*01				*01		*06	*06	*01	*02	*01	*01
0375	A.Control	*01	*04			*01				*05	*03	*04	*13	*01	*03
0750	A.Control	*01	*13	*03						*05	*06			*01	*01
0133	A.Control	ND													
0183	A.Control	*03	*07	*02		*01				*02	*02	*01	*05	*03	*05
0207	A.Control	ND													
0171	A.Control	*11		*02						*03	*03	*04		*05	
0523	A.Control	*15	*03	*01				*01		*06	*04	*04	*11	*01	*04
0630	A.Control	ND													
0167	A.Control	*11	*13	*02	*03					*06	*03	*02	*04	*01	*05
0403	A.Control	*11	*13	*02	*03					*06	*03	*02	*04	*01	*05
0234	A.Control	*11	*11	*02						*03	*03	*04	*13	*05	
0169	A.Control	*11		*03						*06		*03		*01	
0835	A.Control	*15	*07			*01		*01		*06	*02	*01	*04	*01	*02
0381	A.Control	ND													
0156	A.Control	*15	*11	*02				*01		*06		*18	*13	*01	
0413	A.Control	*03	*13	*01	*03					*06	*04	*01	*02	*01	*04
0392	A.Control	*03	*07	*01		*01				*02	*04	*01		*02	*04
0329	A.Control	*01	*15					*01		*05	*06	*04	*18	*01	*01
0339	A.Control	ND													
0474	A.Control	*03	*11	*01	*02					*03	*04	*01	*04	*04	*05
0539	A.Control	*15	*10					*01		*06	*05	*01	*04	*01	*01
0789	A.Control	ND								*04				*04	
0453	A.Control	*03	*13	*01	*02					*06	*02	*01	*04	*01	*05
0614	A.Control	*11	*13	*03						*06	*03	*01	*13	*01	*05
0303	A.Control	*03	*13	*01						*06	*04	*01		*01	*04
0322	A.Control	*03	*08	*01						*03	*04	*01	*02	*04	*05
0408	A.Control	*03	*10	*02						*05	*02	*01	*17	*01	*05
0699	A.Control	*15	*04			*01		*01		*06	*03	*02	*04	*01	*03
0566	A.Control	*07	*08			*01				*02	*03	*04		*02	*04
0094	A.Control	*03	*04	*02		*01				*02	*03	*03	*04	*03	*05
0514	A.Control	*11	*08	*02						*03	*03	*04	*13	*05	
0675	A.Control	*01	*11	*02						*05	*03	*11	*18	*01	*05
1871	A.Control	ND													
0532	A.Control	*01	*03	*02						*05	*02	*01	*02	*01	*05
0715	A.Control	ND													
0366	A.Control	*13	*14	*02	*03					*06	*06	*01	*04	*01	*01
0645	A.Control	*03		*01						*04		*01	*04	*04	
0661	A.Control	*03	*12	*01						*05	*04	*01		*01	*04
0801	A.Control	ND													
0830	A.Control	*12	*07	*01		*01				*05	*02	*04	*13	*01	*03
0142	A.Control	*01	*03	*01						*05	*04	*01		*01	*04
0225	A.Control	*03	*13	*02	*03					*05	*02				

[†] ND = not done.

3.33. Table S33. Top 20 most highly associated functional variants in exome sequencing of bnAbs vs non-bnAbs (dominant genetic model).

Column 1	Col 2	Col 3	Col 4	Col 5	Col 6	Col 7	Col 8	Col 9	Col 10
Rank	RS ID	bnab Count	Non-bnAb Count	bnab MAF	Non-bnAb MAF	EVS AA MAF	Gene	Immune Function	P Value (FET)
1	rs2304877	0/0/50	1/12/36	0.000	0.143	0.055	ANK1	YES	4.25E-05
2	rs13628	0/0/31	2/13/27	0.000	0.202	0.101	RTBDN	NO	7.57E-05
3	rs11101224	3/26/20	1/10/37	0.327	0.125	0.272	OGDHL	NO	4.09E-04
4	rs753686	8/25/8	9/12/27	0.500	0.313	0.323	COL20A1	NO	4.86E-04
5	rs192584273	7/7/21	1/1/35	0.300	0.041	0.000	MUC4	NO	4.88E-04
6	rs2177336	25/17/1	45/5/0	0.221	0.050	0.177	MUC4	NO	5.73E-04
7	chr9_100849907_G	2/8/18	1/24/6	0.214	0.419	0.000	TRIM14	YES	5.93E-04
8	rs2303098	1/4/43	3/16/27	0.063	0.239	0.159	COL5A3	NO	7.82E-04
9	rs7616293	1/11/25	0/2/45	0.176	0.021	0.071	C3orf55	NO	7.93E-04
10	rs115587270	2/15/33	0/3/47	0.190	0.030	0.046	GREB1	NO	8.09E-04
11	rs3732235	0/13/37	0/1/49	0.130	0.010	0.131	ZNF638	NO	8.46E-04
12	rs11542286	0/13/37	0/1/49	0.130	0.010	0.133	ZNF638	NO	8.46E-04
13	rs217086	37/11/2	49/1/0	0.150	0.010	0.089	CTSC	YES	8.46E-04
14	rs4473306	0/1/49	1/12/37	0.010	0.140	0.116	LILRA3	YES	8.46E-04
15	rs882605	29/18/1	45/5/0	0.208	0.050	0.171	MUC4	NO	8.54E-04
16	rs8103406	9/23/9	7/11/25	0.500	0.291	0.372	ZNRF4	NO	8.90E-04
17	rs34077456	0/9/38	0/0/50	0.096	0.000	0.044	USH1C	NO	9.54E-04
18	rs1106502	30/19/1	45/5/0	0.210	0.210	0.174	MUC4	NO	9.67E-04
19	rs1104760	30/19/1	45/5/0	0.210	0.210	0.175	MUC4	NO	9.67E-04
20	rs76864584	0/13/11	0/5/34	0.271	0.064	0.000	C14orf80	YES	0.0011

Table showing the top 20 single nucleotide variants or small indels identified in the association study of HIV-1 broad neutralization. Functional coding variants for the top 50 subjects on PC1 were compared against 50 subjects with the lowest score along PC1, using Fisher's Exact Test (FET) with a dominant genetic model.

Column 2 lists the rs ID number or genomic coordinates (build37) for each variant.

Columns 3 and 4 show raw genotype counts for each variant, using the format: #homozygous_mt/#heterozygous/#homozygous_wt.

Columns 5 and 6 show the corresponding minor allele frequencies, while column 7 shows the frequency of the minor allele among African-Americans in the Exome Variant Server (EVS) dataset.

Column 9 indicates whether the gene impacted by the variant has a reported immune function or role in HIV-1 biology.

Column 10 shows the significance score for each variant in the FET. The Bonferroni threshold for significance in this analysis was 9.633×10^{-7} .

3.34. Table S34. Top 20 most highly associated functional variants in exome sequencing of autoimmune-bnAbs vs non-bnAbs (dominant genetic model).

Column 1	Col 2	Col 3	Col 4	Col 5	Col 6	Col 7	Col 8	Col 9	Col 10
Rank	Variant ID	bnab Count	Non-bnAb Count	bnab MAF	Non-bnAb MAF	EVS AA MAF	Gene	Immune Function	P Value (FET)
1	rs13628	26/0/0	14/10/1	0.000	0.240	0.101	RTBDN	NO	9.36E-05
2	rs753686	6/21/7	19/7/3	0.515	0.224	0.323	COL20A1	NO	2.21E-04
3	rs35091611	18/16/4	27/3/0	0.316	0.050	0.232	CEA	NO	2.46E-04
4	rs12520799	35/1/0	18/11/1	0.014	0.217	0.138	C5ORF20	YES	2.71E-04
5	rs12520809	35/1/0	18/11/1	0.014	0.217	0.138	C5ORF20	YES	2.71E-04
6	rs1031844	35/1/0	18/11/1	0.014	0.217	0.140	C5ORF20	YES	2.71E-04
7	rs75095706	38/0/0	21/8/1	0.000	0.167	0.050	SH3TC1	YES	2.90E-04
8	rs7542760	10/23/5	20/8/0	0.434	0.143	0.206	PIGR	YES	4.12E-04
9	rs7036568	9/25/6	19/5/5	0.463	0.259	0.335	C9ORF84	NO	4.76E-04
10	rs34155934	18/15/3	27/3/0	0.292	0.050	0.248	CEA	NO	5.45E-04
11	rs340151	12/23/5	22/5/3	0.413	0.183	0.204	TMPRSS7	NO	6.06E-04
12	rs11264875	17/21/2	25/5/0	0.313	0.083	0.161	NUP210L	YES	6.13E-04
13	rs13021	40/0/0	22/7/1	0.000	0.150	0.076	PNN	YES	6.20E-04
14	rs4473306	40/0/0	22/7/1	0.000	0.150	0.116	LILRA3	YES	6.20E-04
15	rs77835065	35/1/0	19/10/1	0.014	0.200	0.044	PXDNL	YES	6.71E-04
16	rs3732235	28/12/0	30/0/0	0.150	0.000	0.131	ZNF638	NO	7.39E-04
17	rs11542286	28/12/0	30/0/0	0.150	0.000	0.133	ZNF638	NO	7.39E-04
18	rs11640138	28/8/0	11/16/3	0.111	0.367	0.272	TNP2	YES	0.001
19	rs115587270	26/12/2	29/1/0	0.200	0.017	0.046	GREB1	NO	0.0012
20	rs11101224	15/22/2	23/5/1	0.333	0.121	0.272	OGDHL	NO	0.0012

Table showing the top 20 single nucleotide variants or small indels identified in the sub-group analysis of HIV-1 broad neutralization after restricting the broad neutralizer group to only those with autoimmune serology and removing those subjects with evidence of autoimmunity from the non-bnAb control group. Functional coding variants for the top 50 subjects on PC1 were compared against 50 subjects with the lowest PC1 scores, using Fisher's Exact Test (FET) with a dominant genetic model.

Column 2 lists the rs ID number or genomic coordinates (build37) for each variant.

Columns 3 and 4 show raw genotype counts for each variant, using the format: #homozygous_mt/#heterozygous/#homozygous_wt.

Columns 5 and 6 show the corresponding minor allele frequencies, while column 7 shows the frequency of the minor allele among African-Americans in the Exome Variant Server (EVS) dataset.

Column 9 indicates whether the gene impacted by the variant has a reported immune function or role in HIV-1 biology.

Column 10 shows the significance score for each variant in the FET. The Bonferroni threshold for significance in this analysis was 1.134×10^{-6} .

4. References

1. G. D. Tomaras, J. M. Binley, E. S. Gray, E. T. Crooks, K. Osawa, P. L. Moore, N. Tumba, T. Tong, X. Shen, N. L. Yates, J. Decker, C. K. Wibmer, F. Gao, S. M. Alam, P. Easterbrook, S. Abdool Karim, G. Kamanga, J. A. Crump, M. Cohen, G. M. Shaw, J. R. Mascola, B. F. Haynes, D. C. Montefiori, L. Morris, Polyclonal B cell responses to conserved neutralization epitopes in a subset of HIV-1-infected individuals, *J Virol* **85**, 11502–11519 (2011).
2. P. R. Rosenbaum, D. B. Rubin, The Central Role of the Propensity Score in Observational Studies for Causal Effects, *Biometrika* **70**, 41–55 (1983).
3. J. J. Heckman, Sample Selection Bias as a Specification Error, *Econometrica* **47**, 153–161 (1979).
4. K. Pearson, On lines and planes of closest fit to systems of points in space, *Phil Mag* **2**, 559–572 (1901).
5. H. Hotelling, Analysis of a complex of statistical variables into principal components, *Journal of Educational Psychology* **24**, 417–441 (1933).
6. J. E. Jackson, *A User's Guide to Principal Components* (John Wiley & Sons, 1991).
7. M. S. Seaman, H. Janes, N. Hawkins, L. E. Grandpre, C. Devoy, A. Giri, R. T. Coffey, L. Harris, B. Wood, M. G. Daniels, T. Bhattacharya, A. Lapedes, V. R. Polonis, F. E. McCutchan, P. B. Gilbert, S. G. Self, B. T. Korber, D. C. Montefiori, J. R. Mascola, Tiered categorization of a diverse panel of HIV-1 Env pseudoviruses for assessment of neutralizing antibodies, *J Virol* **84**, 1439–1452 (2010).
8. N. A. Doria-Rose, R. M. Klein, M. G. Daniels, S. O'Dell, M. Nason, A. Lapedes, T. Bhattacharya, S. A. Migueles, R. T. Wyatt, B. T. Korber, J. R. Mascola, M. Connors, Breadth of human immunodeficiency virus-specific neutralizing activity in sera: clustering analysis and association with clinical variables, *J Virol* **84**, 1631–1636 (2010).
9. B. F. Haynes, Cardiolipin Polyspecific Autoreactivity in Two Broadly Neutralizing HIV-1 Antibodies, *Science* **308**, 1906–1908 (2005).
10. H.-X. Liao, R. Lynch, T. Zhou, F. Gao, S. M. Alam, S. D. Boyd, A. Z. Fire, K. M. Roskin, C. A. Schramm, Z. Zhang, J. Zhu, L. Shapiro, NISC Comparative Sequencing Program, J. C. Mullikin, S. Gnanakaran, P. Hraber, K. Wiehe, G. Kelsoe, G. Yang, S.-M. Xia, D. C. Montefiori, R. Parks, K. E. Lloyd, R. M. Scearce, K. A. Soderberg, M. Cohen, G. Kamanga, M. K. Louder, L. M. Tran, Y. Chen, F. Cai, S. Chen, S. Moquin, X. Du, M. G. Joyce, S. Srivatsan, B. Zhang, A. Zheng, G. M. Shaw, B. H. Hahn, T. B. Kepler, B. T. M. Korber, P. D. Kwong, J. R. Mascola, B. F. Haynes, Co-evolution of a broadly neutralizing HIV-1 antibody and founder virus, *Nature* **496**, 469–476 (2013).
11. R. M. Lynch, L. Tran, M. K. Louder, S. D. Schmidt, M. Cohen, CHAVI 001 Clinical Team Members, R. Dersimonian, Z. Euler, E. S. Gray, S. Abdool Karim, J. Kirchherr, D. C. Montefiori, S. Sibeko, K. Soderberg, G. Tomaras, Z.-Y. Yang, G. J. Nabel, H. Schuitemaker, L. Morris, B. F. Haynes, J. R. Mascola, The development of CD4 binding site antibodies during HIV-1 infection, *J Virol* **86**, 7588–7595 (2012).
12. H.-X. Liao, X. Chen, S. Munshaw, R. Zhang, D. J. Marshall, N. Vandergrift, J. F. Whitesides, X. Lu, J.-S. Yu, K.-K. Hwang, F. Gao, M. Markowitz, S. L. Heath, K. J. Bar, P. A. Goepfert, D. C. Montefiori, G. C. Shaw, S. M. Alam, D. M. Margolis, T. N. Denny, S. D. Boyd, E. Marshal, M. Egholm, B. B. Simen, B. Hanczaruk, A. Z. Fire, G. Voss, G. Kelsoe, G. D. Tomaras, M. A. Moody, T. B. Kepler, B. F. Haynes, Initial antibodies binding to HIV-1 gp41 in acutely infected subjects are polyreactive and highly mutated, *Journal of Experimental Medicine* **208**, 2237–2249 (2011).
13. M. A. Moody, R. Zhang, E. B. Walter, C. W. Woods, G. S. Ginsburg, M. T. McClain, T. N. Denny, X. Chen, S. Munshaw, D. J. Marshall, J. F. Whitesides, M. S. Drinker, J. D. Amos, T. C. Gurley, J. A. Eudailey, A.

Foulger, K. R. DeRosa, R. Parks, R. R. Meyerhoff, J.-S. Yu, D. M. Kozink, B. E. Barefoot, E. A. Ramsburg, S. Khurana, H. Golding, N. A. Vandergrift, S. M. Alam, G. D. Tomaras, T. B. Kepler, G. Kelsoe, B. F. Haynes, H3N2 influenza infection elicits more cross-reactive and less clonally expanded anti-hemagglutinin antibodies than influenza vaccination, *PLoS ONE* **6**, e25797 (2011).

14. M. Locci, C. Havenar-Daughton, E. Landais, J. Wu, M. A. Kroenke, C. L. Arlehamn, L. F. Su, R. Cubas, M. M. Davis, A. Sette, E. K. Haddad, A. V. I. P. C. P. I. International, P. Poignard, S. Crotty, Human circulating PD-1+CXCR3-CXCR5+ memory Tfh cells are highly functional and correlate with broadly neutralizing HIV antibody responses, *Immunity* **39**, 758–769 (2013).

15. D. Q. Tran, H. Ramsey, E. M. Shevach, Induction of FOXP3 expression in naive human CD4+FOXP3 T cells by T-cell receptor stimulation is transforming growth factor-beta dependent but does not confer a regulatory phenotype, *Blood* **110**, 2983–2990 (2007).

16. M. E. Himmel, K. G. MacDonald, R. V. Garcia, T. S. Steiner, M. K. Levings, Helios+ and Helios- cells coexist within the natural FOXP3+ T regulatory cell subset in humans, *J. Immunol.* **190**, 2001–2008 (2013).

17. Y. Benjamini, Y. Hochberg, Controlling the false discovery rate: a practical and powerful approach to multiple testing, *J R Statist Soc B* **57**, 289–300 (1995).